Appendix D: Power Analysis Results for the Non-zero Count Model

Caption for figures:
Power curves (top panel) show the estimated power to detect a hotspot/coldspot of various effect sizes for each sample size (number of transect segments with sightings) from 1 to 200. Red solid, dashed, and dotted lines represent the estimated power to detect a hotspot of 3, 10, and 20 times the reference mean, respectively. Blue solid, dashed, and dotted lines represent the estimated power to detect a coldspot of ⅓, 1/10, and 1/20 times the reference mean, respectively. Blue lines that are absent indicate that the estimated power to detect a coldspot was undefined because the effect size times the reference mean was less than or equal to one. Boxplots (bottom panel) show the distribution of estimated power to detect a hotspot/coldspot of various effect sizes based on the number of transect segments with sightings within each grid cell for each spatial resolution. The number of grid cells with sightings of the given species and the percentage of grid cells that achieve 80% power to detect a hotspot/coldspot are shown below the horizontal axis.

Citation for main document:
Leirness JB, Kinlan BP. 2018. Additional statistical analyses to support guidelines for marine avian sampling. Sterling (VA): US Department of the Interior, Bureau of Ocean Energy Management. OCS Study BOEM 2018-063. iii+43 p.

List of Figures

Figure D1. Common Eider spring D-5

Figure D2. Common Eider summer D-6

Figure D3. Common Eider fall D-7

Figure D4. Common Eider winter D-8

Figure D5. Surf Scoter spring D-9

Figure D6. Surf Scoter fall D-10

Figure D7. Surf Scoter winter D-11

Figure D8. White-winged Scoter spring D-12

Figure D9. White-winged Scoter fall D-13

Figure D10. White-winged Scoter winter D-14

Figure D11. Long-tailed Duck spring D-15

Figure D12. Long-tailed Duck fall D-16

Figure D13. Long-tailed Duck winter D-17

Figure D14. Razorbill spring D-18

Figure D15. Razorbill summer D-19

Figure D16. Razorbill fall D-20

Figure D17. Razorbill winter D-21

Figure D18. Atlantic Puffin spring D-22

Figure D19. Atlantic Puffin summer D-23

Figure D20. Atlantic Puffin fall D-24

Figure D21. Atlantic Puffin winter D-25

Figure D22. Laughing Gull spring D-26

Figure D23. Laughing Gull summer D-27

Figure D24. Laughing Gull fall D-28

Figure D25. Laughing Gull winter D-29

Figure D26. Herring Gull spring D-30
Figure D27. Herring Gull summer D-31
Figure D28. Herring Gull fall D-32
Figure D29. Herring Gull winter D-33
Figure D30. Least Tern summer D-34
Figure D31. Least Tern fall D-35
Figure D32. Roseate Tern spring D-36
Figure D33. Roseate Tern summer D-37
Figure D34. Roseate Tern fall D-38
Figure D35. Common Tern spring D-39
Figure D36. Common Tern summer D-40
Figure D37. Common Tern fall D-41
Figure D38. Royal Tern spring D-42
Figure D39. Royal Tern summer D-43
Figure D40. Royal Tern fall D-44
Figure D41. Red-throated Loon spring D-45
Figure D42. Red-throated Loon fall D-46
Figure D43. Red-throated Loon winter D-47
Figure D44. Common Loon spring D-48
Figure D45. Common Loon summer D-49
Figure D46. Common Loon fall D-50
Figure D47. Common Loon winter D-51
Figure D48. Black-capped Petrel spring D-52
Figure D49. Black-capped Petrel summer D-53
Figure D50. Black-capped Petrel fall D-54
Figure D51. Black-capped Petrel winter D-55

Figure D52. Cory's Shearwater spring D-56
Figure D53. Cory's Shearwater summer D-57
Figure D54. Cory's Shearwater fall D-58
Figure D55. Sooty Shearwater spring D-59
Figure D56. Sooty Shearwater summer D-60
Figure D57. Sooty Shearwater fall D-61
Figure D58. Great Shearwater spring D-62
Figure D59. Great Shearwater summer D-63
Figure D60. Great Shearwater fall D-64
Figure D61. Great Shearwater winter D-65
Figure D62. Audubon's Shearwater spring D-66
Figure D63. Audubon's Shearwater summer D-67
Figure D64. Audubon's Shearwater fall D-68
Figure D65. Audubon's Shearwater winter D-69
Figure D66. Northern Gannet spring D-70
Figure D67. Northern Gannet summer D-71
Figure D68. Northern Gannet fall D-72
Figure D69. Northern Gannet winter D-73

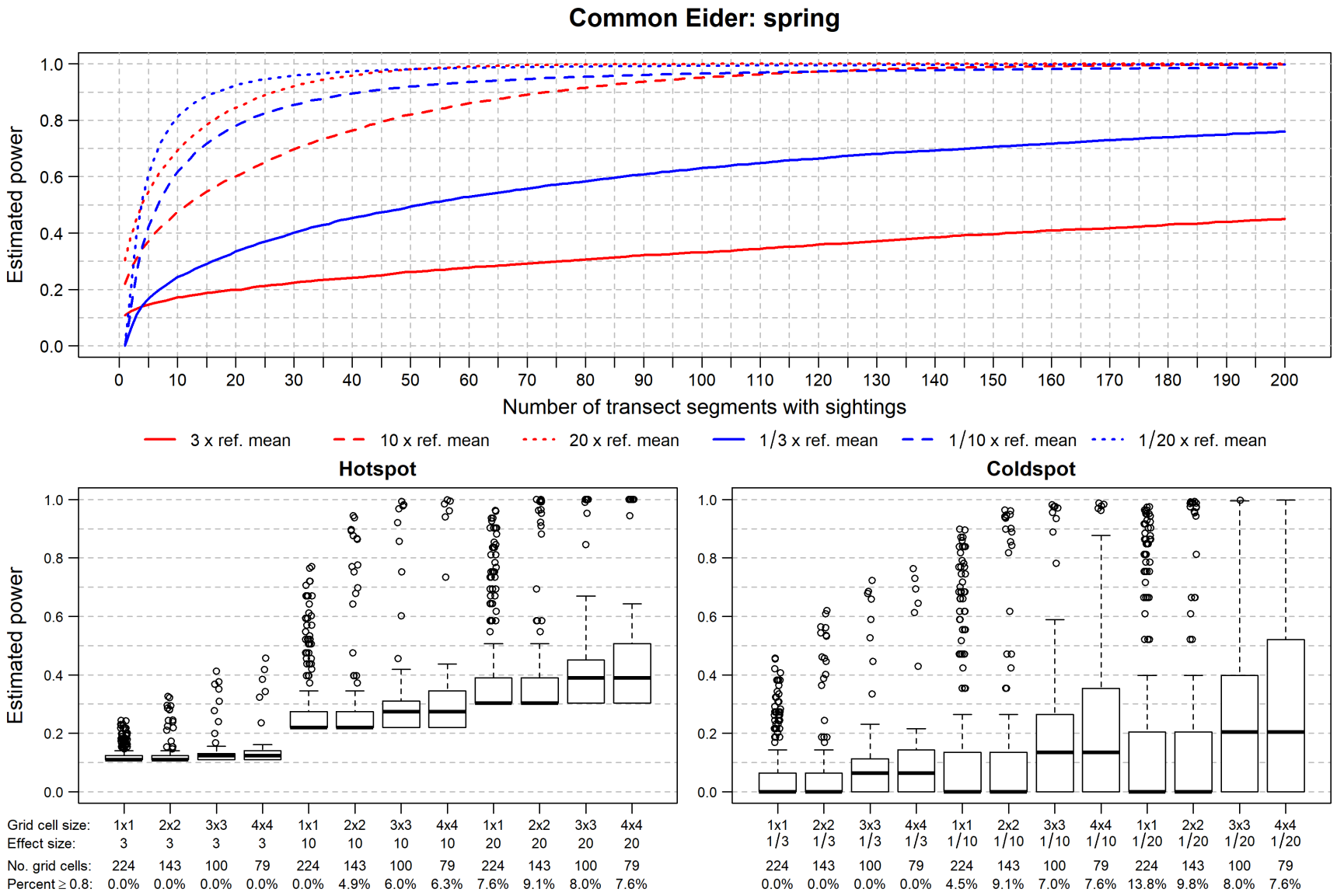

Figure D1. Power analysis results for Common Eider during spring based on the non-zero count model (type I error rate = 0.05)

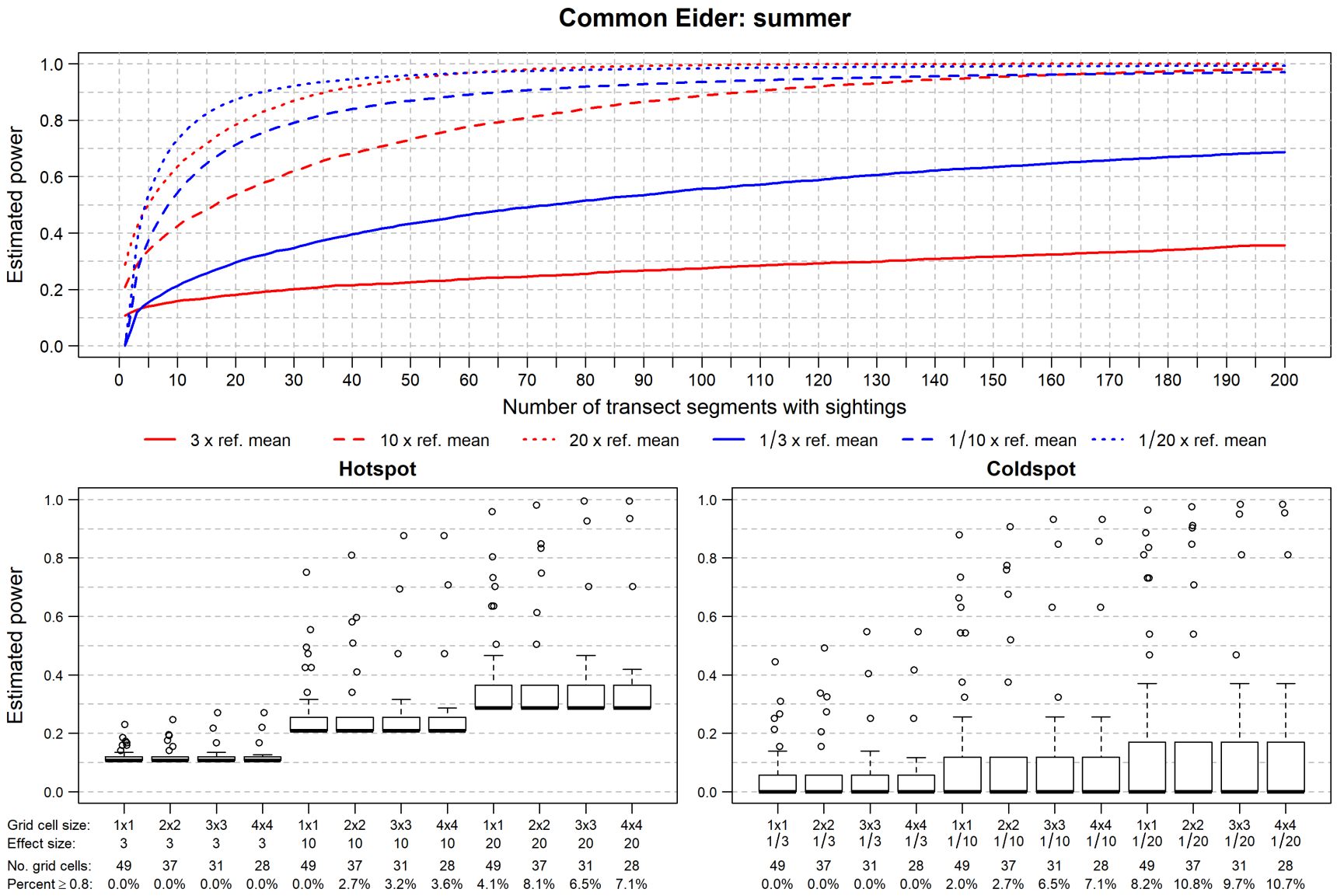

Figure D2. Power analysis results for Common Eider during summer based on the non-zero count model (type I error rate = 0.05)

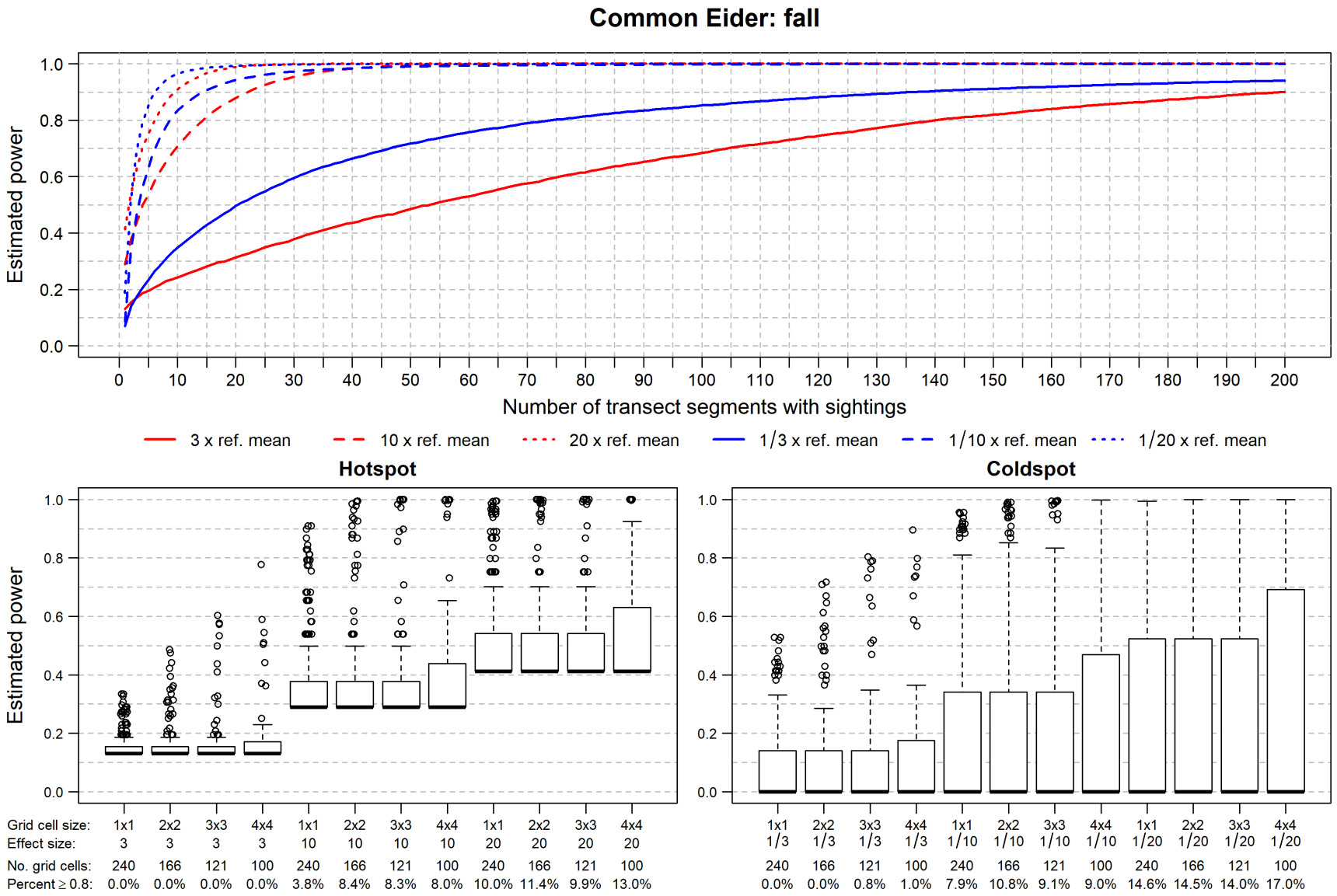

Figure D3. Power analysis results for Common Eider during fall based on the non-zero count model (type I error rate = 0.05)

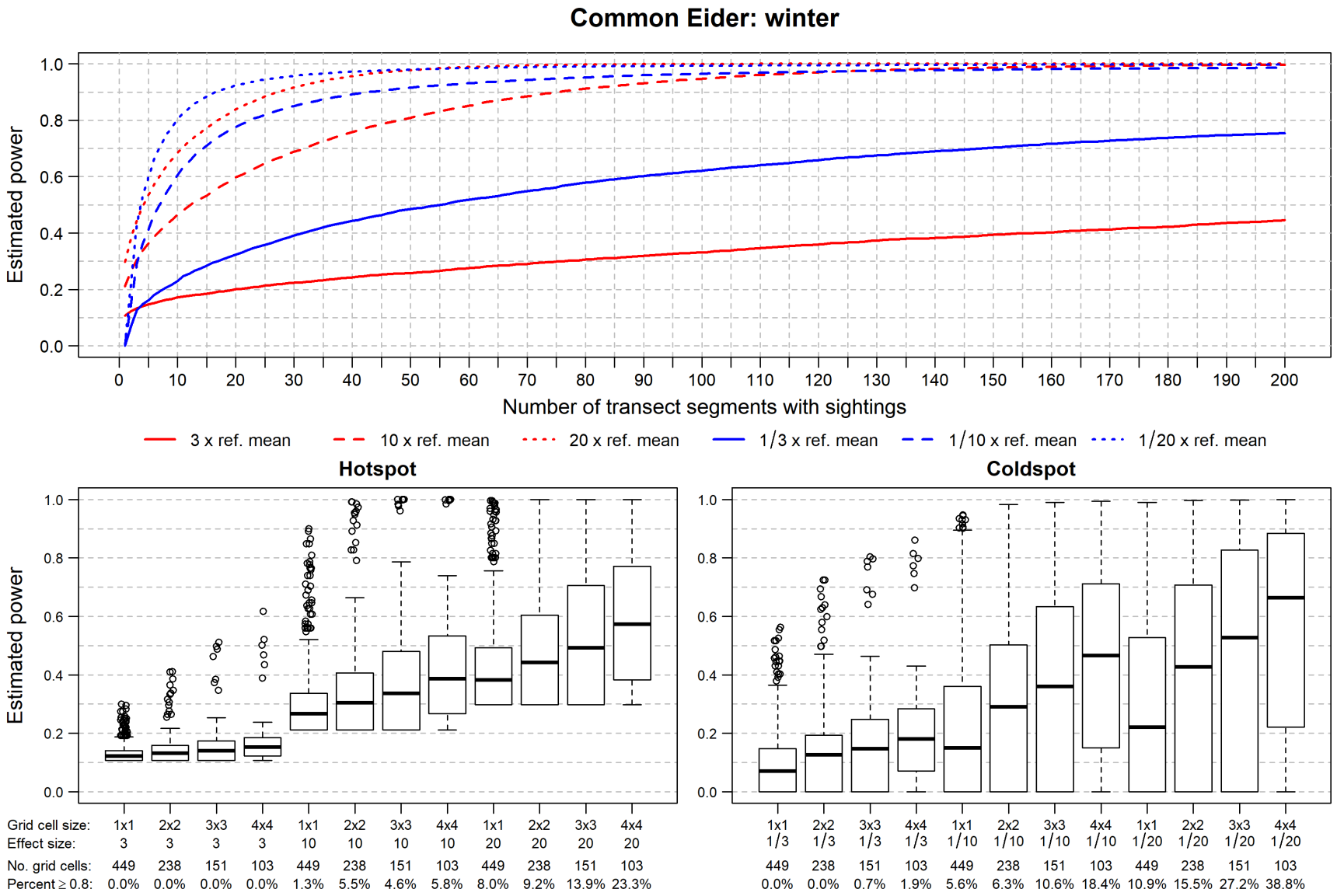

Figure D4. Power analysis results for Common Eider during winter based on the non-zero count model (type I error rate = 0.05)

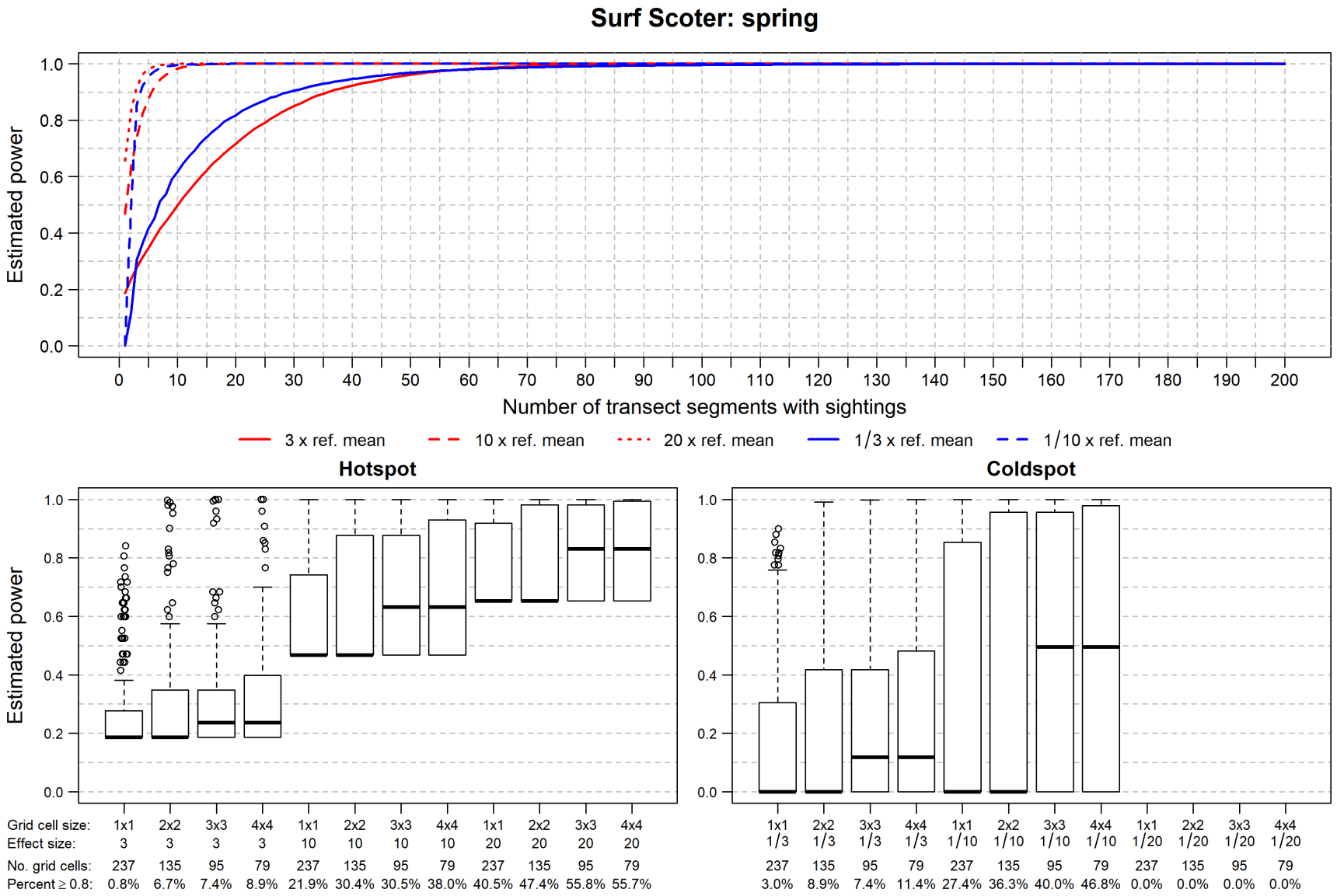

Figure D5. Power analysis results for Surf Scoter during spring based on the non-zero count model (type I error rate = 0.05)

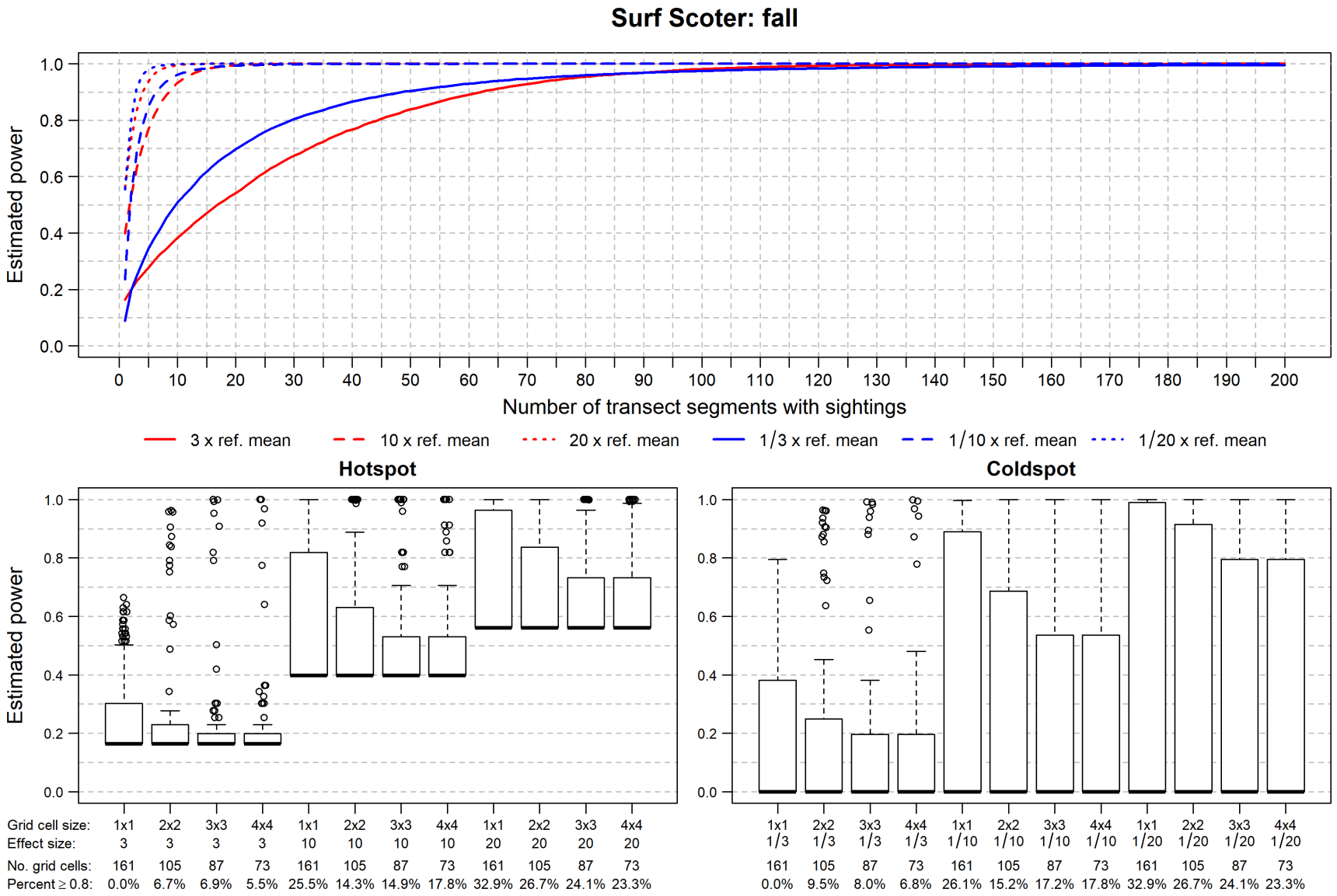

Figure D6. Power analysis results for Surf Scoter during fall based on the non-zero count model (type I error rate = 0.05)

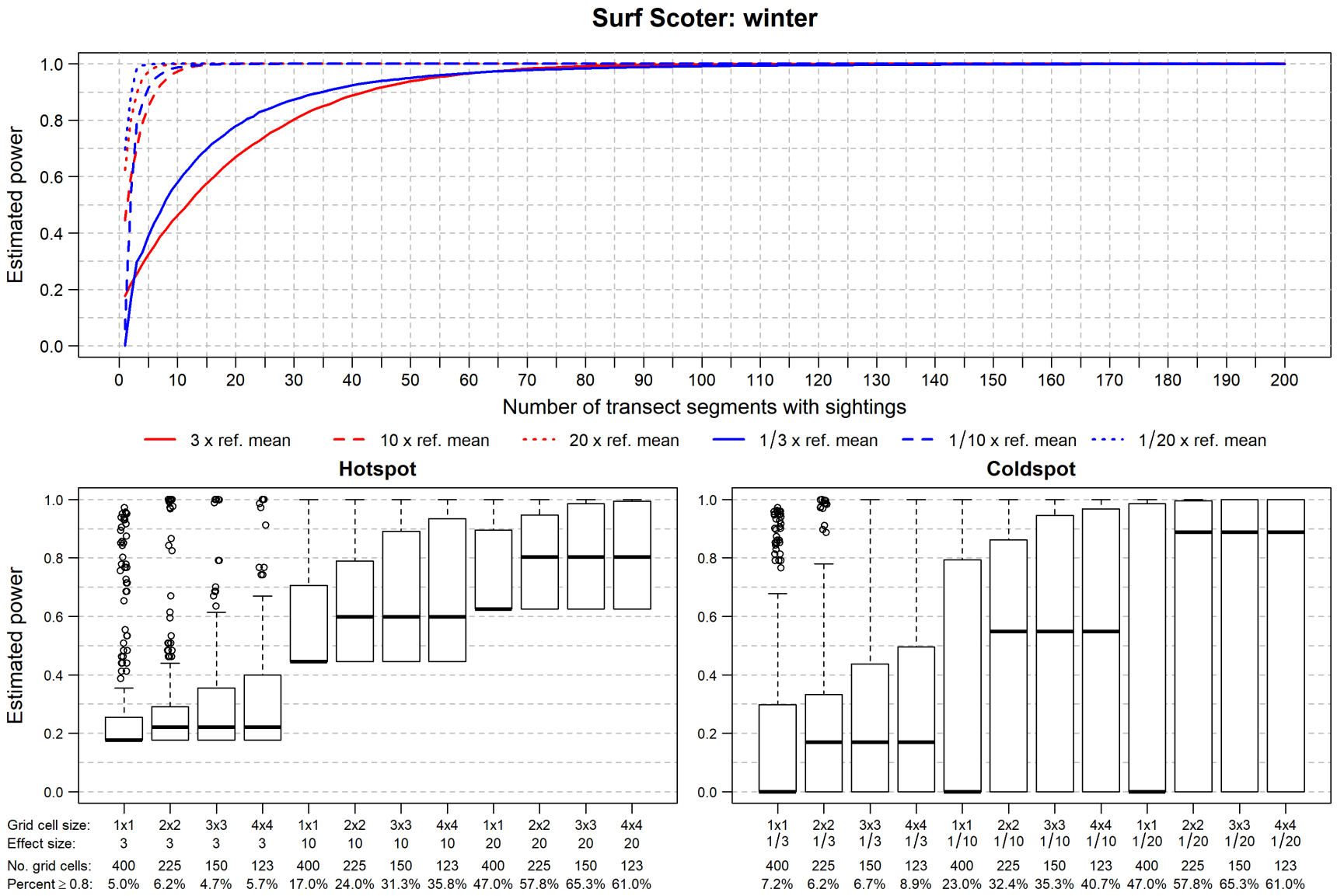

Figure D7. Power analysis results for Surf Scoter during winter based on the non-zero count model (type I error rate = 0.05)

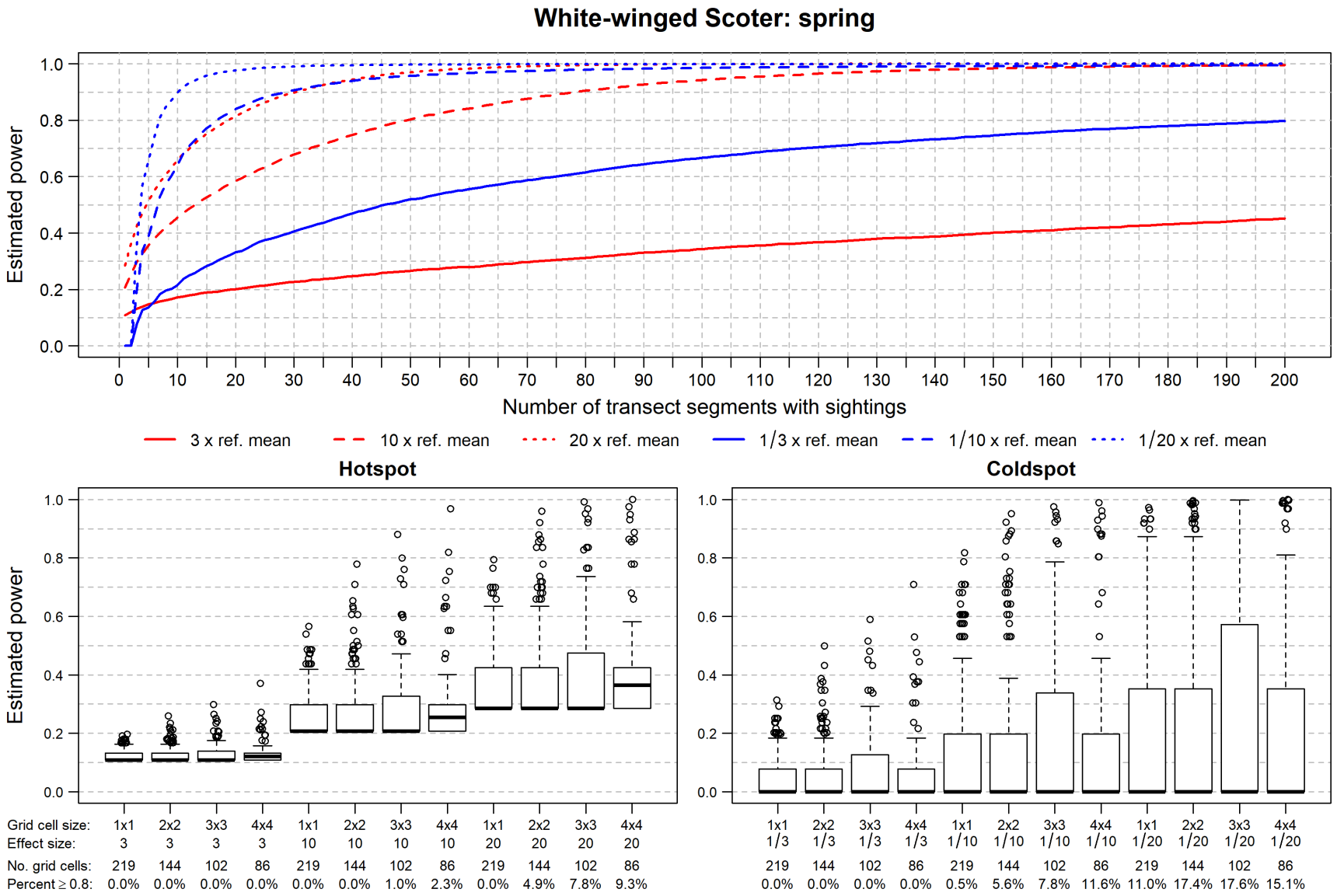

Figure D8. Power analysis results for White-winged Scoter during spring based on the non-zero count model (type I error rate = 0.05)

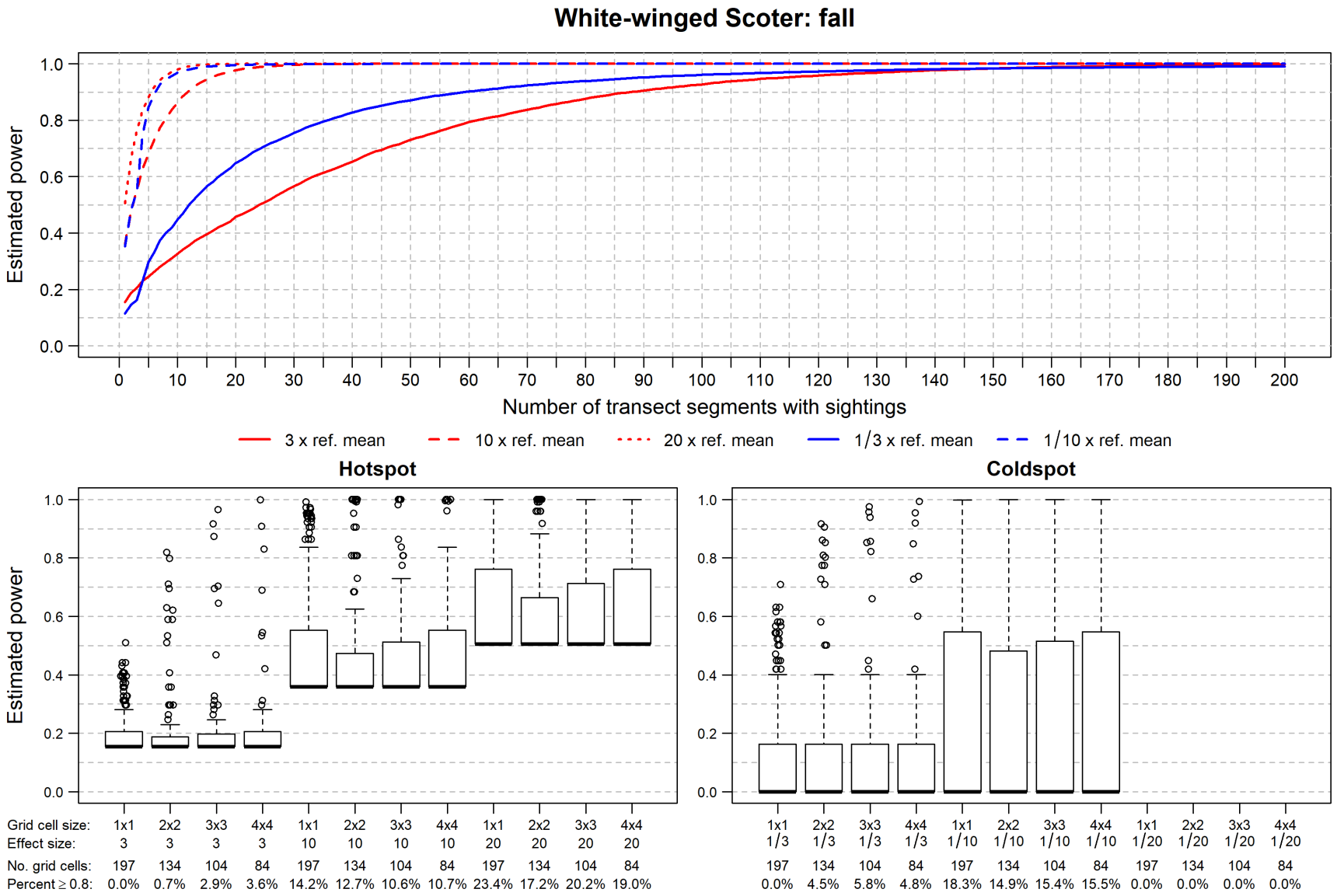

Figure D9. Power analysis results for White-winged Scoter during fall based on the non-zero count model (type I error rate = 0.05)

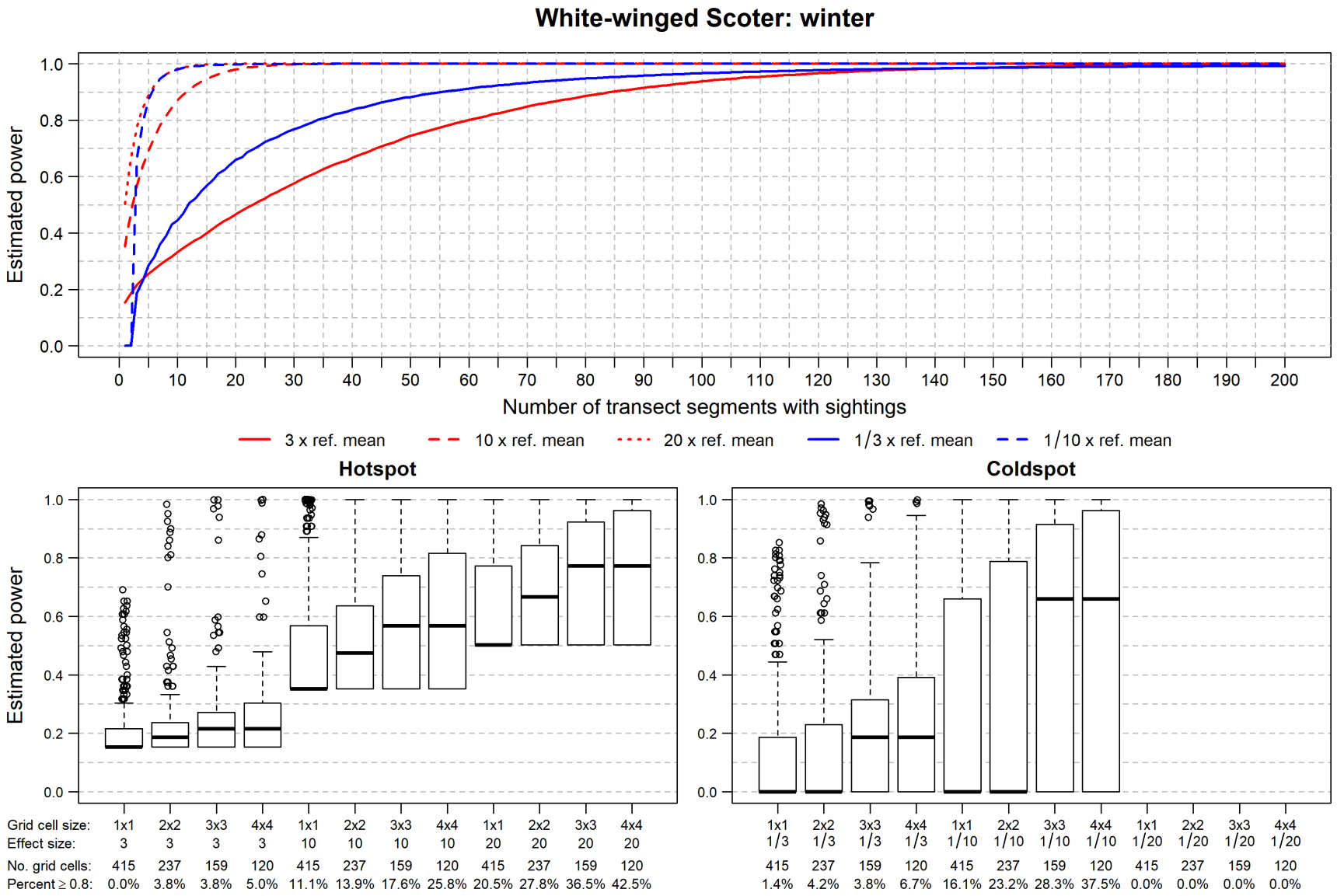

Figure D10. Power analysis results for White-winged Scoter during winter based on the non-zero count model (type I error rate = 0.05)

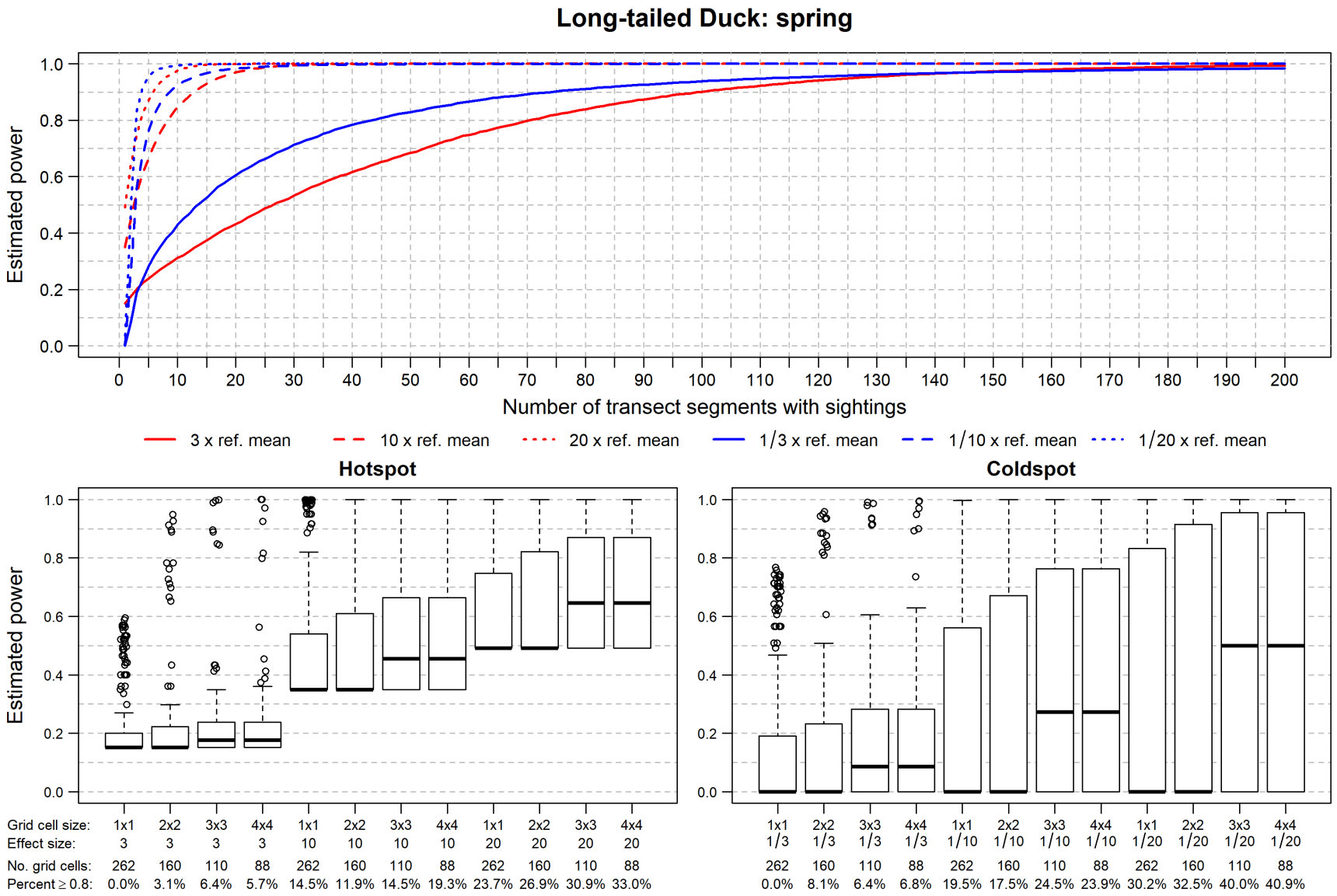

Figure D11. Power analysis results for Long-tailed Duck during spring based on the non-zero count model (type I error rate = 0.05)

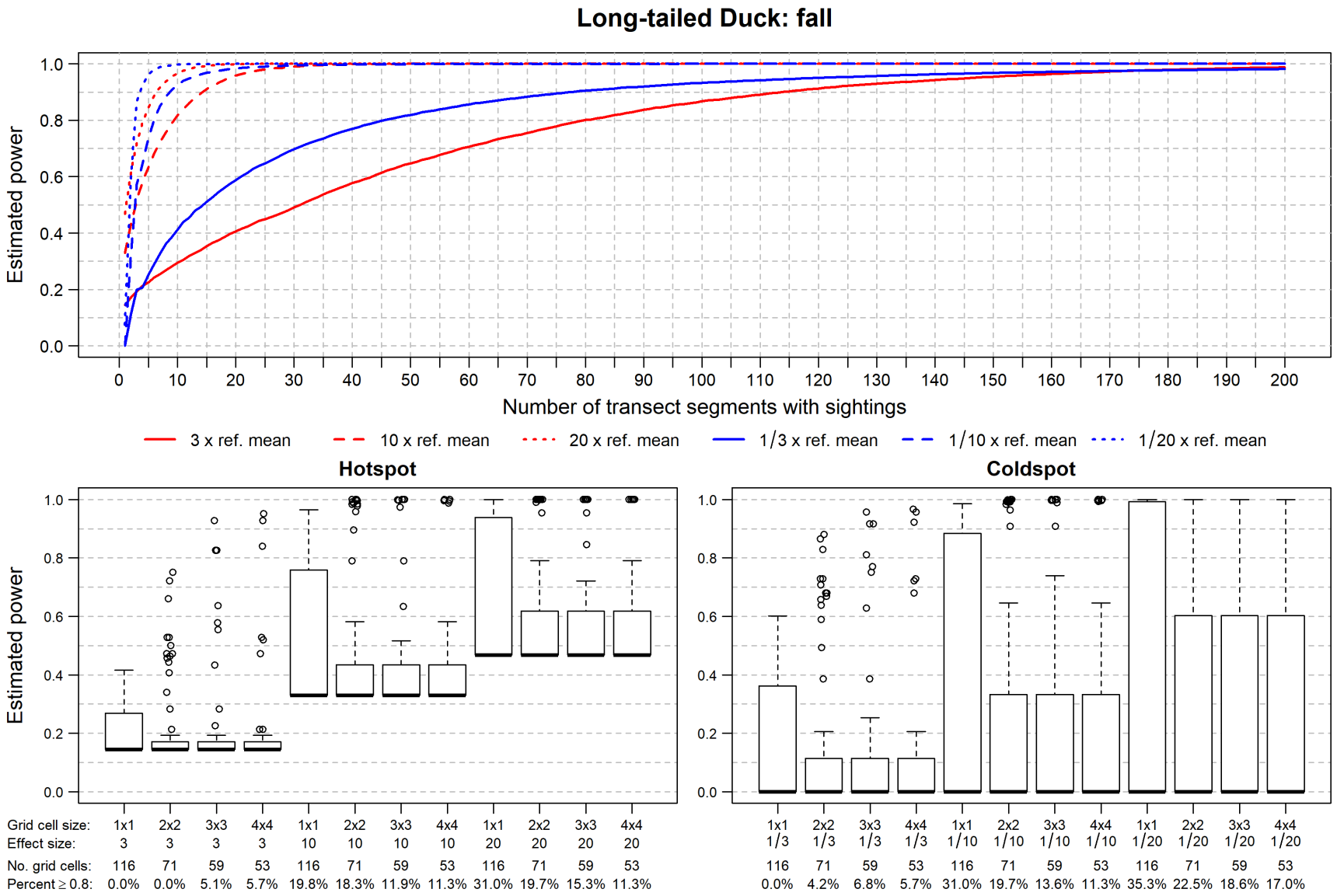

Figure D12. Power analysis results for Long-tailed Duck during fall based on the non-zero count model (type I error rate = 0.05)

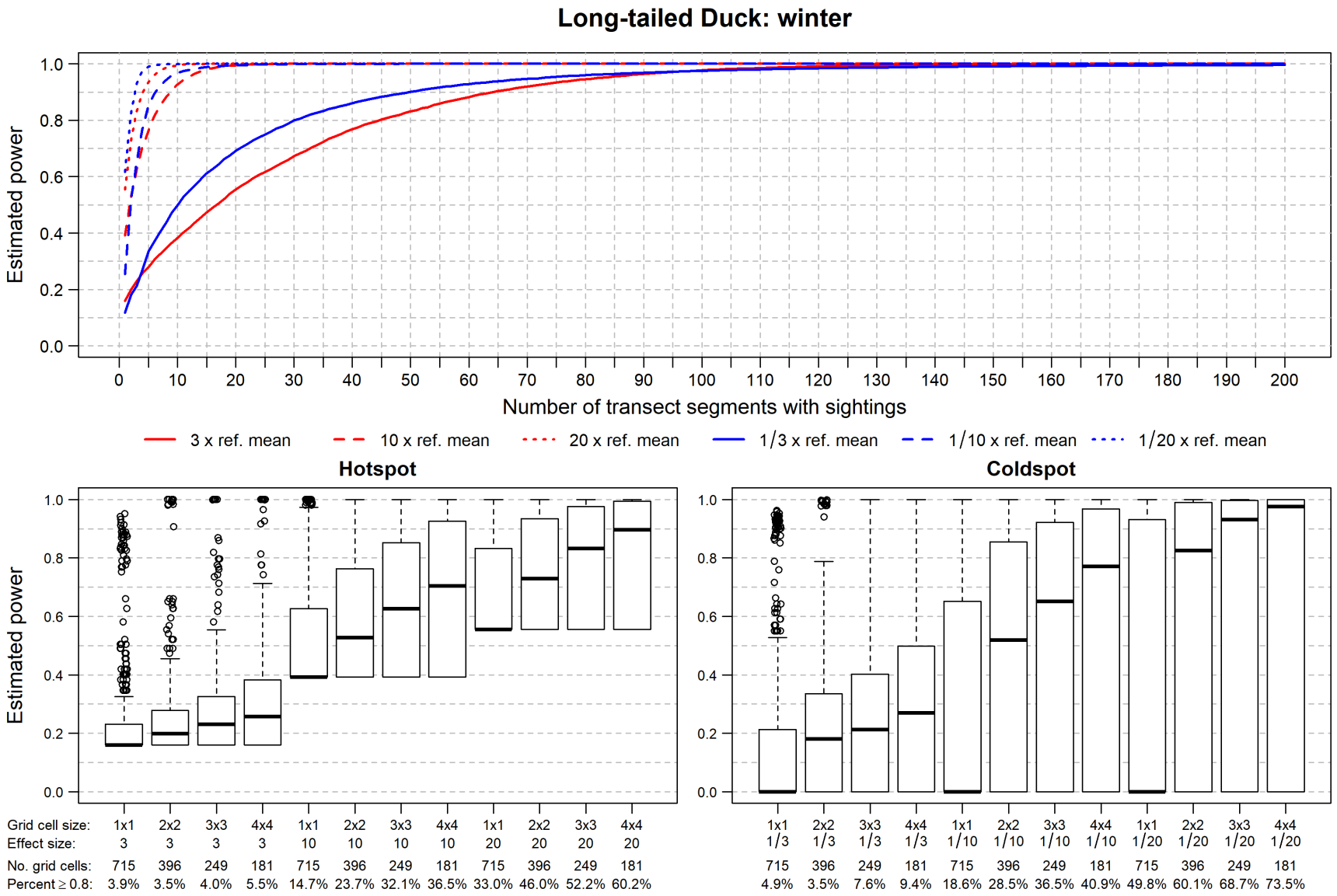

Figure D13. Power analysis results for Long-tailed Duck during winter based on the non-zero count model (type I error rate = 0.05)

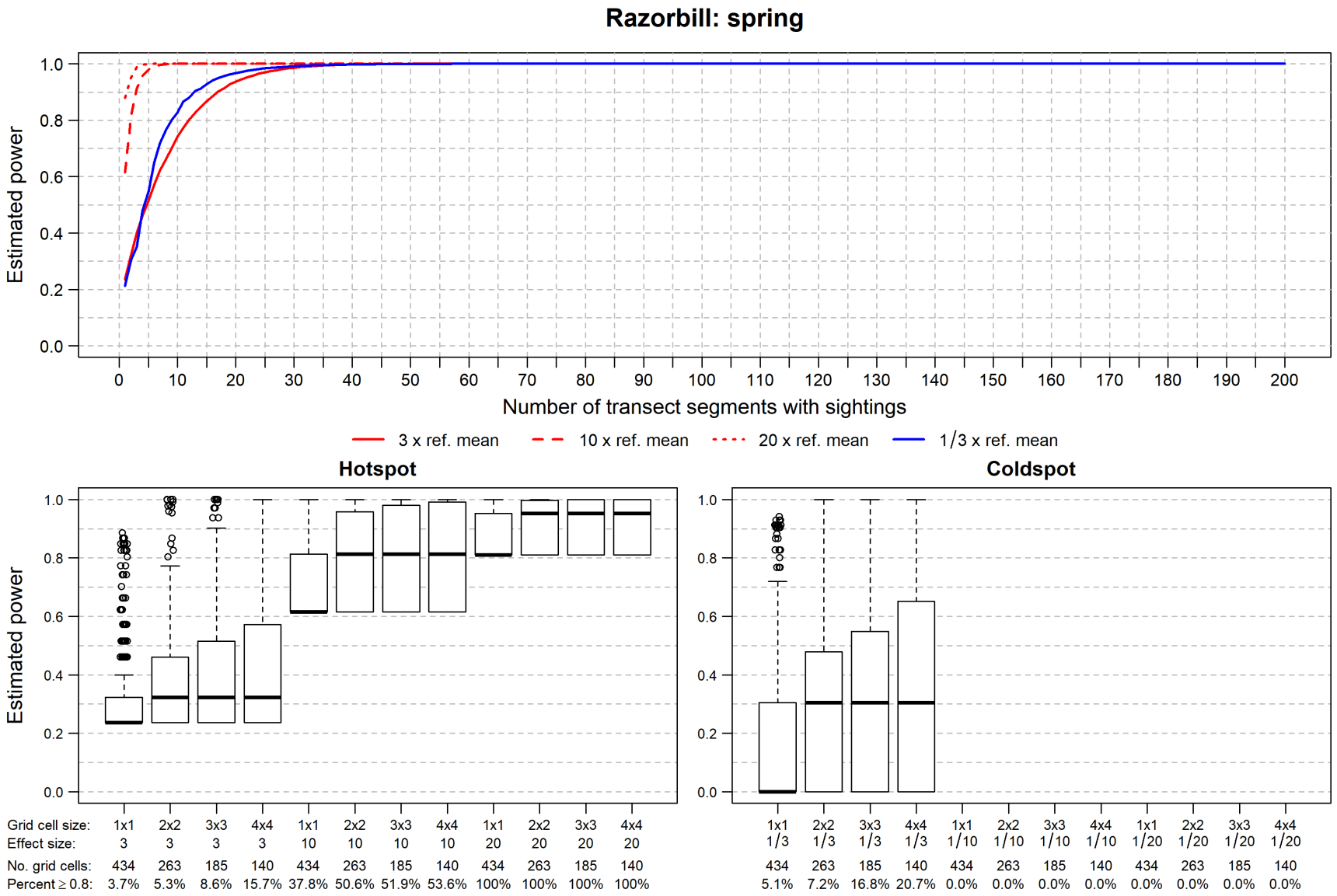

Figure D14. Power analysis results for Razorbill during spring based on the non-zero count model (type I error rate = 0.05)

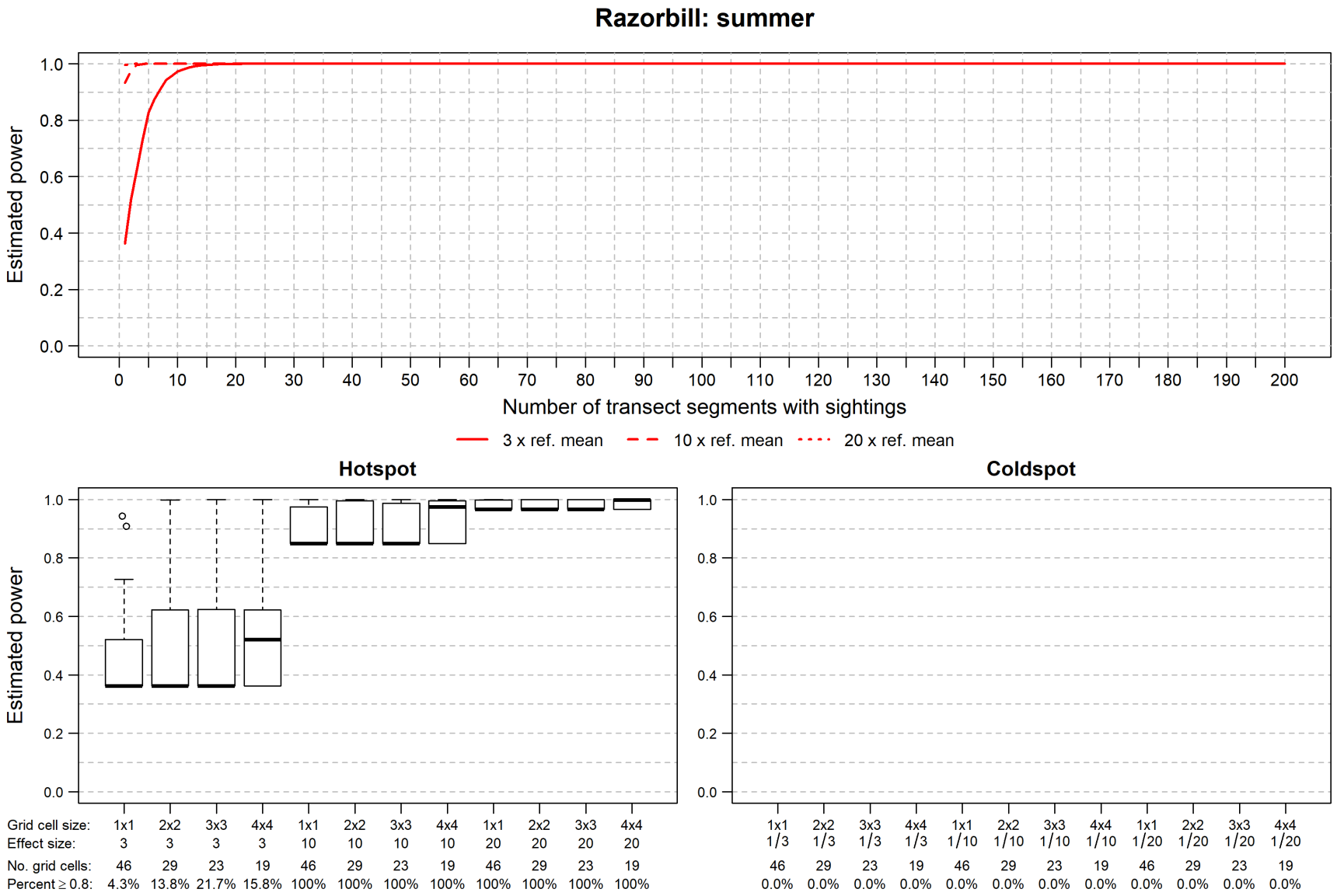

Figure D15. Power analysis results for Razorbill during summer based on the non-zero count model (type I error rate = 0.05)

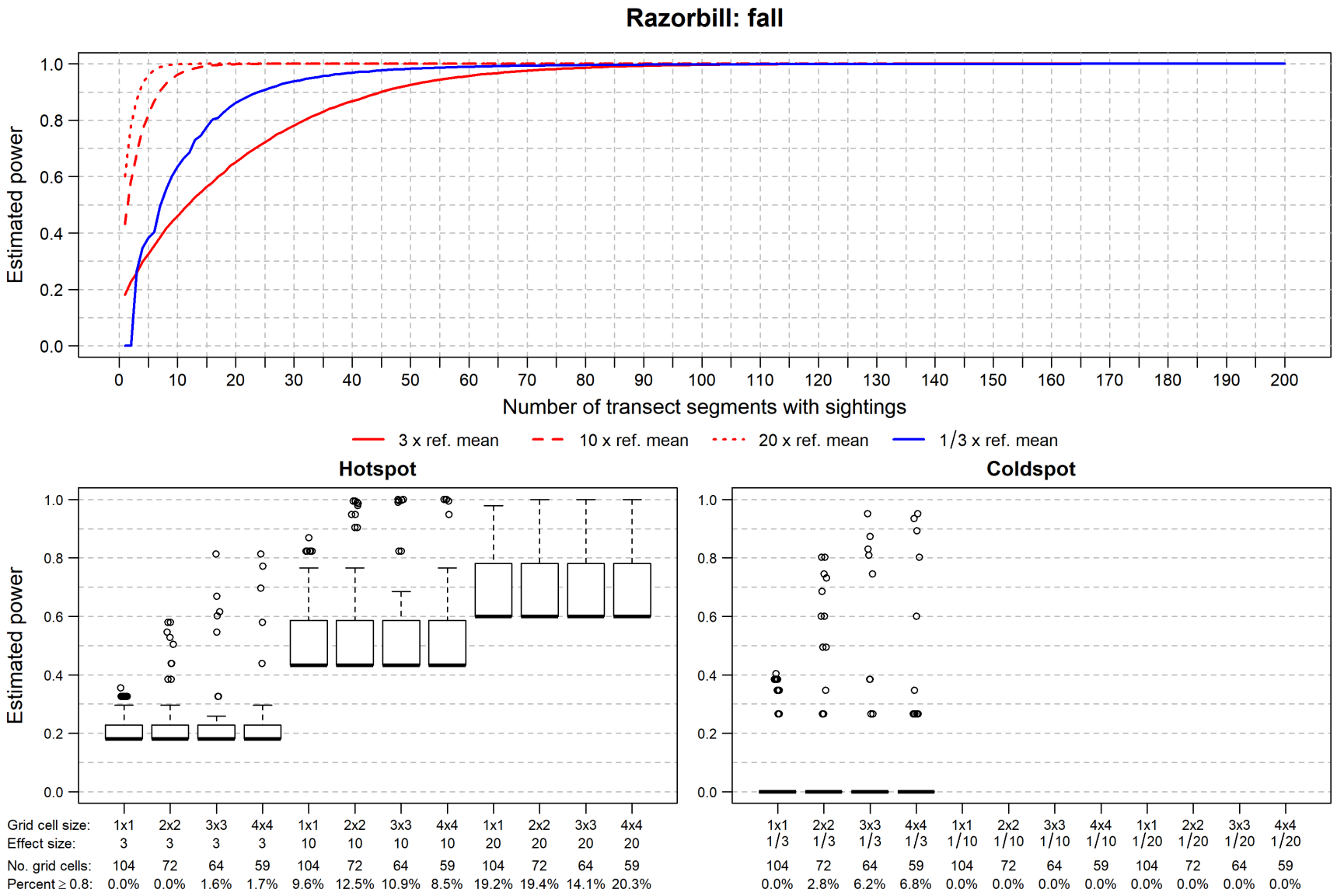

Figure D16. Power analysis results for Razorbill during fall based on the non-zero count model (type I error rate = 0.05)

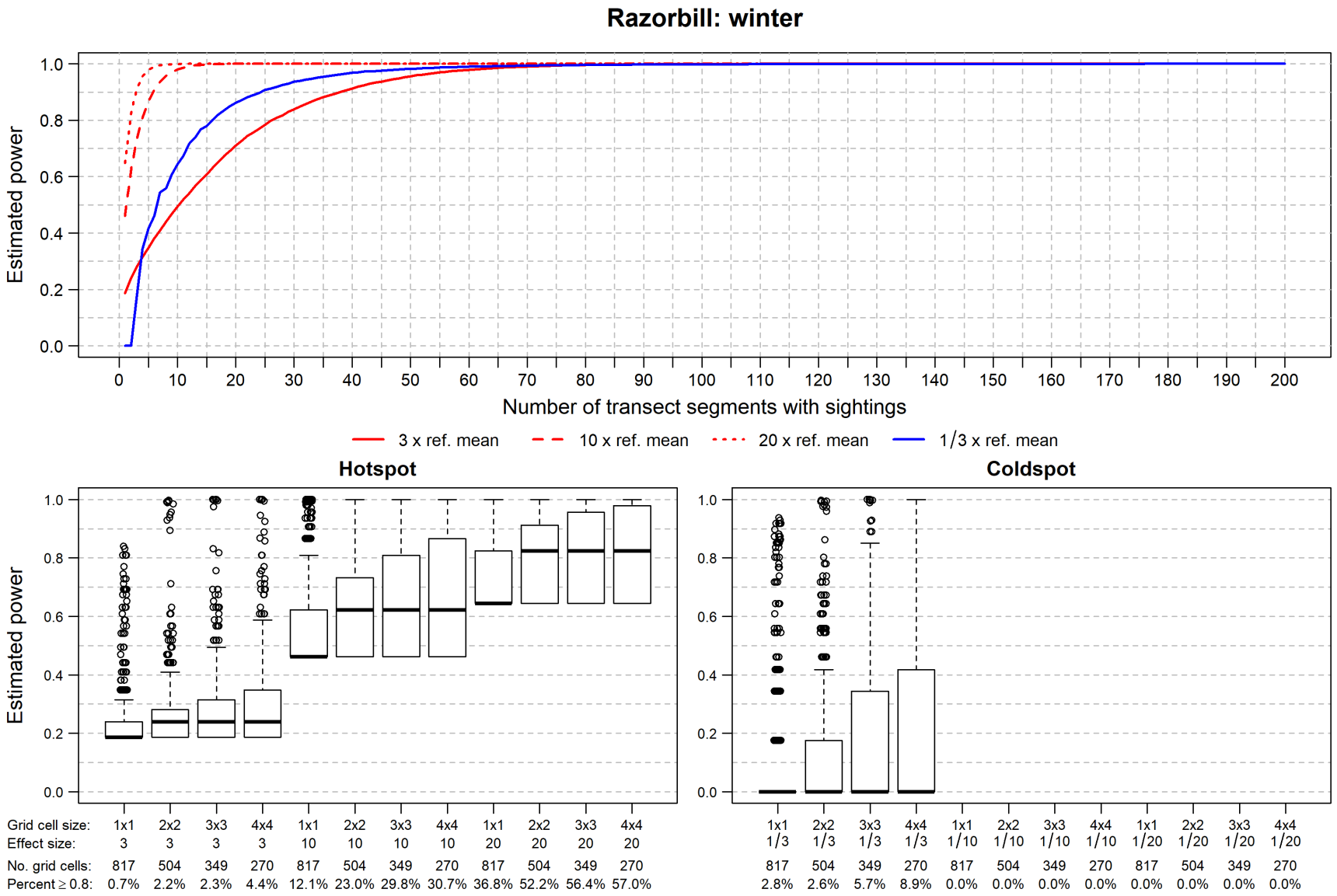

Figure D17. Power analysis results for Razorbill during winter based on the non-zero count model (type I error rate = 0.05)

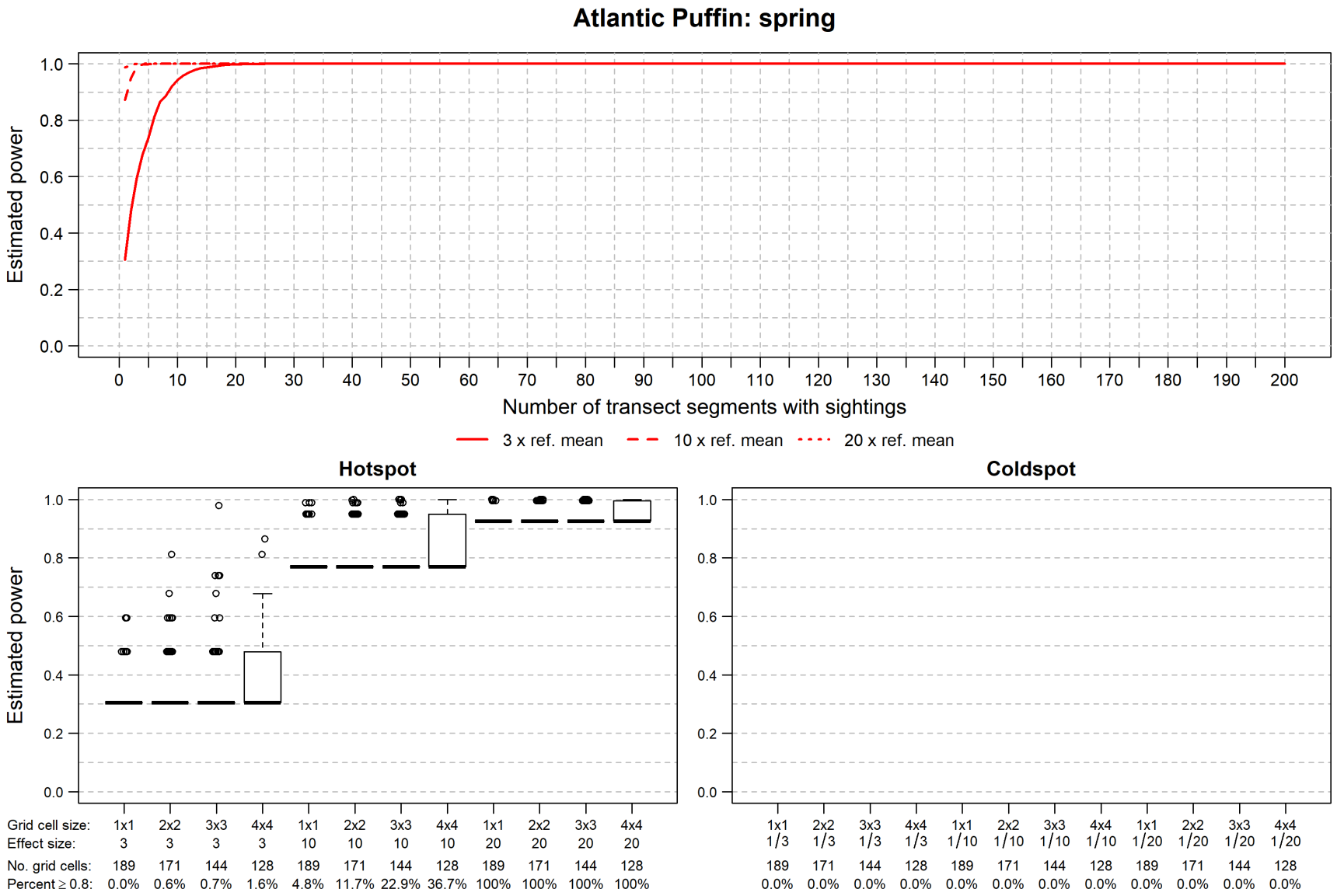

Figure D18. Power analysis results for Atlantic Puffin during spring based on the non-zero count model (type I error rate = 0.05)

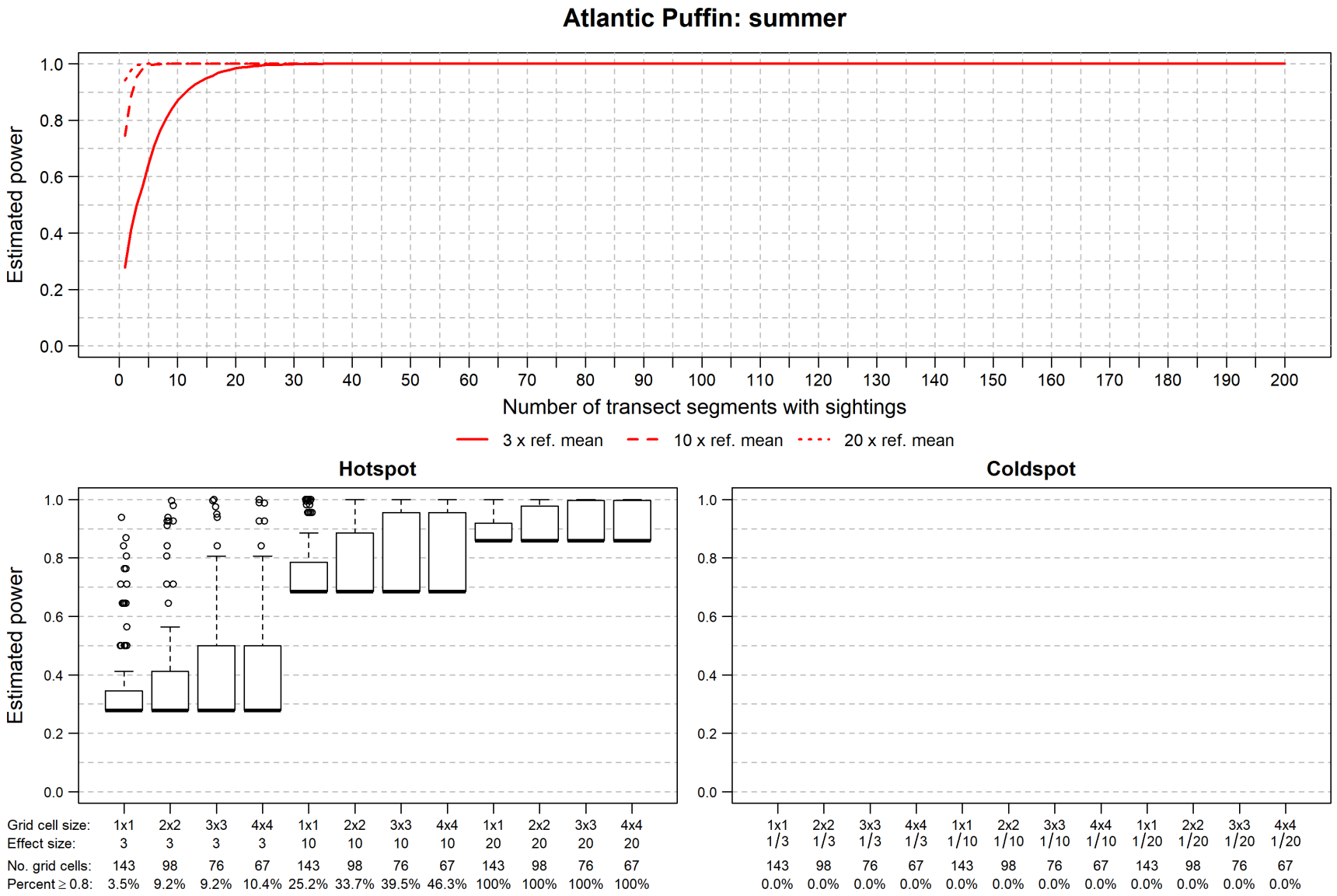

Figure D19. Power analysis results for Atlantic Puffin during summer based on the non-zero count model (type I error rate = 0.05)

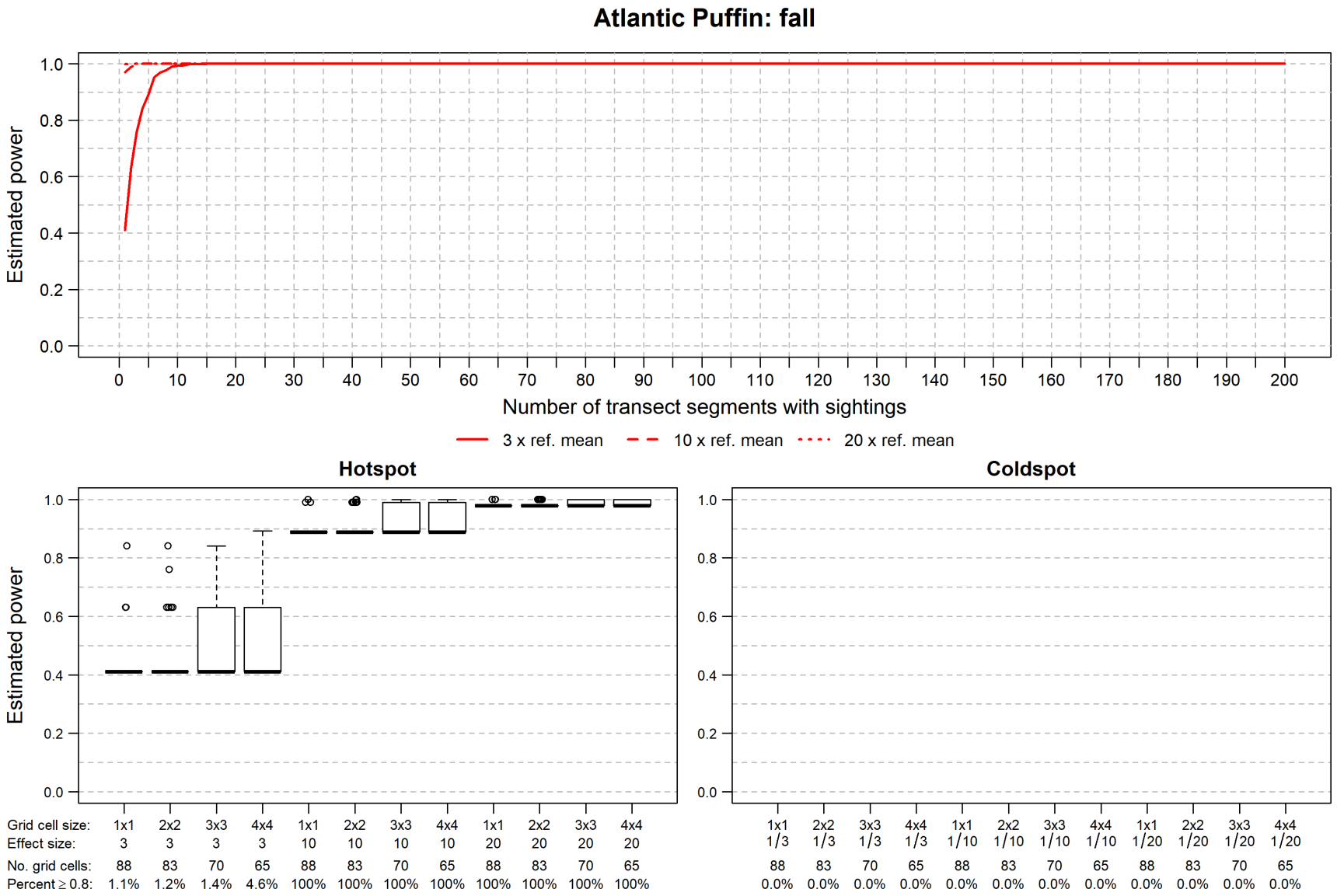

Figure D20. Power analysis results for Atlantic Puffin during fall based on the non-zero count model (type I error rate = 0.05)

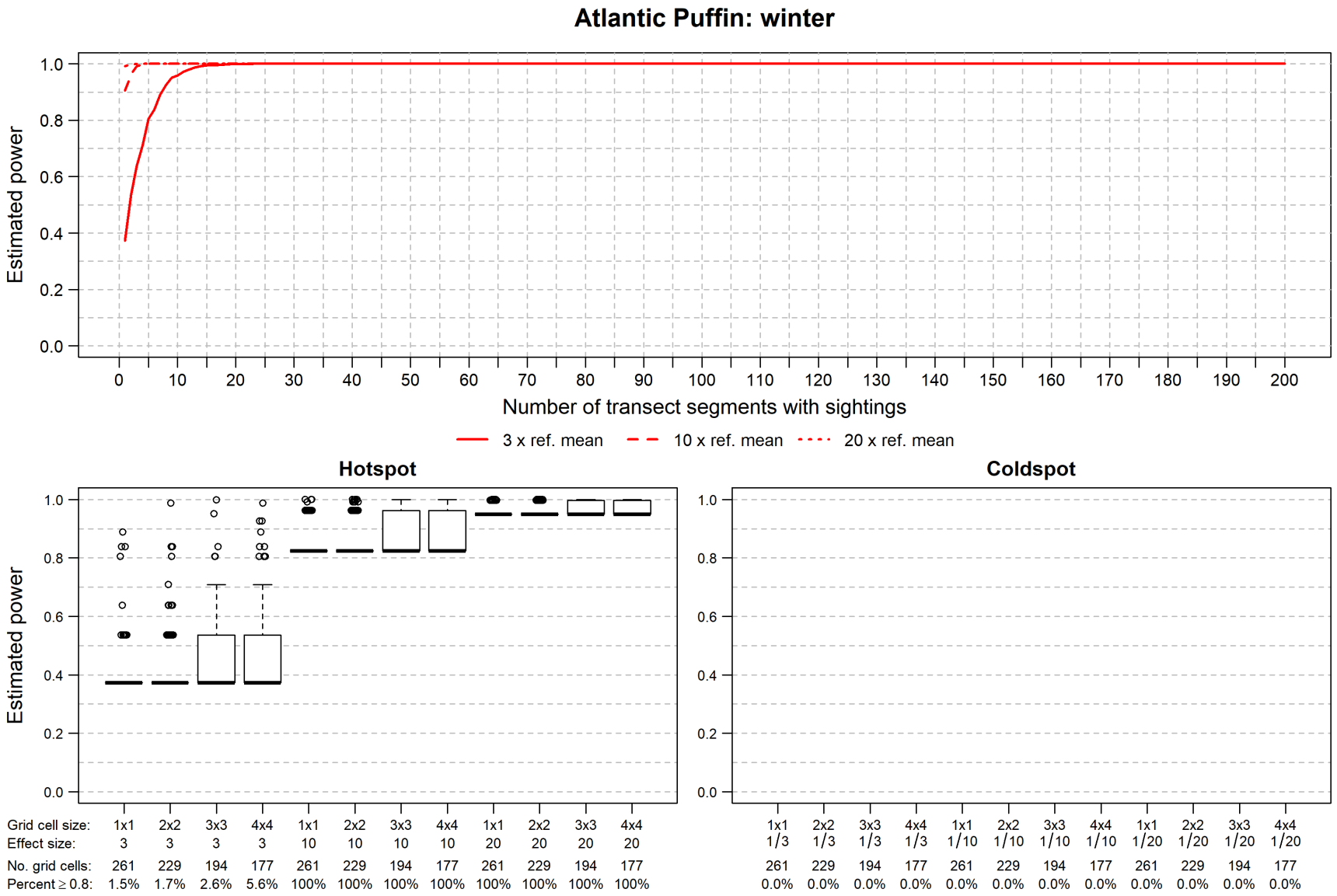

Figure D21. Power analysis results for Atlantic Puffin during winter based on the non-zero count model (type I error rate = 0.05)

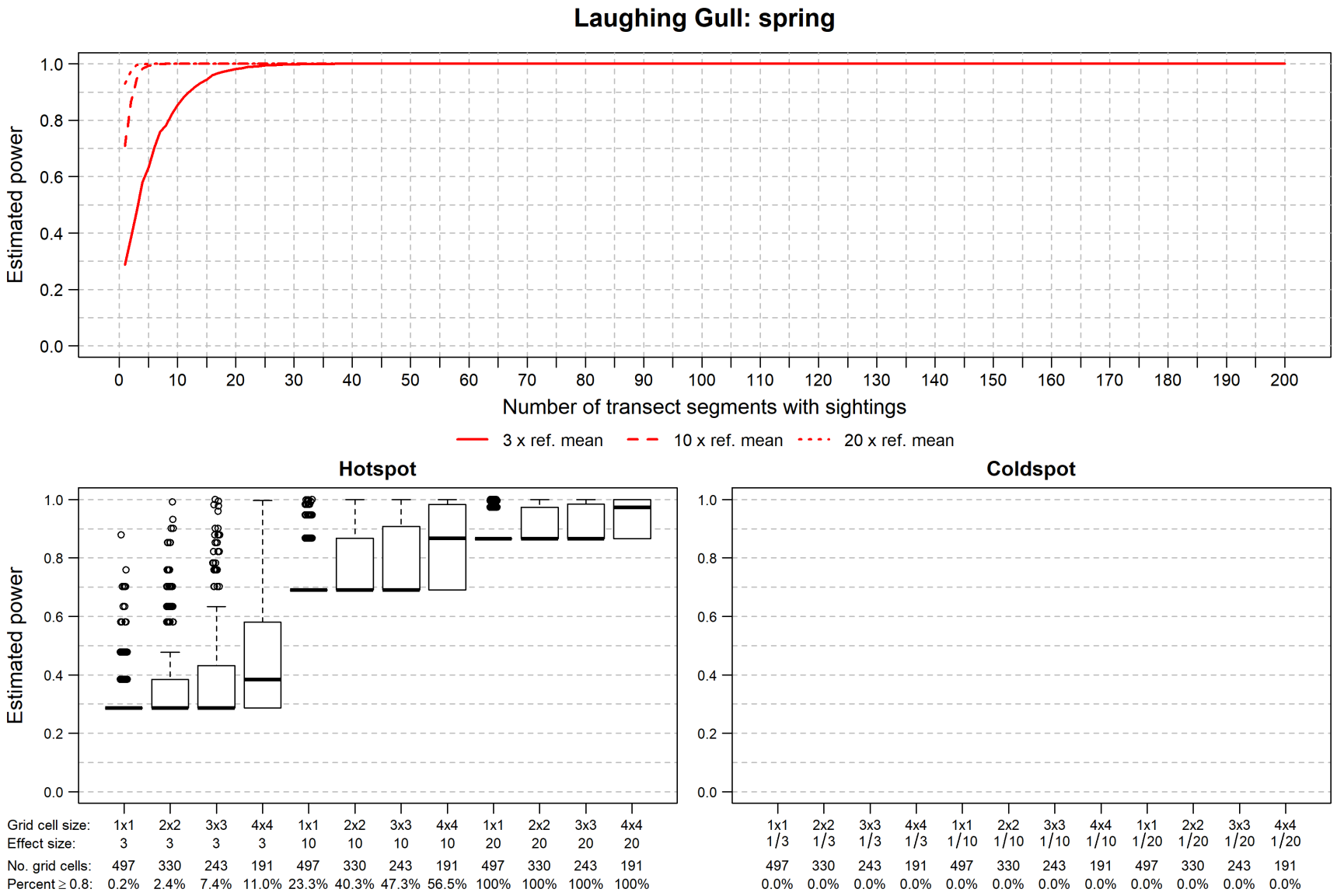

Figure D22. Power analysis results for Laughing Gull during spring based on the non-zero count model (type I error rate = 0.05)

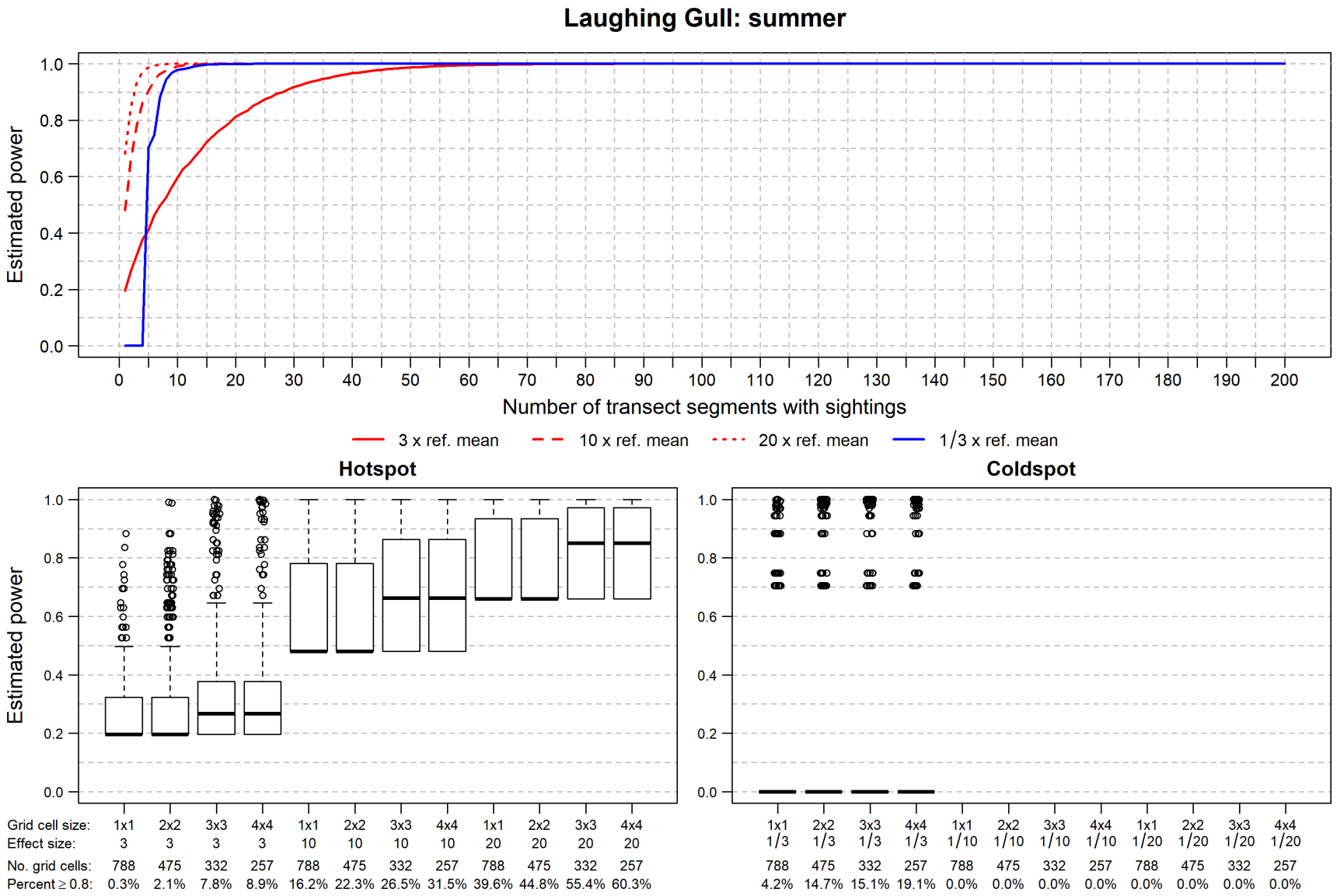

Figure D23. Power analysis results for Laughing Gull during summer based on the non-zero count model (type I error rate = 0.05)

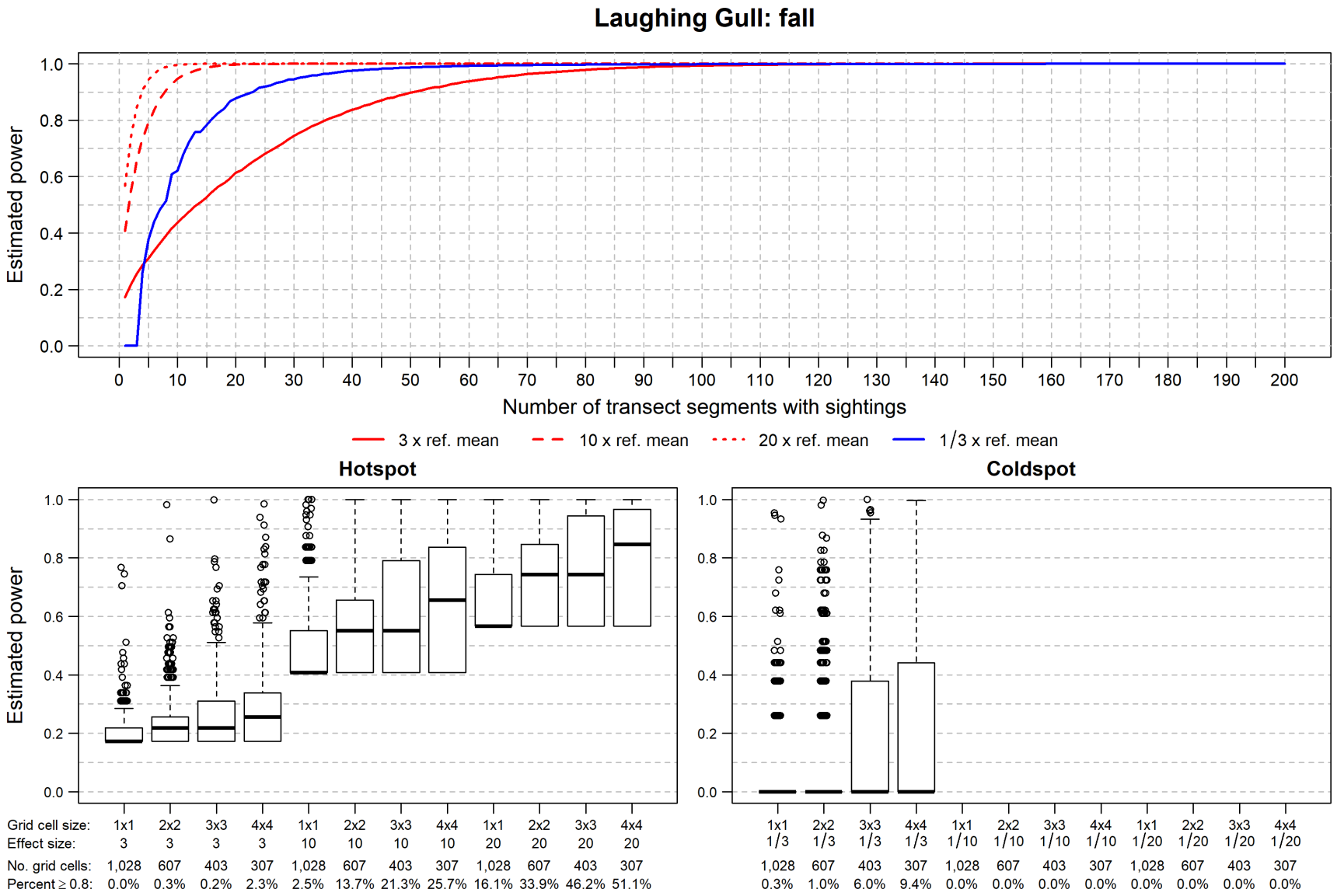

Figure D24. Power analysis results for Laughing Gull during fall based on the non-zero count model (type I error rate = 0.05)

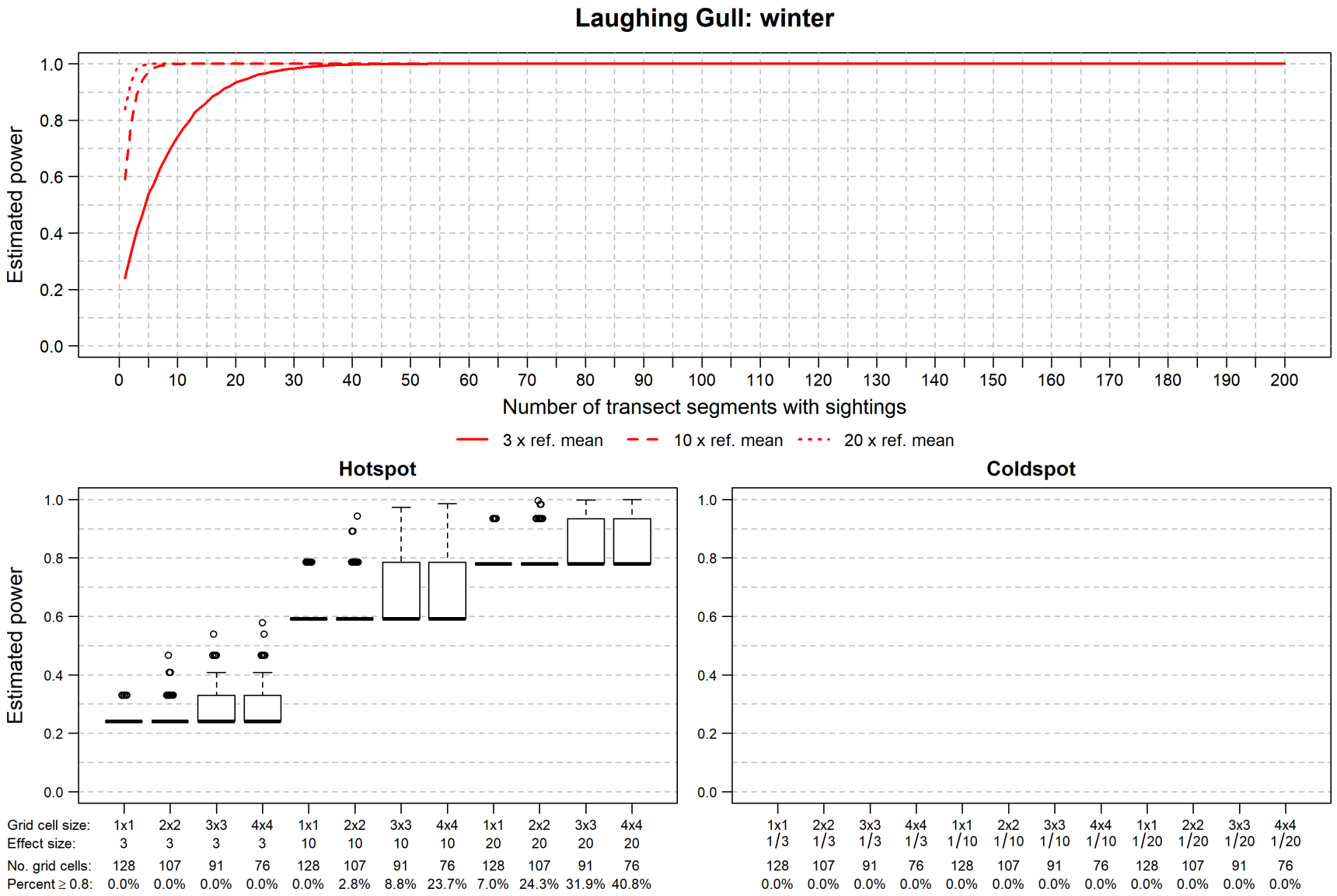

Figure D25. Power analysis results for Laughing Gull during winter based on the non-zero count model (type I error rate = 0.05)

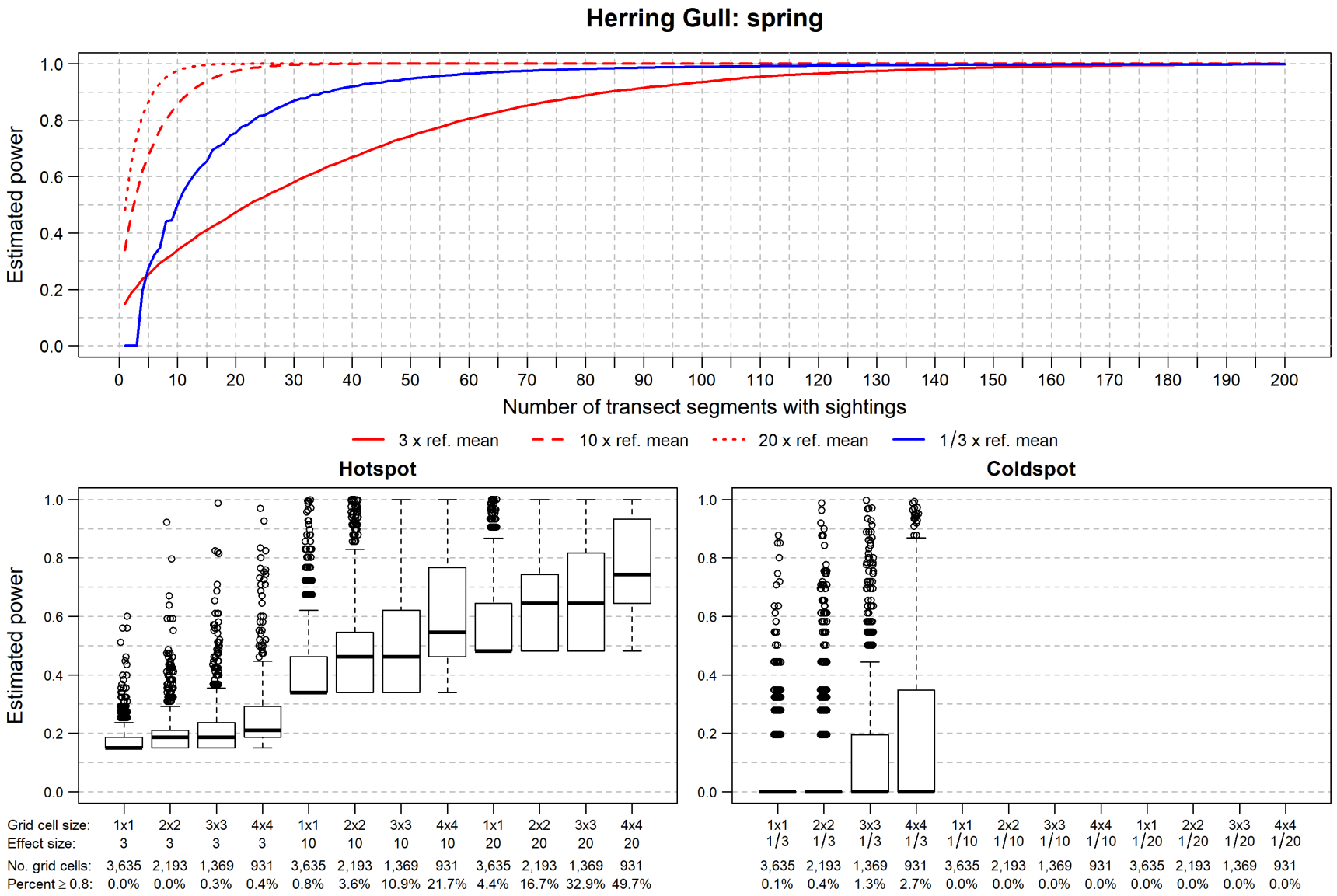

Figure D26. Power analysis results for Herring Gull during spring based on the non-zero count model (type I error rate = 0.05)

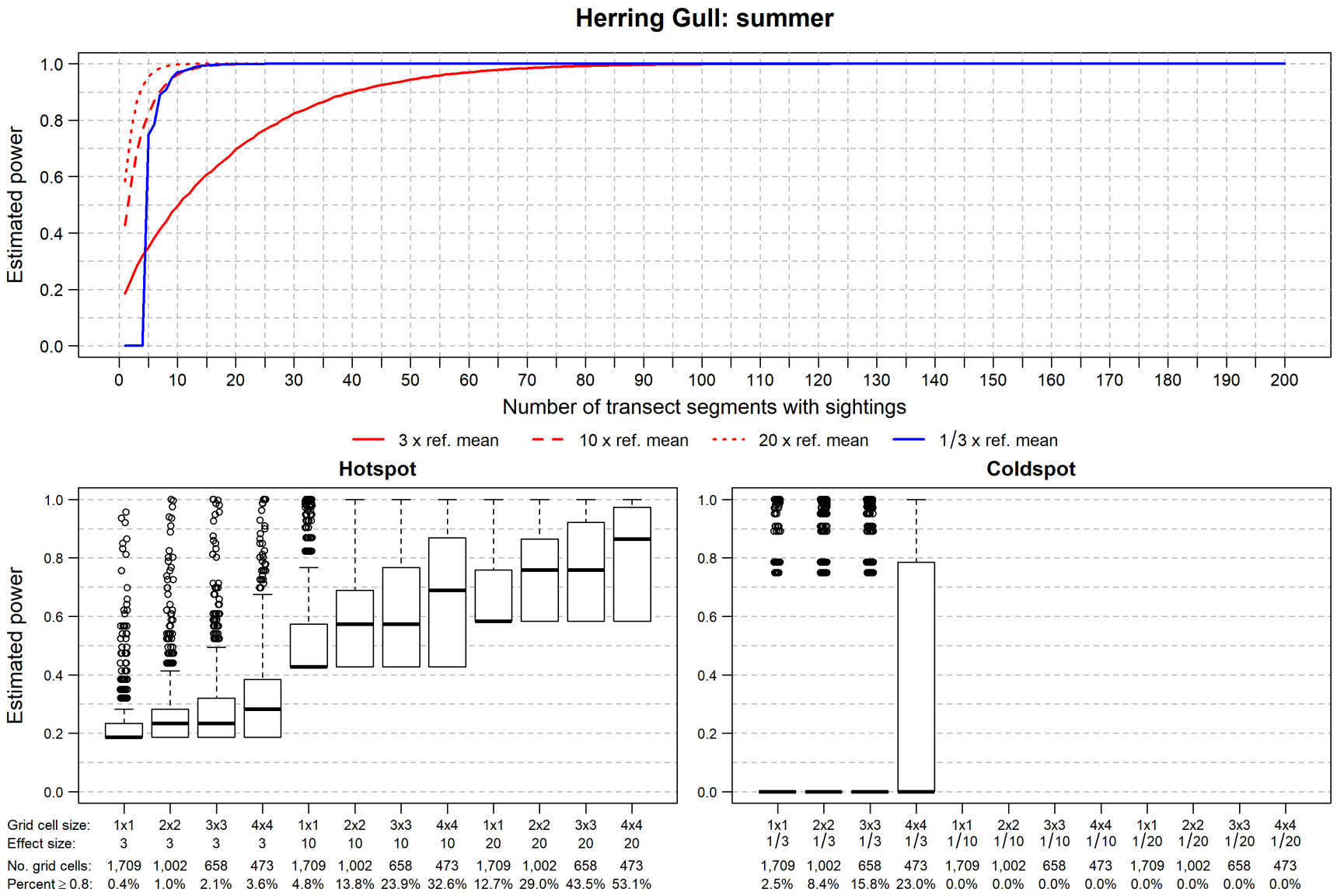

Figure D27. Power analysis results for Herring Gull during summer based on the non-zero count model (type I error rate = 0.05)

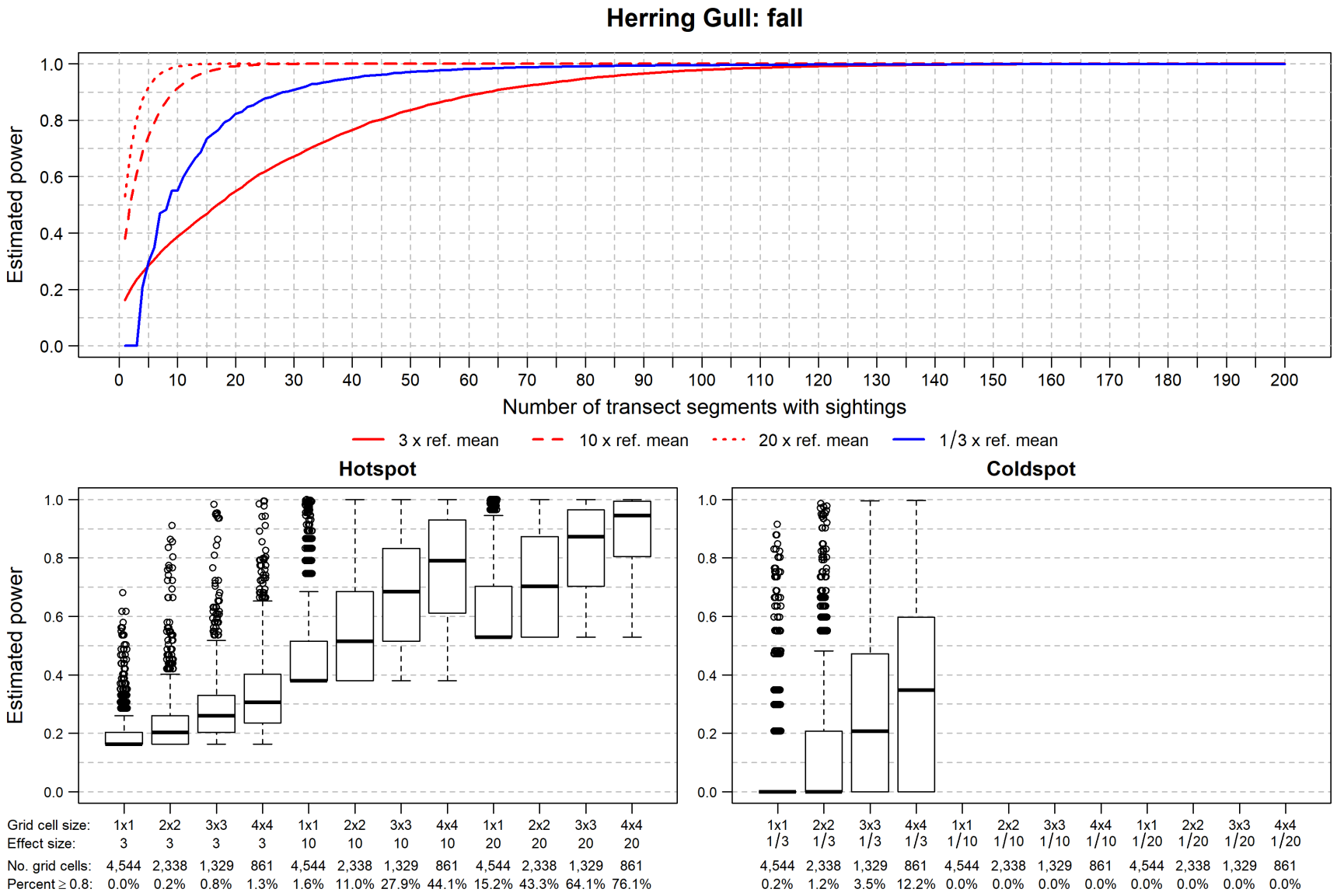

Figure D28. Power analysis results for Herring Gull during fall based on the non-zero count model (type I error rate = 0.05)

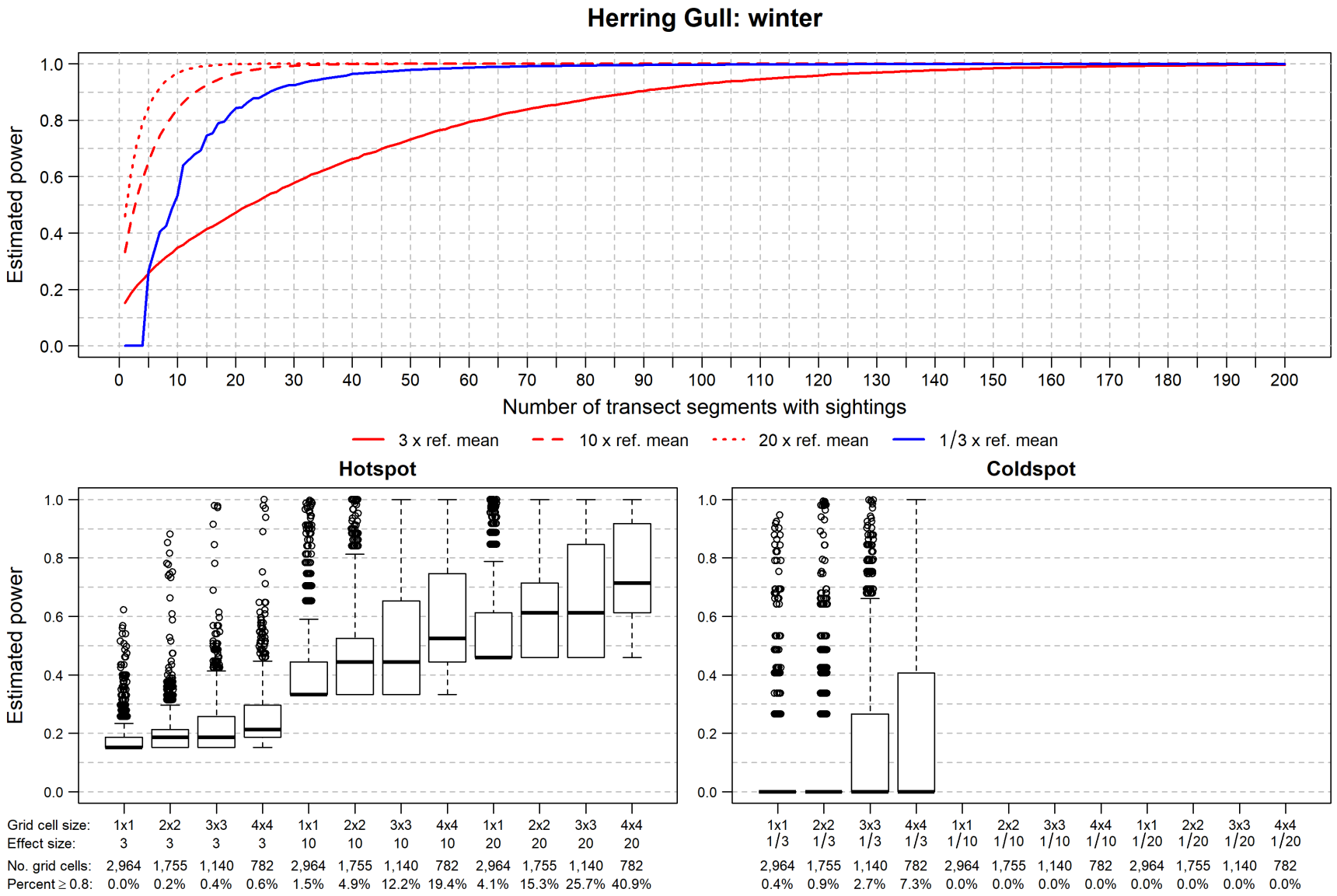

Figure D29. Power analysis results for Herring Gull during winter based on the non-zero count model (type I error rate = 0.05)

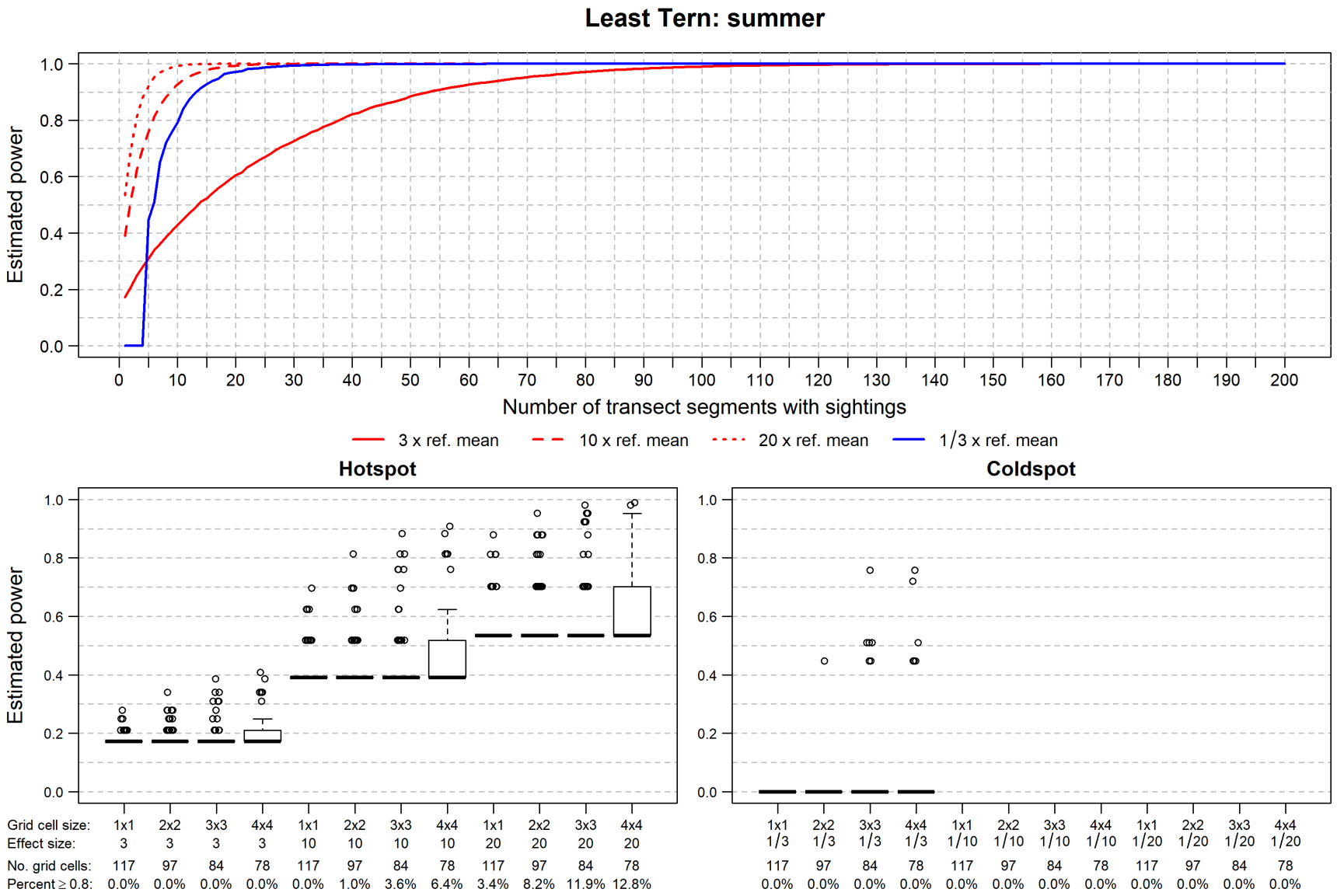

Figure D30. Power analysis results for Least Tern during summer based on the non-zero count model (type I error rate = 0.05)

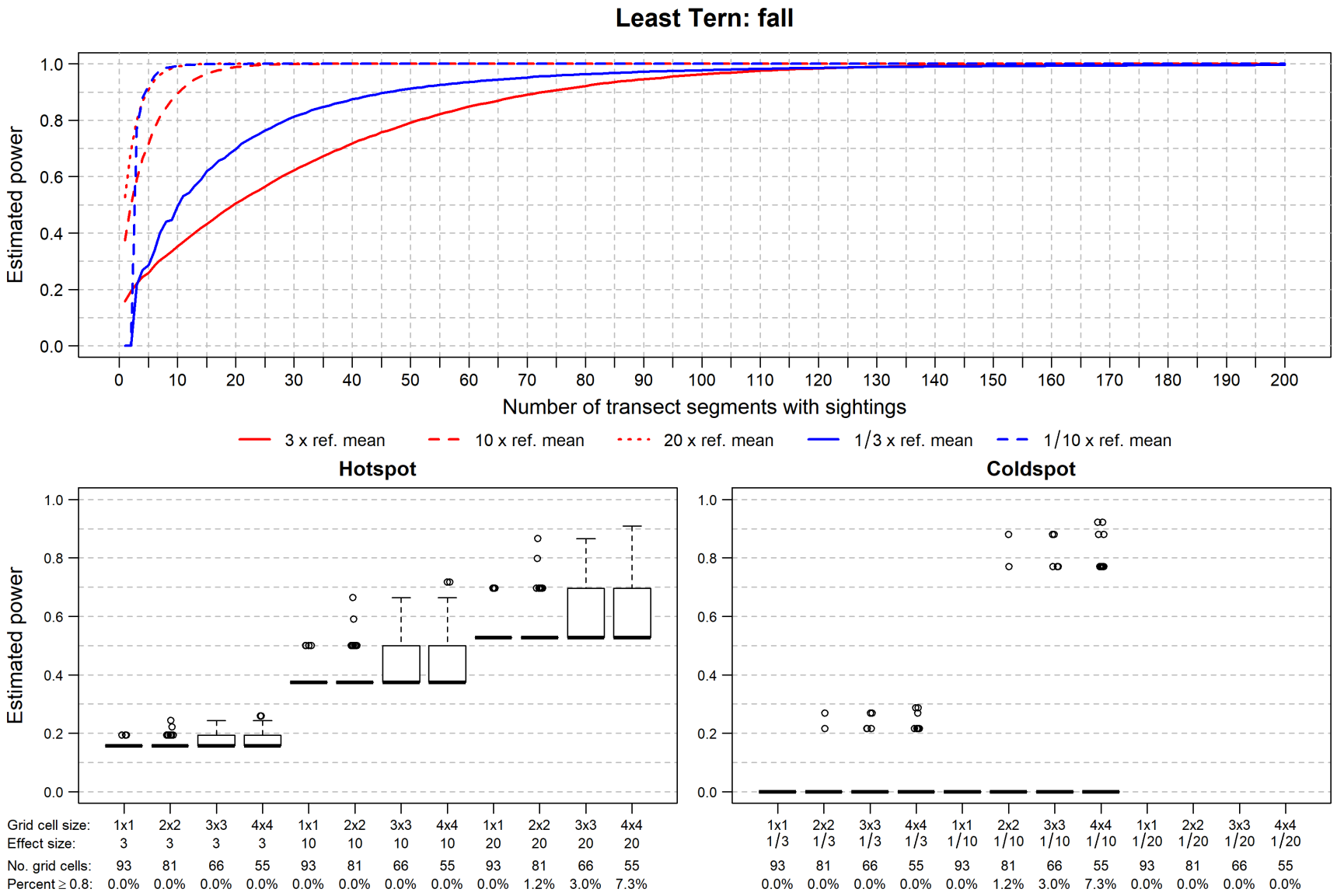

Figure D31. Power analysis results for Least Tern during fall based on the non-zero count model (type I error rate = 0.05)

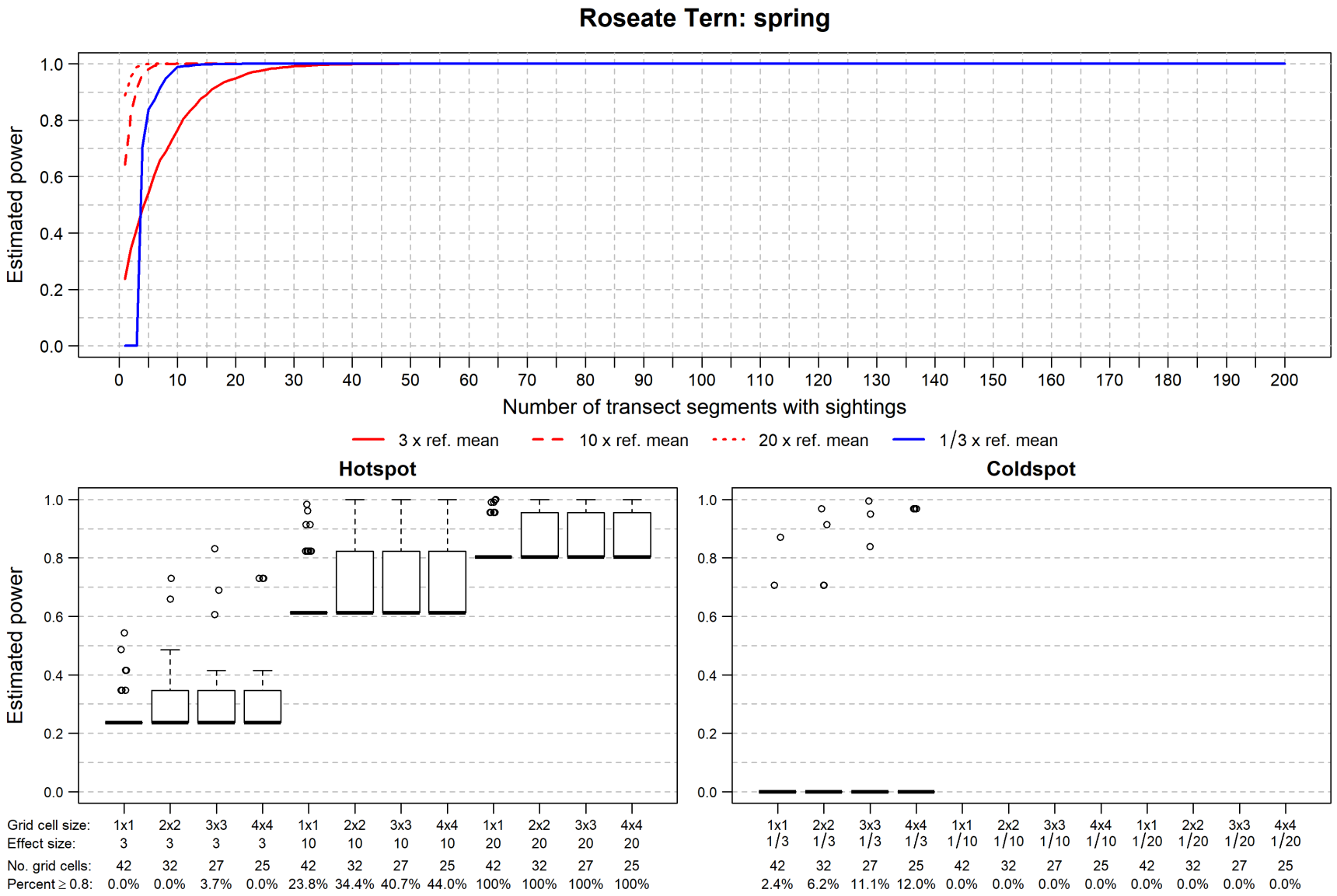

Figure D32. Power analysis results for Roseate Tern during spring based on the non-zero count model (type I error rate = 0.05)

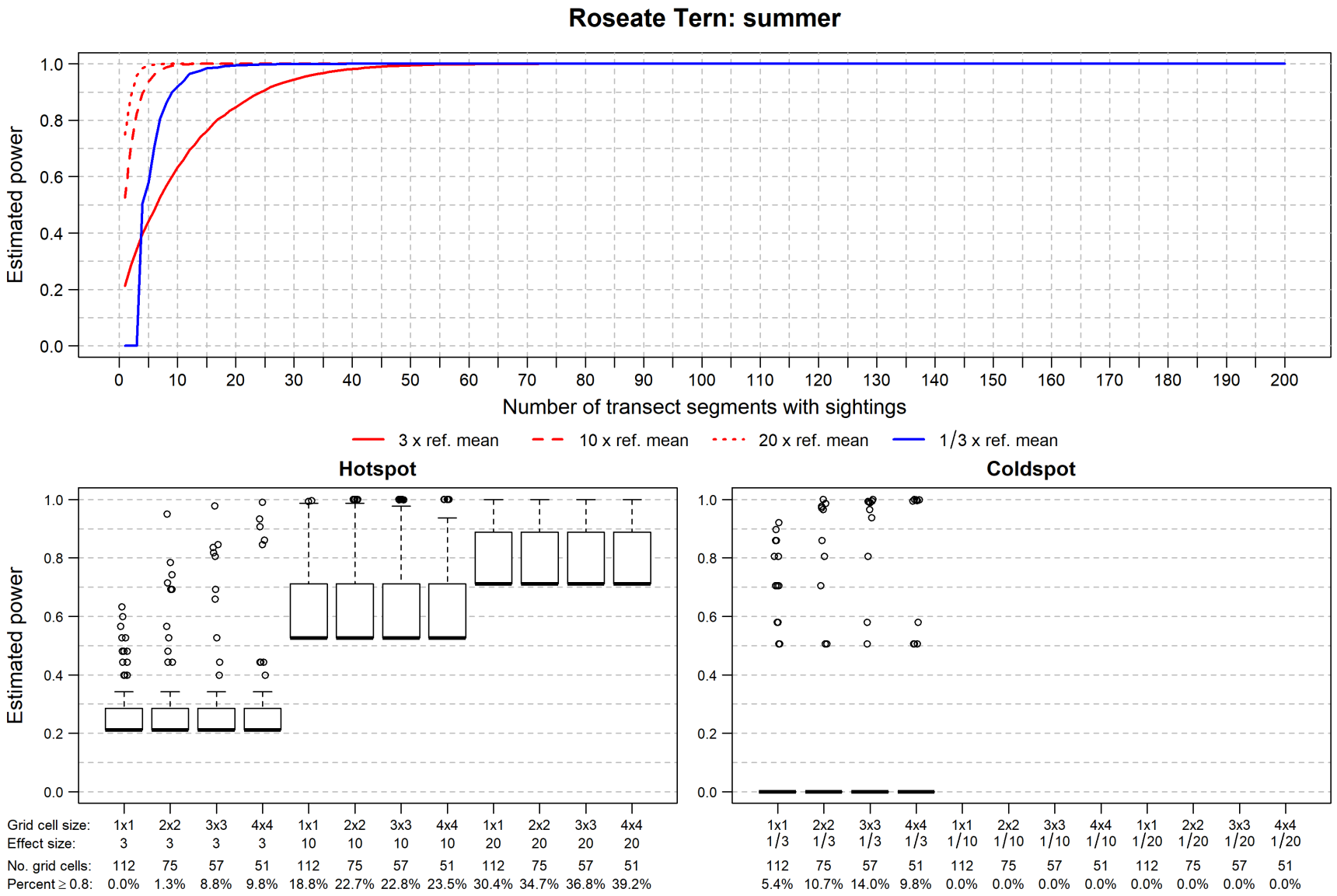

Figure D33. Power analysis results for Roseate Tern during summer based on the non-zero count model (type I error rate = 0.05)

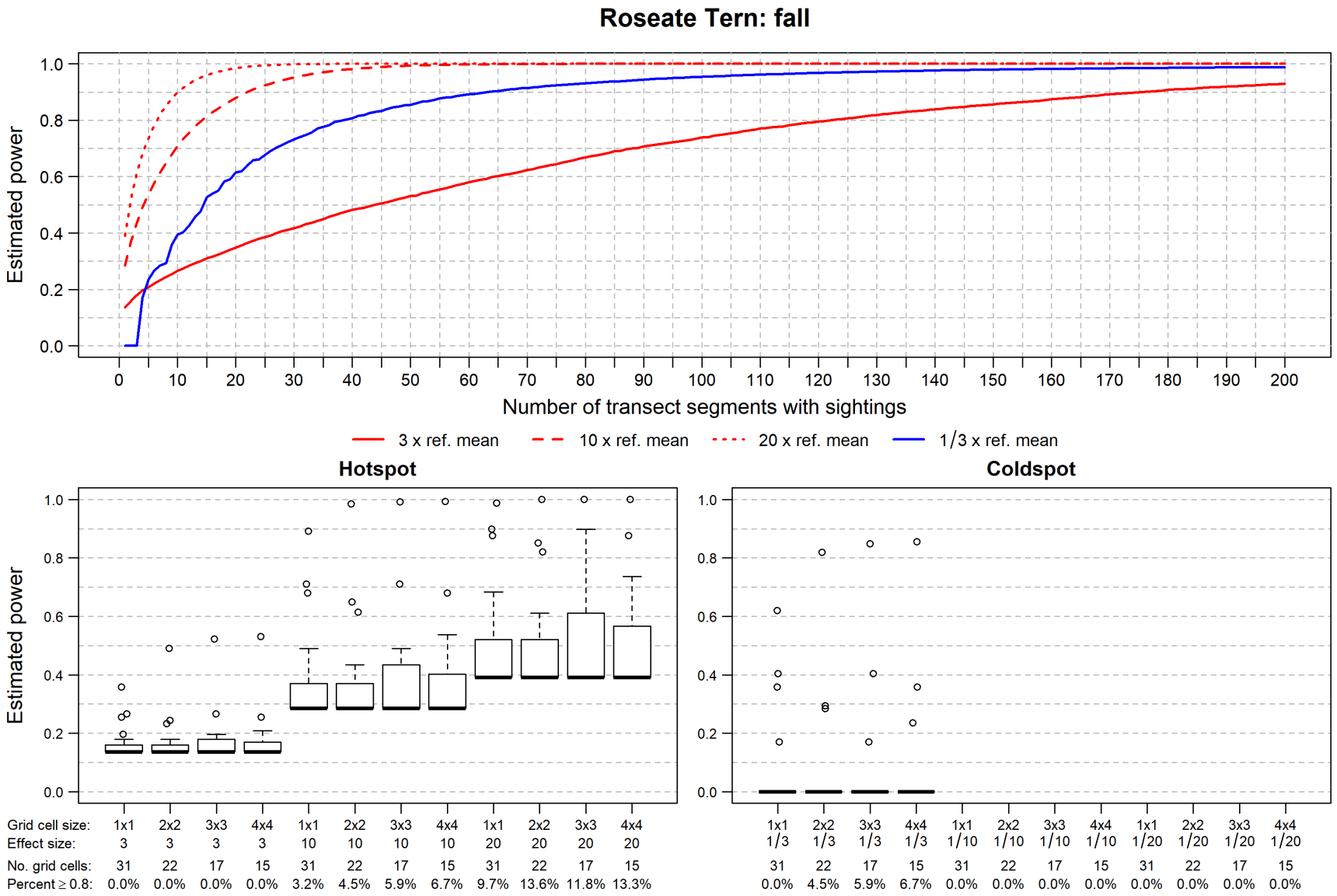

Figure D34. Power analysis results for Roseate Tern during fall based on the non-zero count model (type I error rate = 0.05)

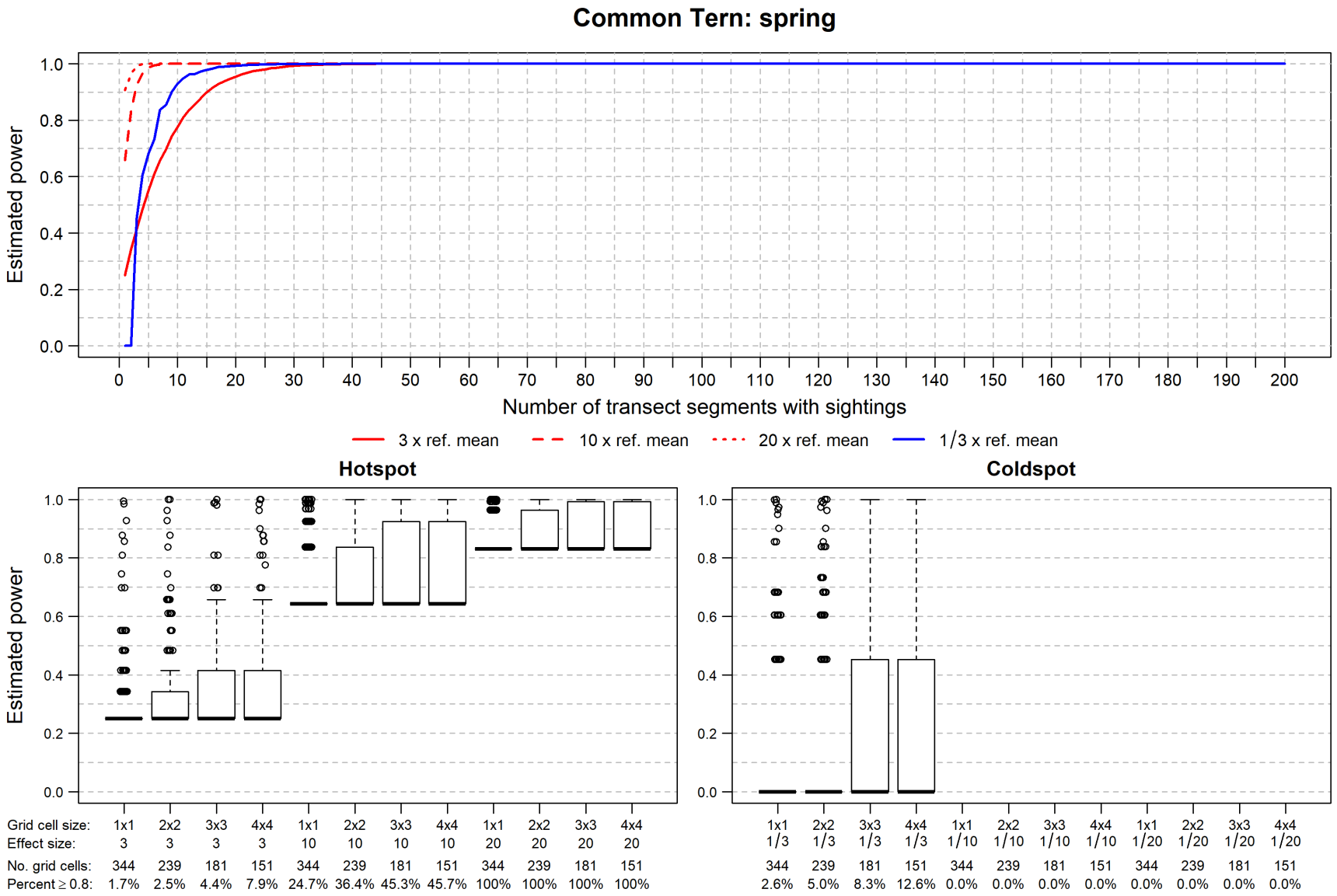

Figure D35. Power analysis results for Common Tern during spring based on the non-zero count model (type I error rate = 0.05)

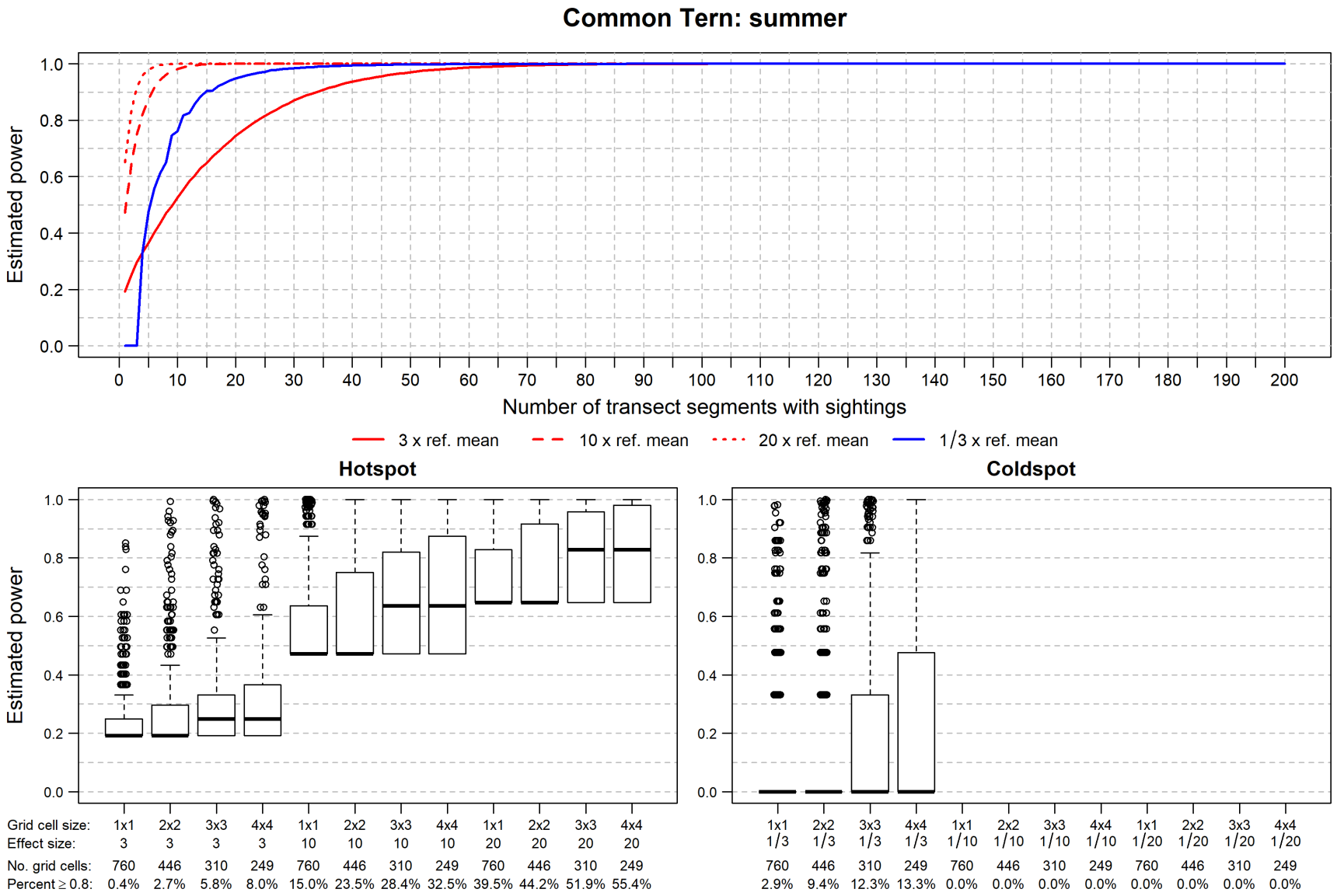

Figure D36. Power analysis results for Common Tern during summer based on the non-zero count model (type I error rate = 0.05)

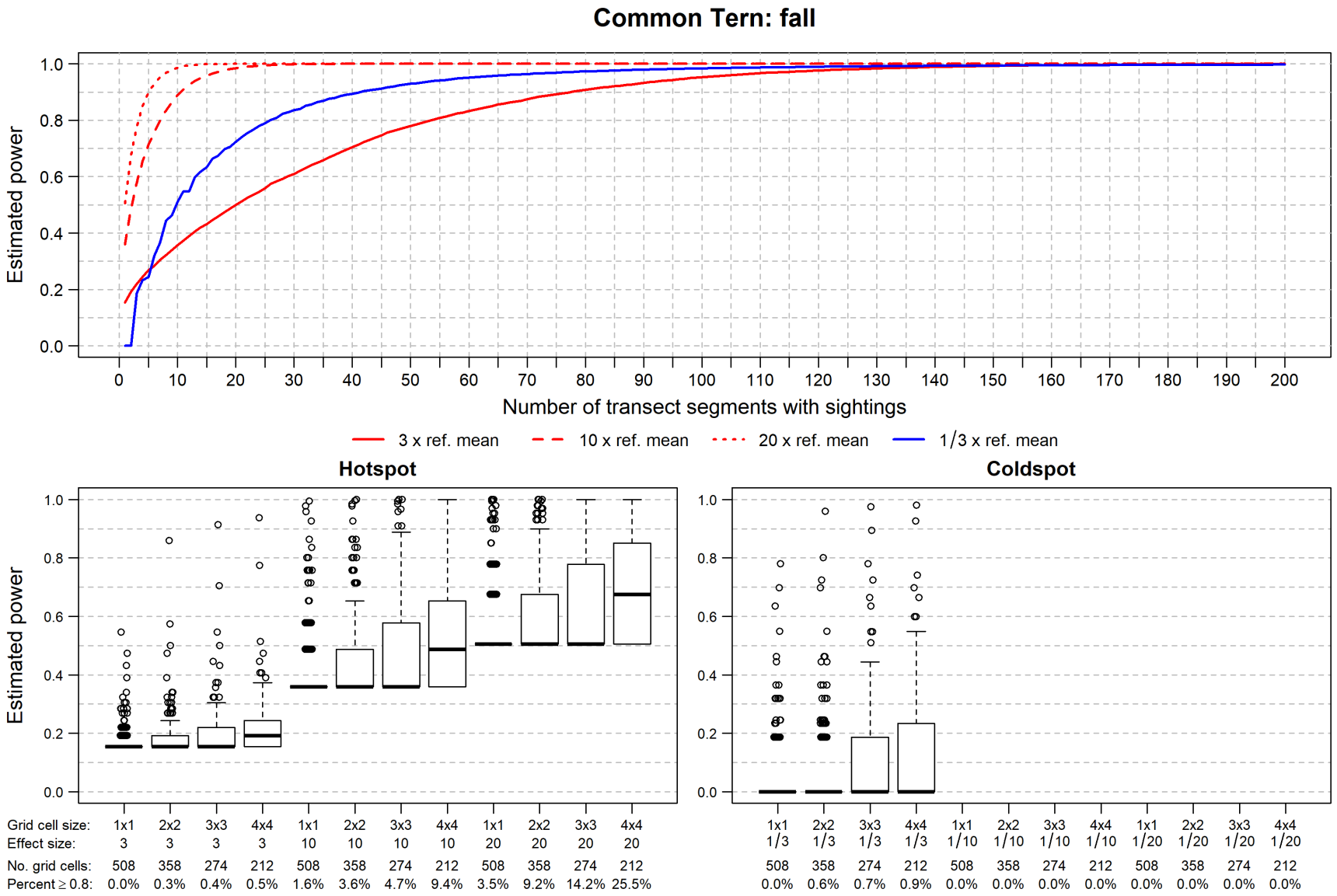

Figure D37. Power analysis results for Common Tern during fall based on the non-zero count model (type I error rate = 0.05)

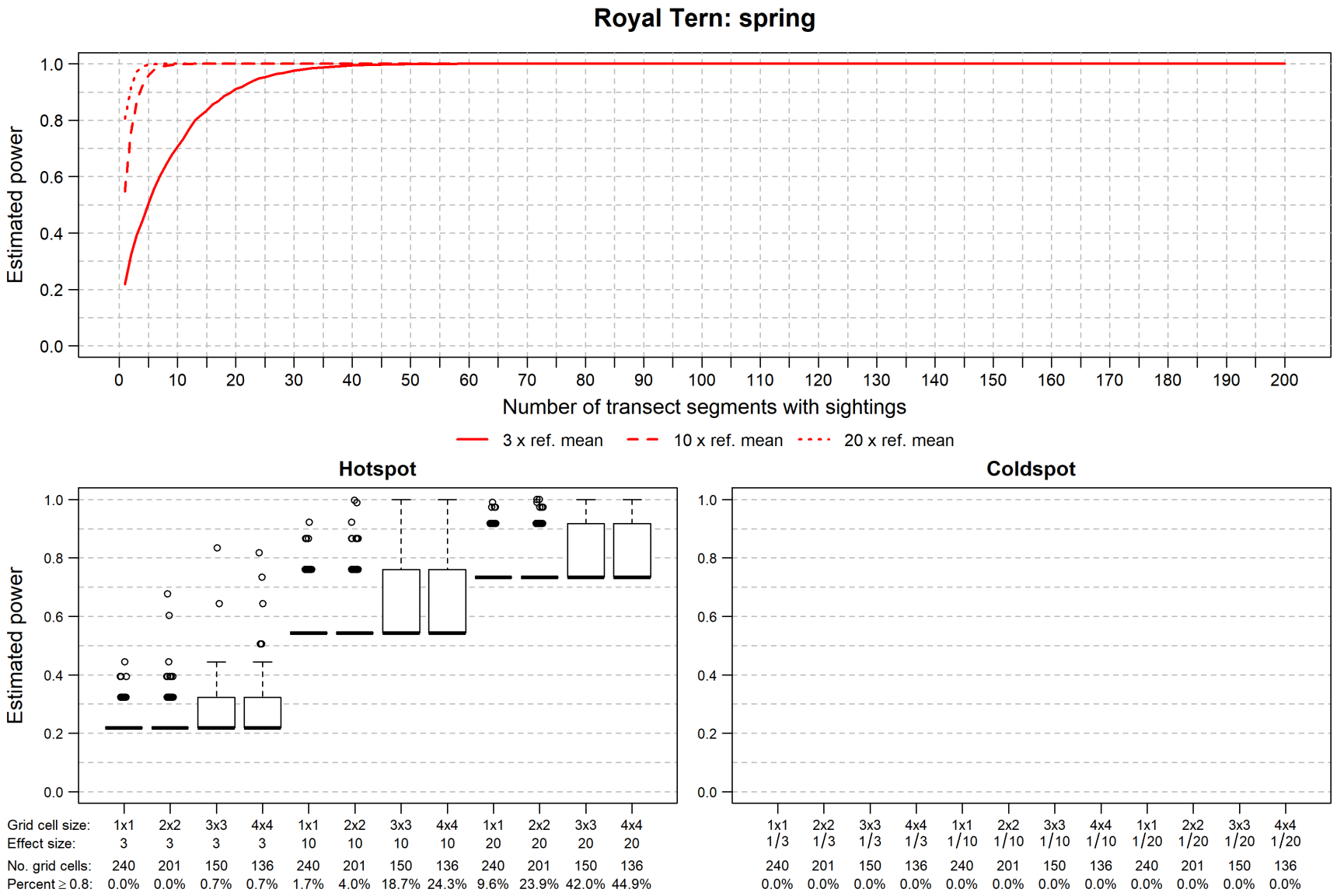

Figure D38. Power analysis results for Royal Tern during spring based on the non-zero count model (type I error rate = 0.05)

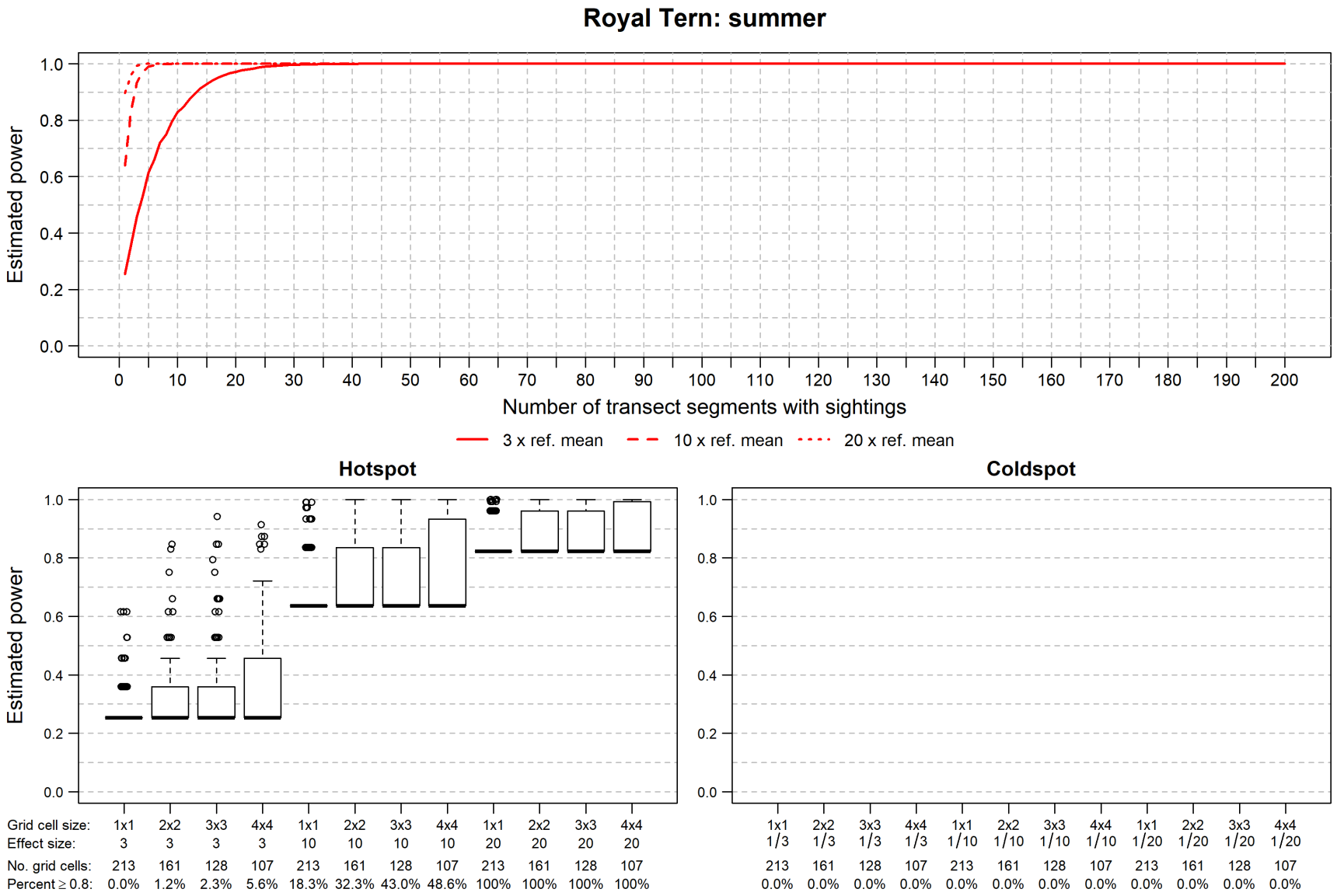

Figure D39. Power analysis results for Royal Tern during summer based on the non-zero count model (type I error rate = 0.05)

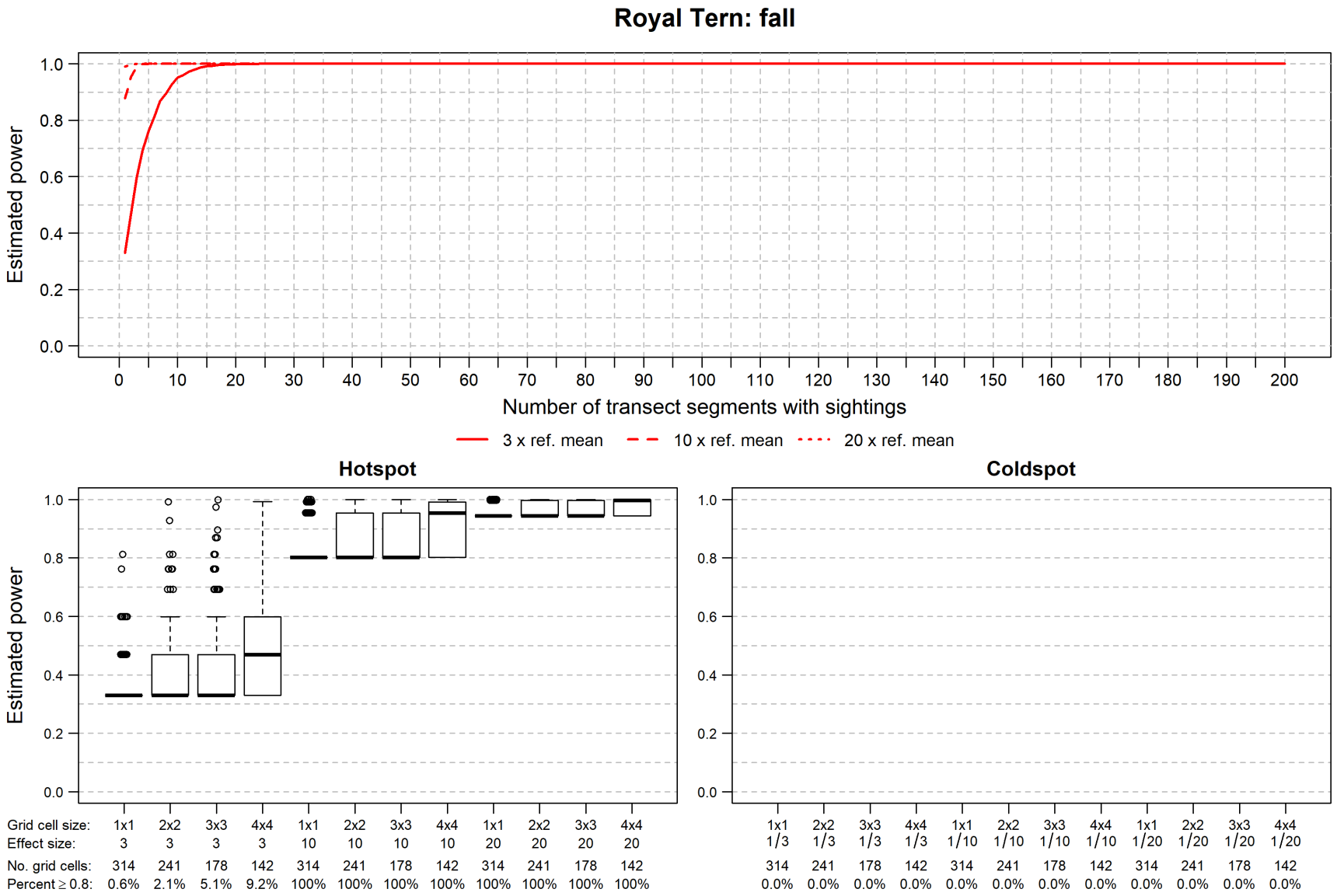

Figure D40. Power analysis results for Royal Tern during fall based on the non-zero count model (type I error rate = 0.05)

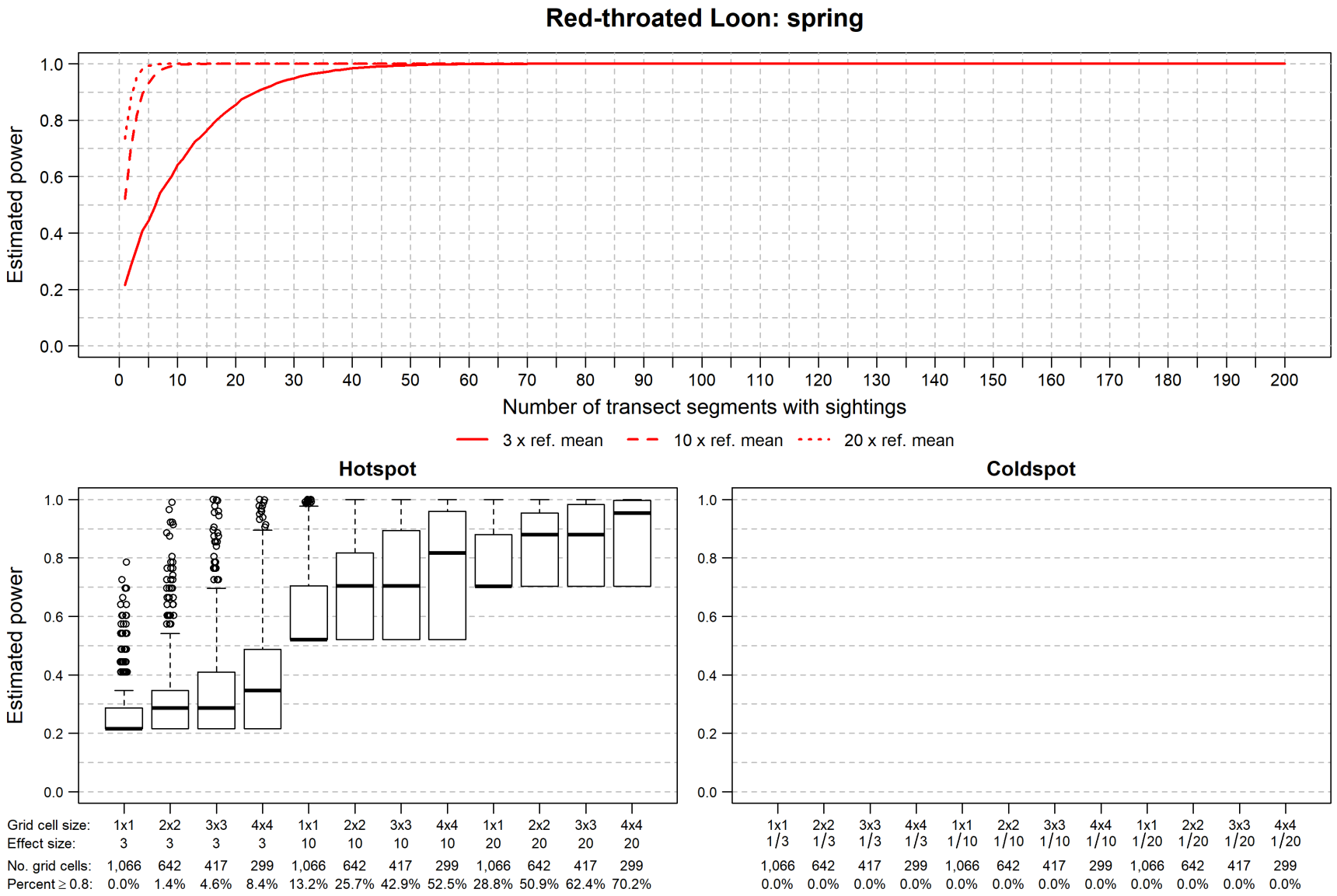

Figure D41. Power analysis results for Red-throated Loon during spring based on the non-zero count model (type I error rate = 0.05)

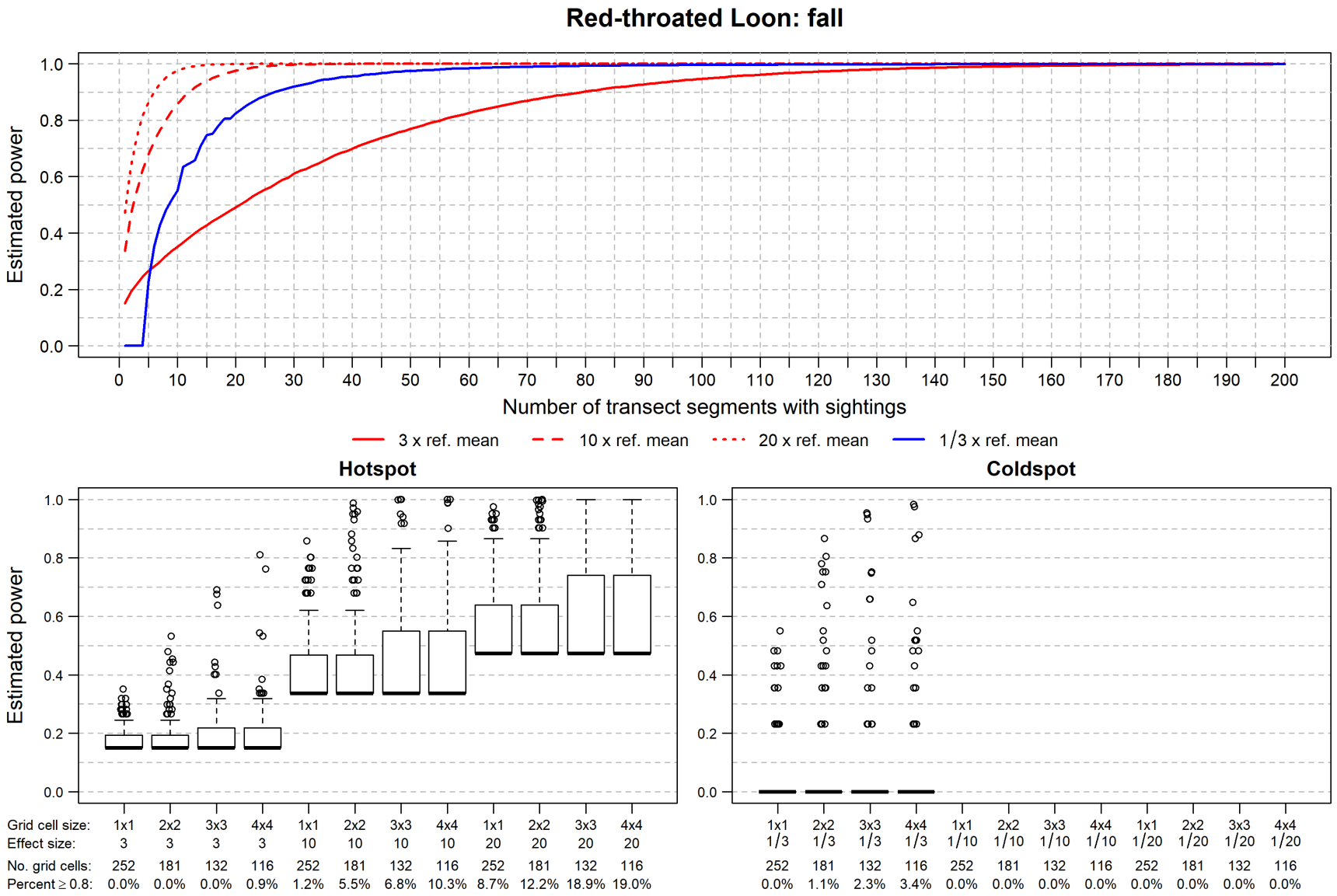

Figure D42. Power analysis results for Red-throated Loon during fall based on the non-zero count model (type I error rate = 0.05)

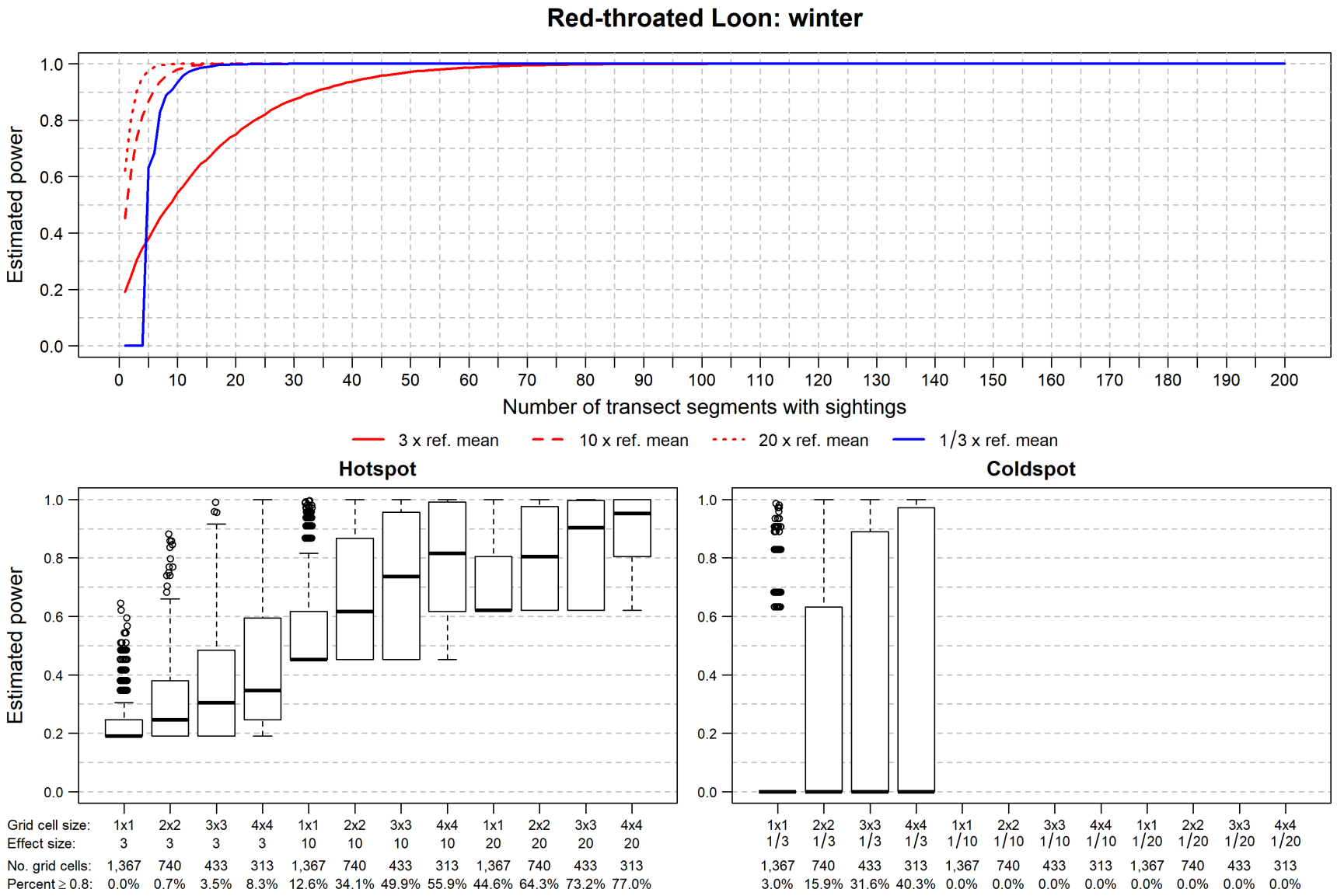

Figure D43. Power analysis results for Red-throated Loon during winter based on the non-zero count model (type I error rate = 0.05)

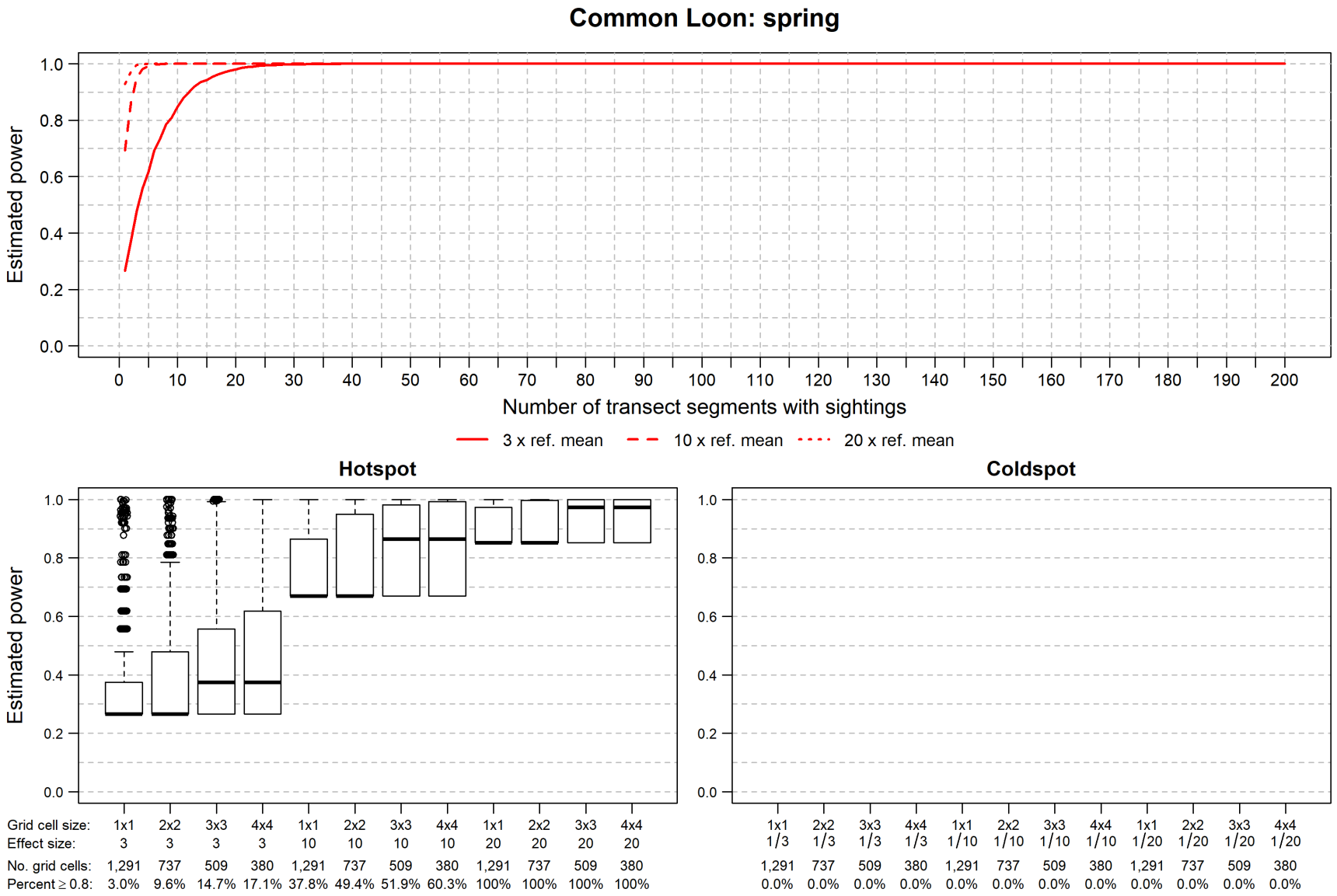

Figure D44. Power analysis results for Common Loon during spring based on the non-zero count model (type I error rate = 0.05)

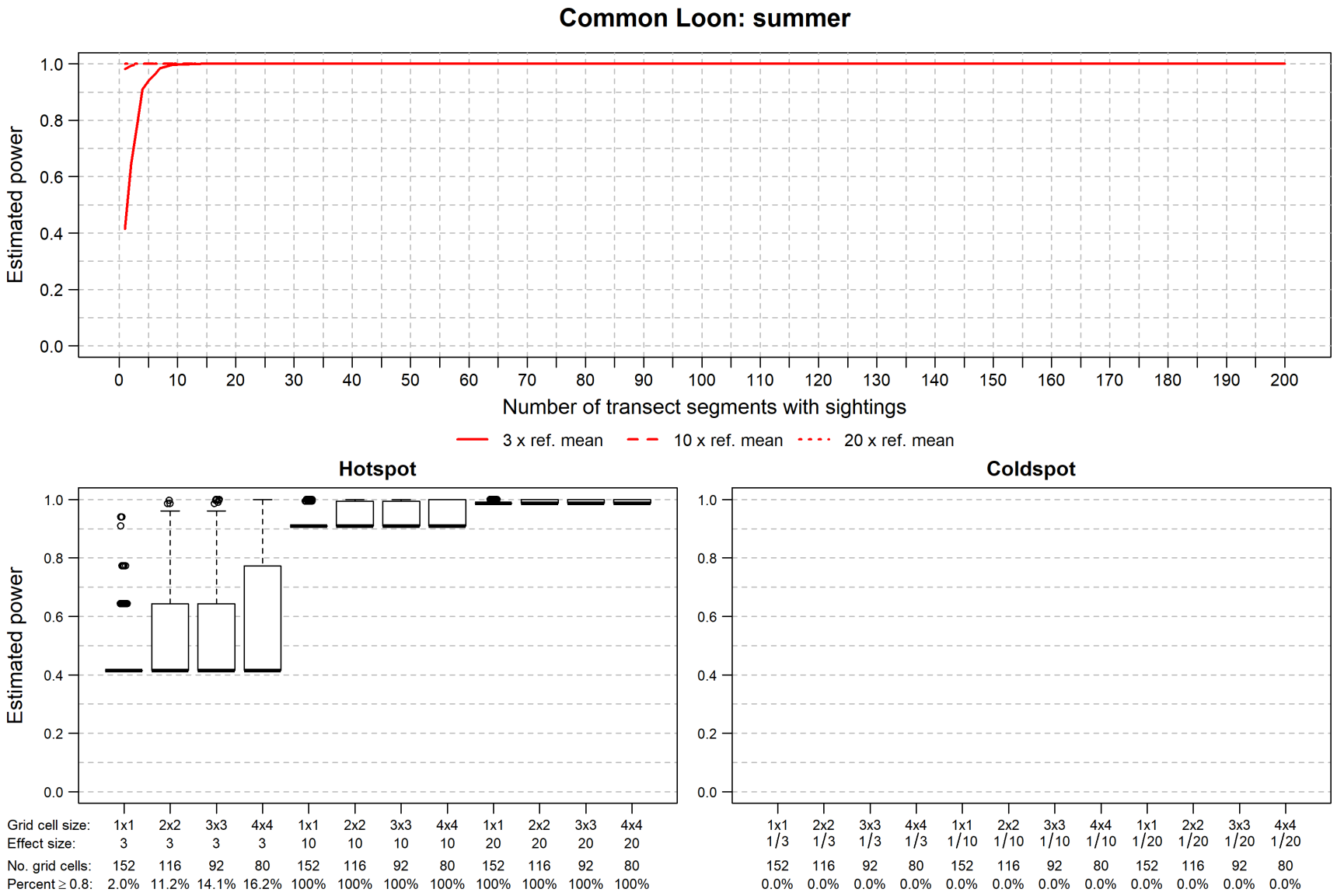

Figure D45. Power analysis results for Common Loon during summer based on the non-zero count model (type I error rate = 0.05)

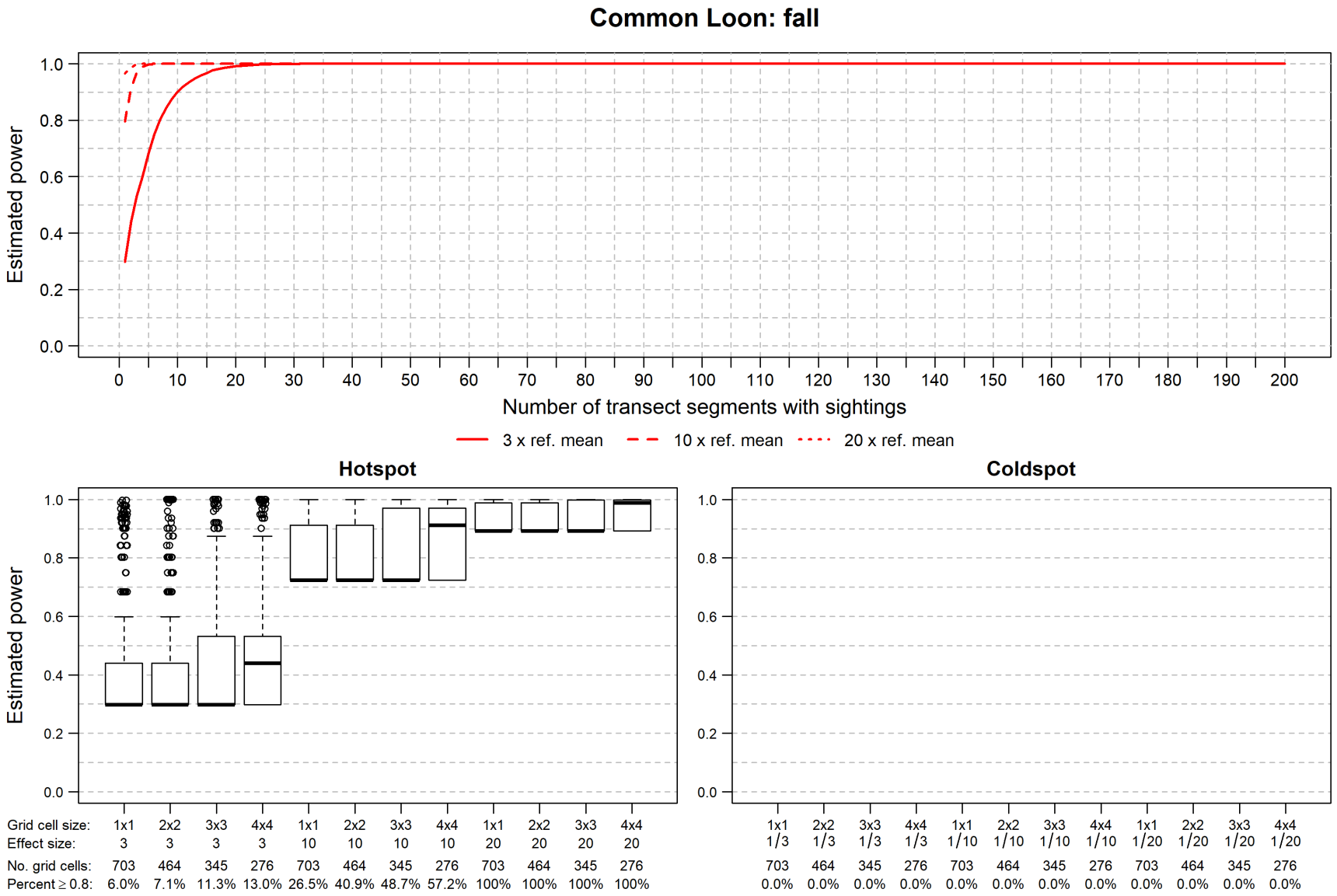

Figure D46. Power analysis results for Common Loon during fall based on the non-zero count model (type I error rate = 0.05)

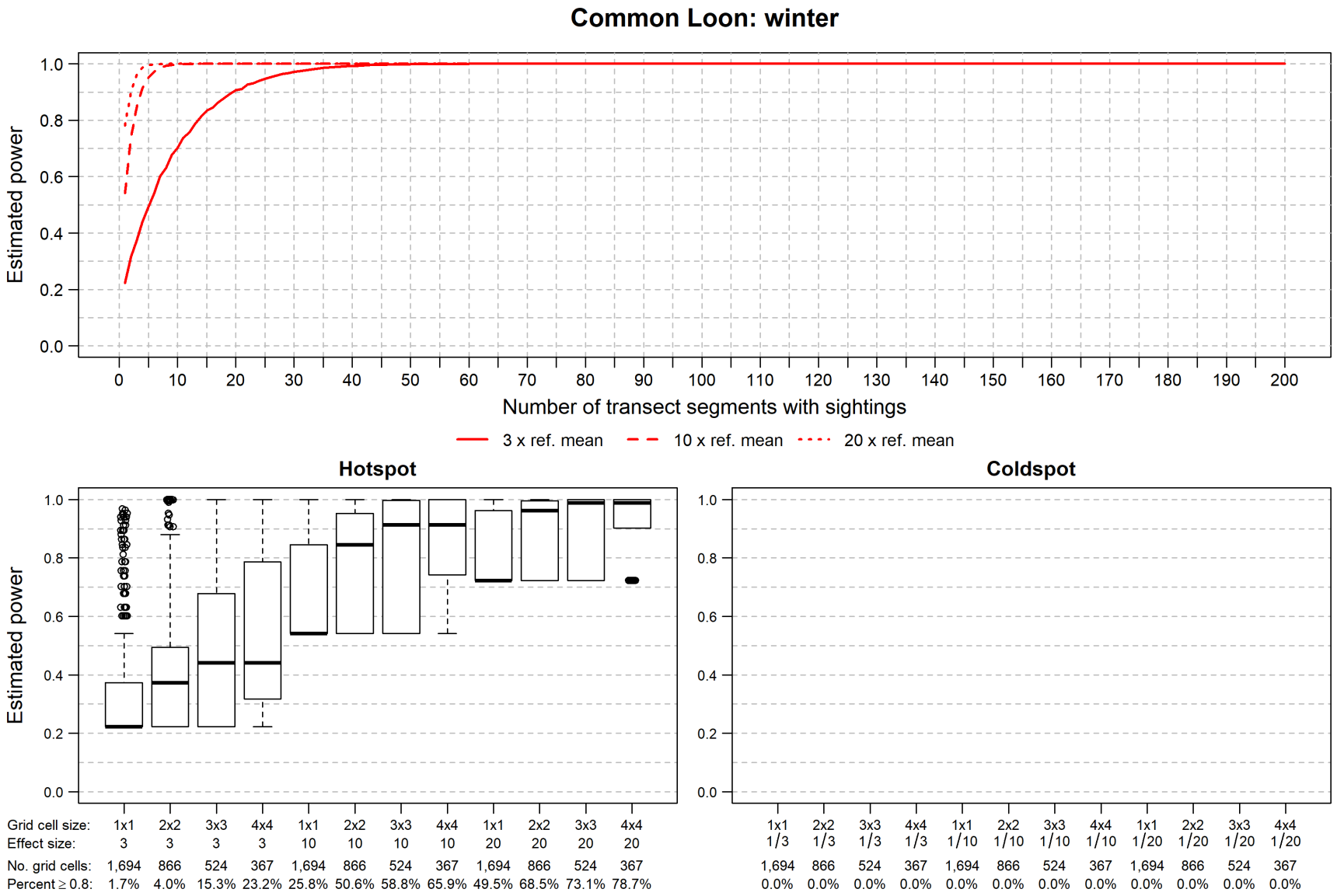

Figure D47. Power analysis results for Common Loon during winter based on the non-zero count model (type I error rate = 0.05)

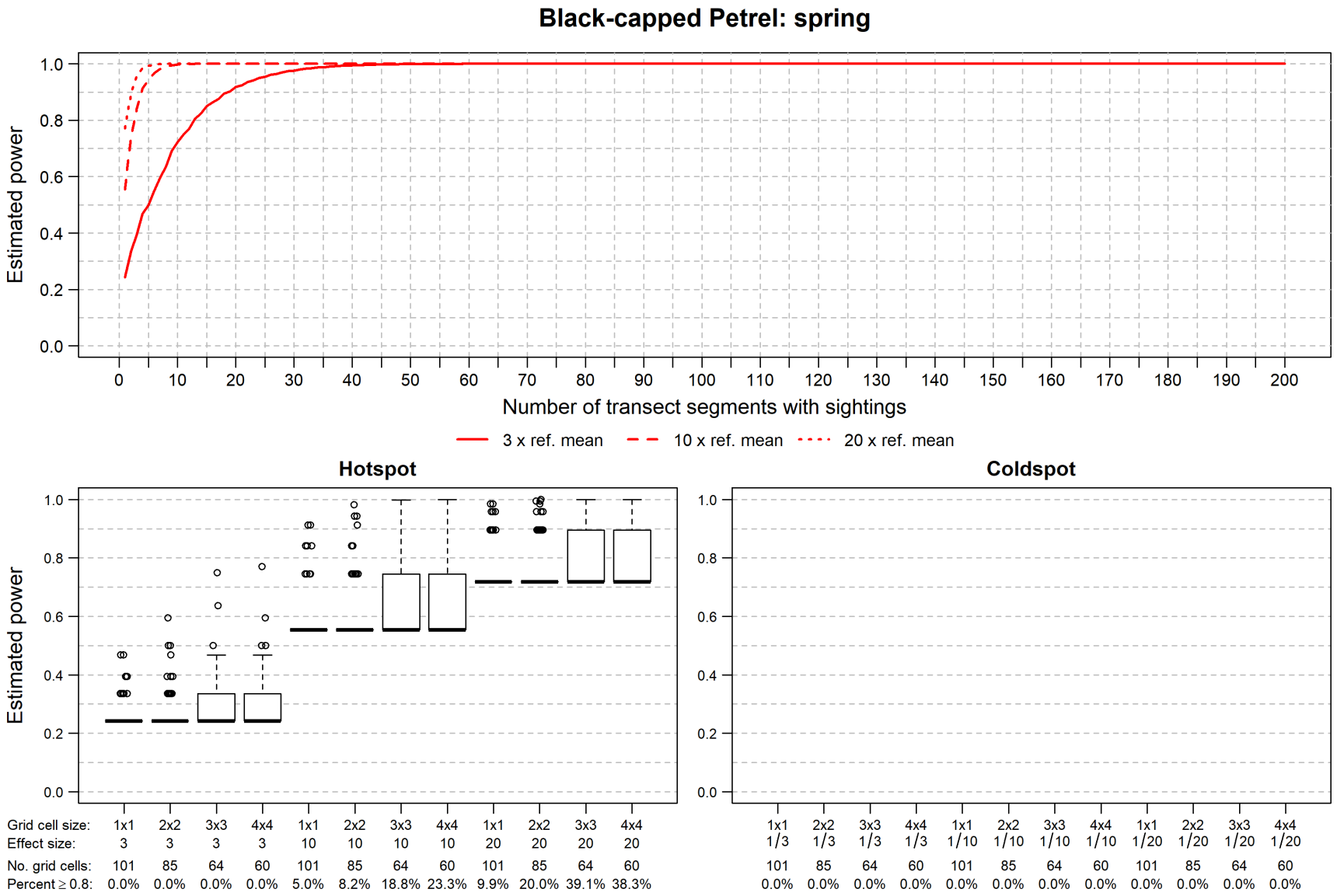

Figure D48. Power analysis results for Black-capped Petrel during spring based on the non-zero count model (type I error rate = 0.05)

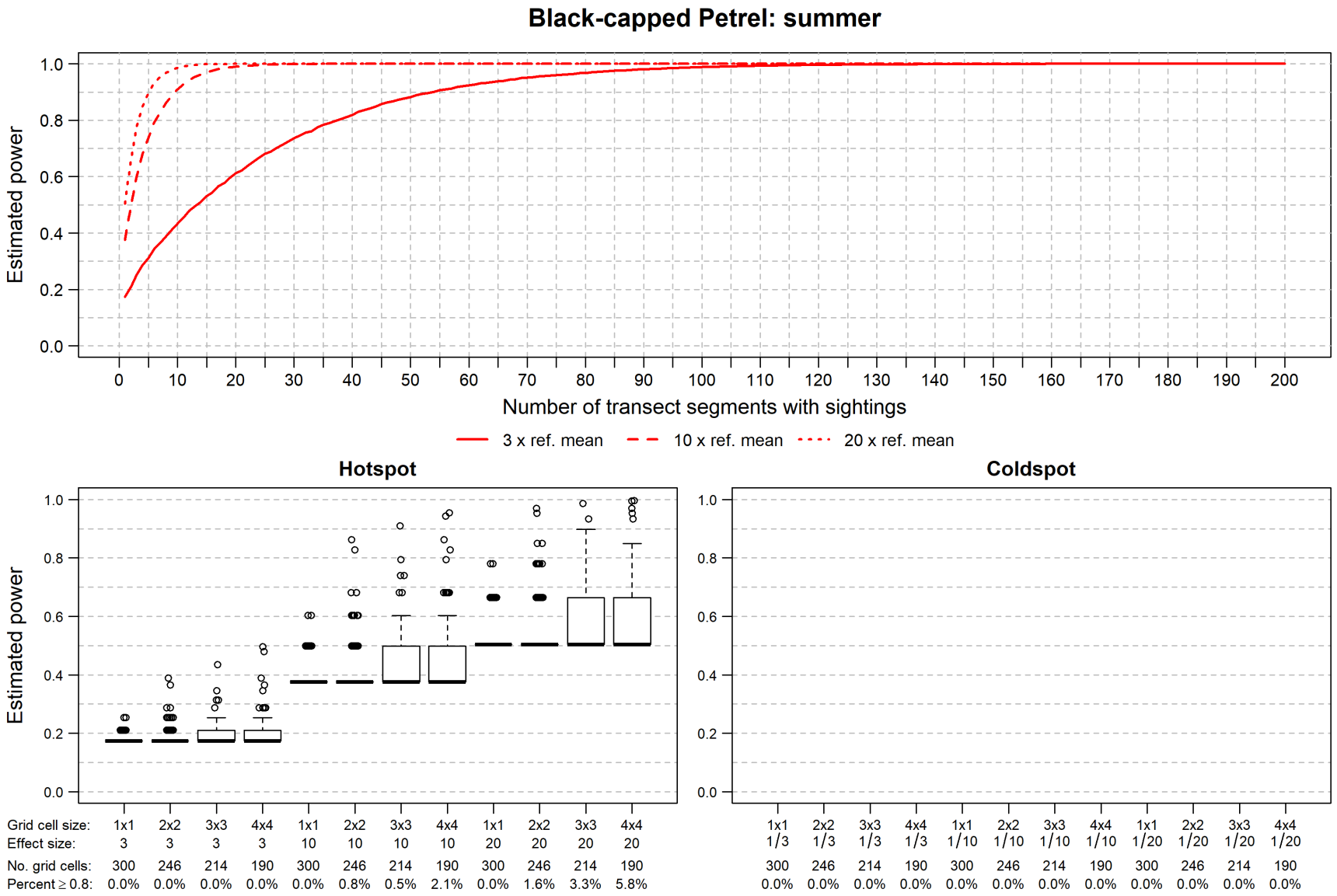

Figure D49. Power analysis results for Black-capped Petrel during summer based on the non-zero count model (type I error rate = 0.05)

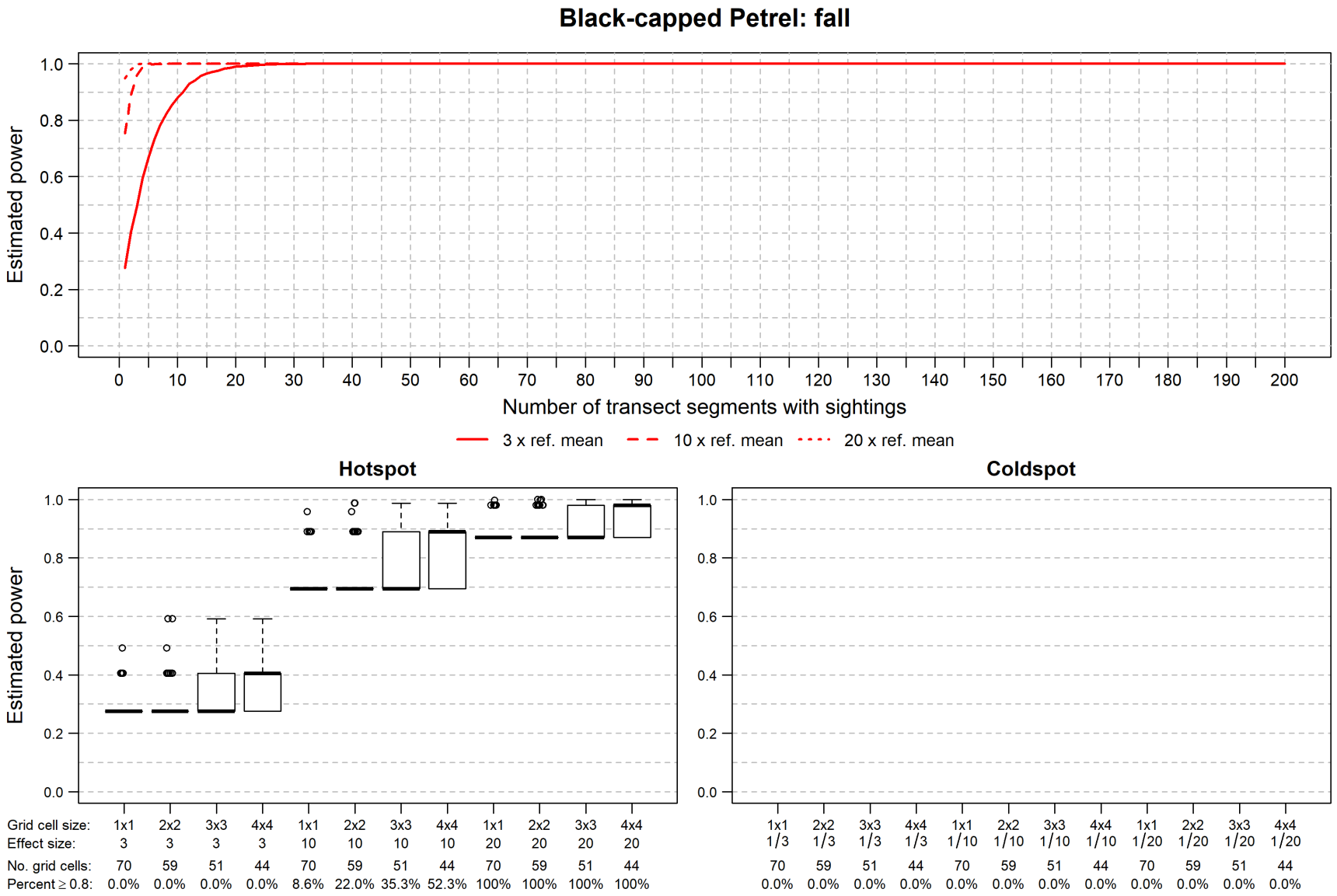

Figure D50. Power analysis results for Black-capped Petrel during fall based on the non-zero count model (type I error rate = 0.05)

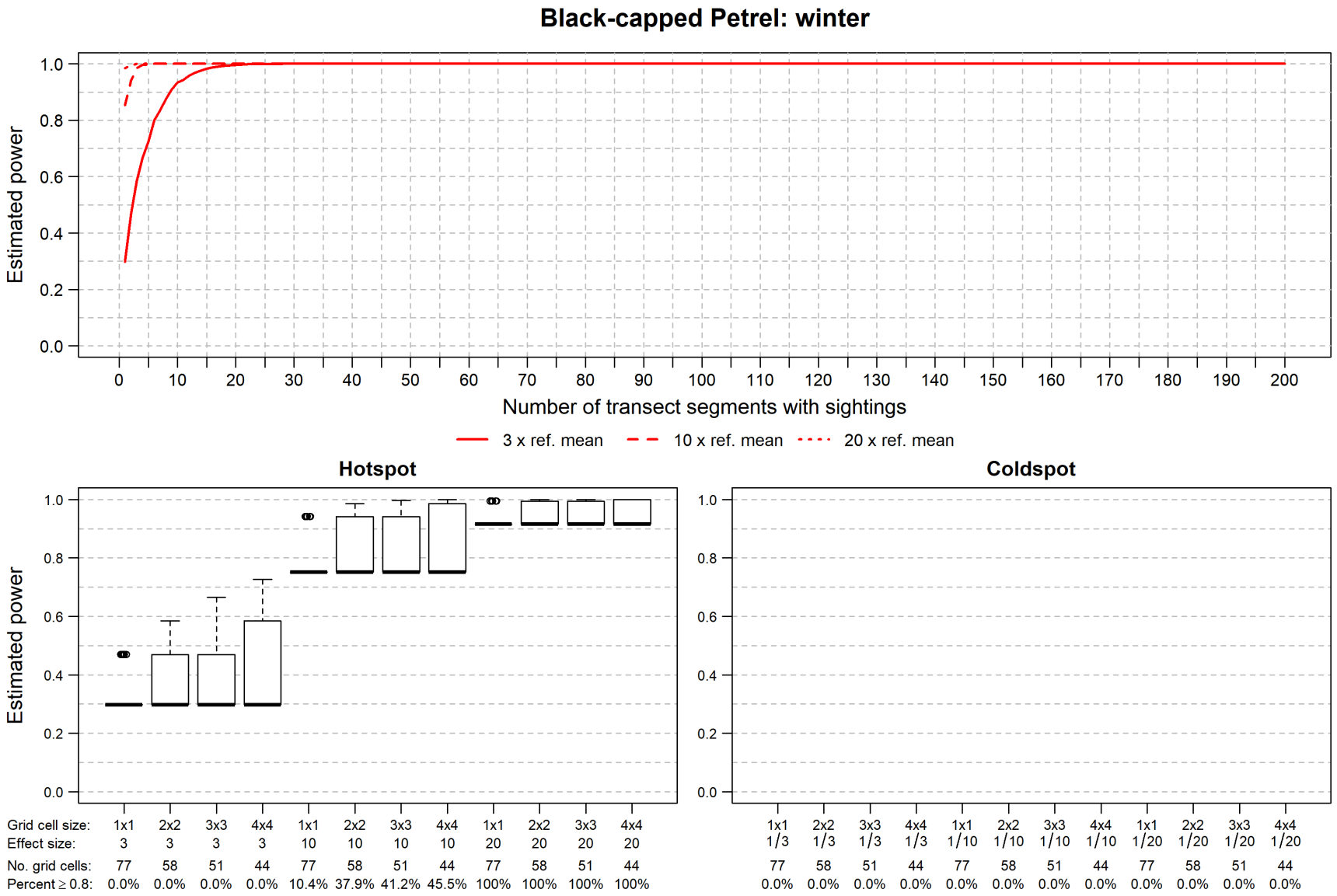

Figure D51. Power analysis results for Black-capped Petrel during winter based on the non-zero count model (type I error rate = 0.05)

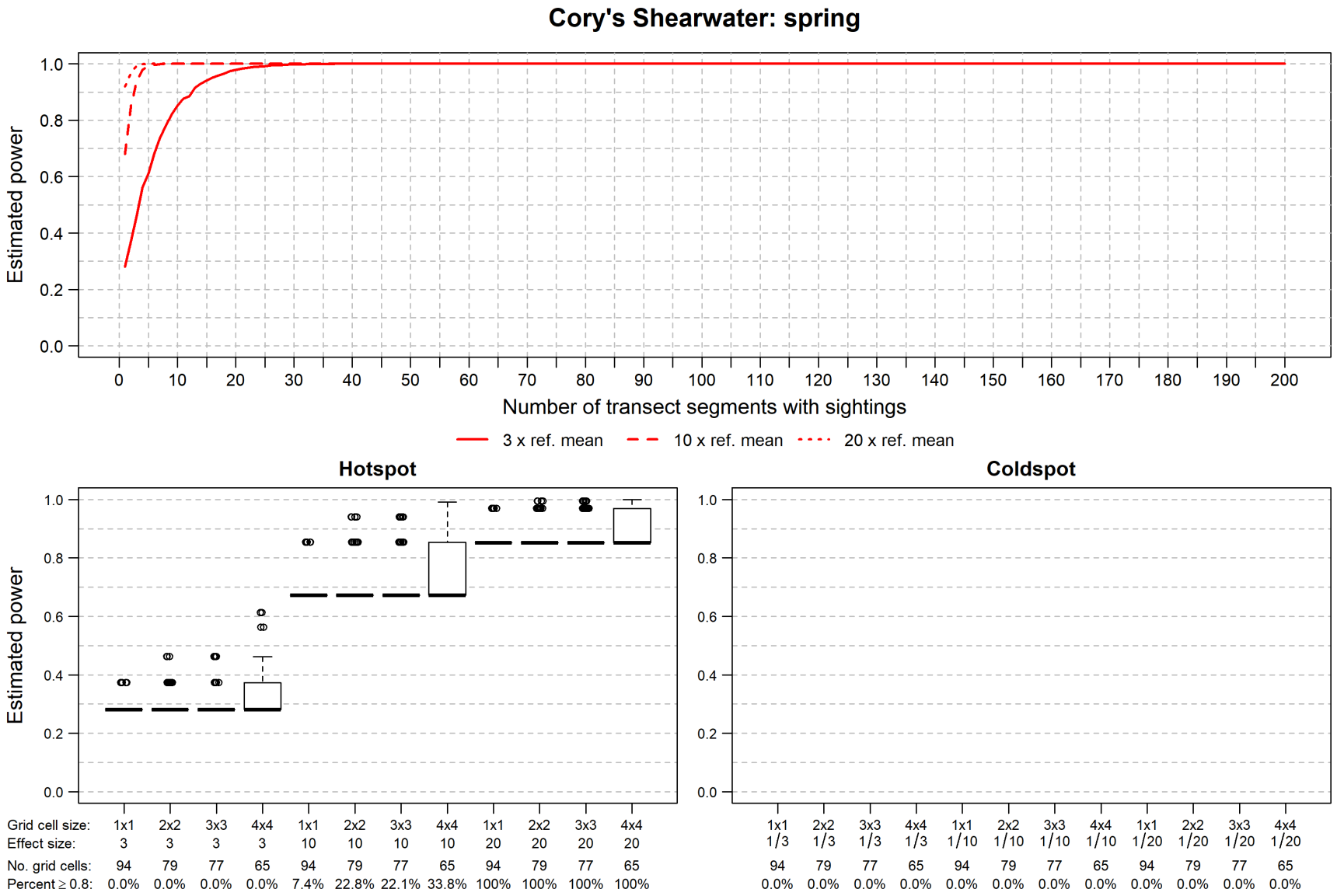

Figure D52. Power analysis results for Cory's Shearwater during spring based on the non-zero count model (type I error rate = 0.05)

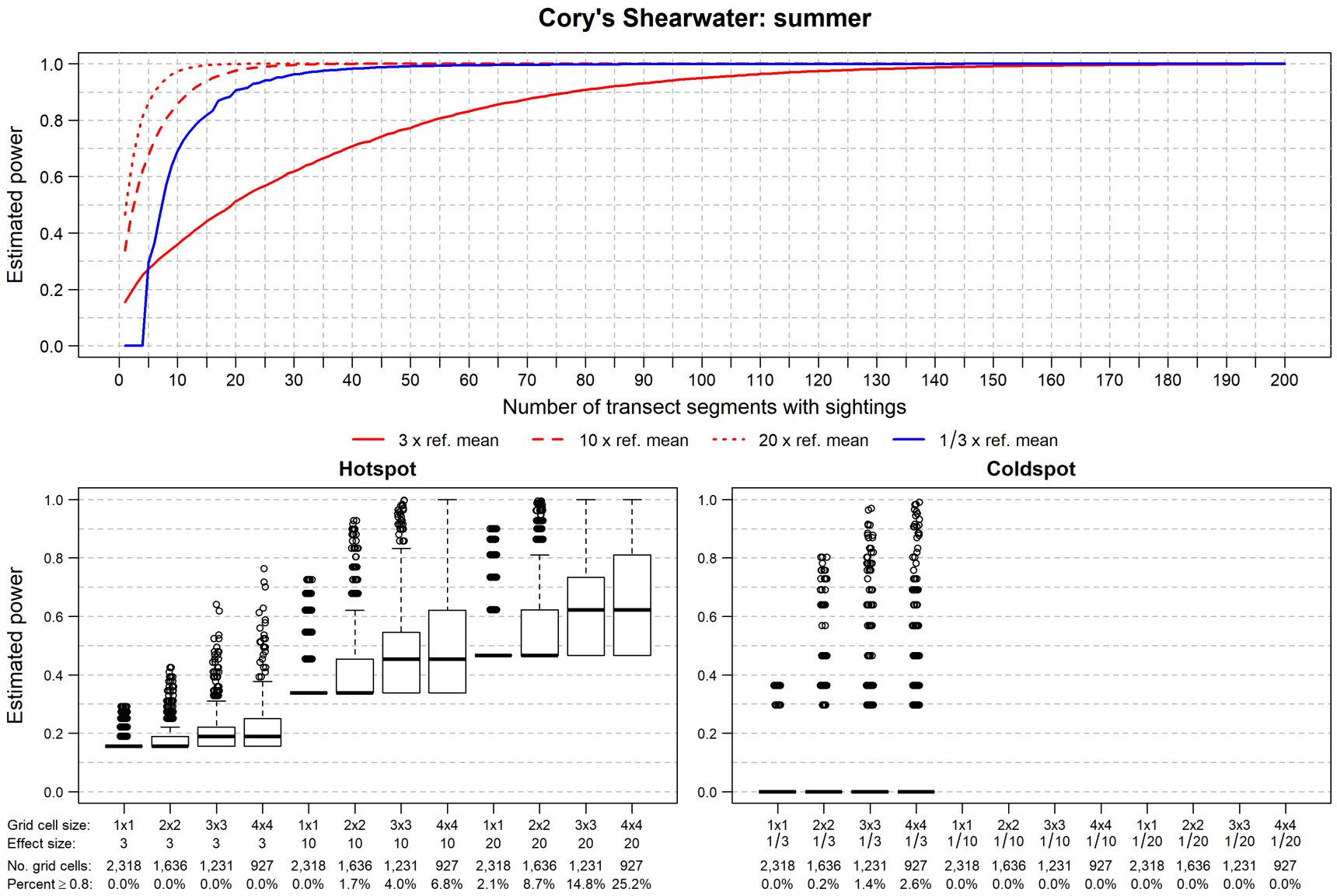

Figure D53. Power analysis results for Cory's Shearwater during summer based on the non-zero count model (type I error rate = 0.05)

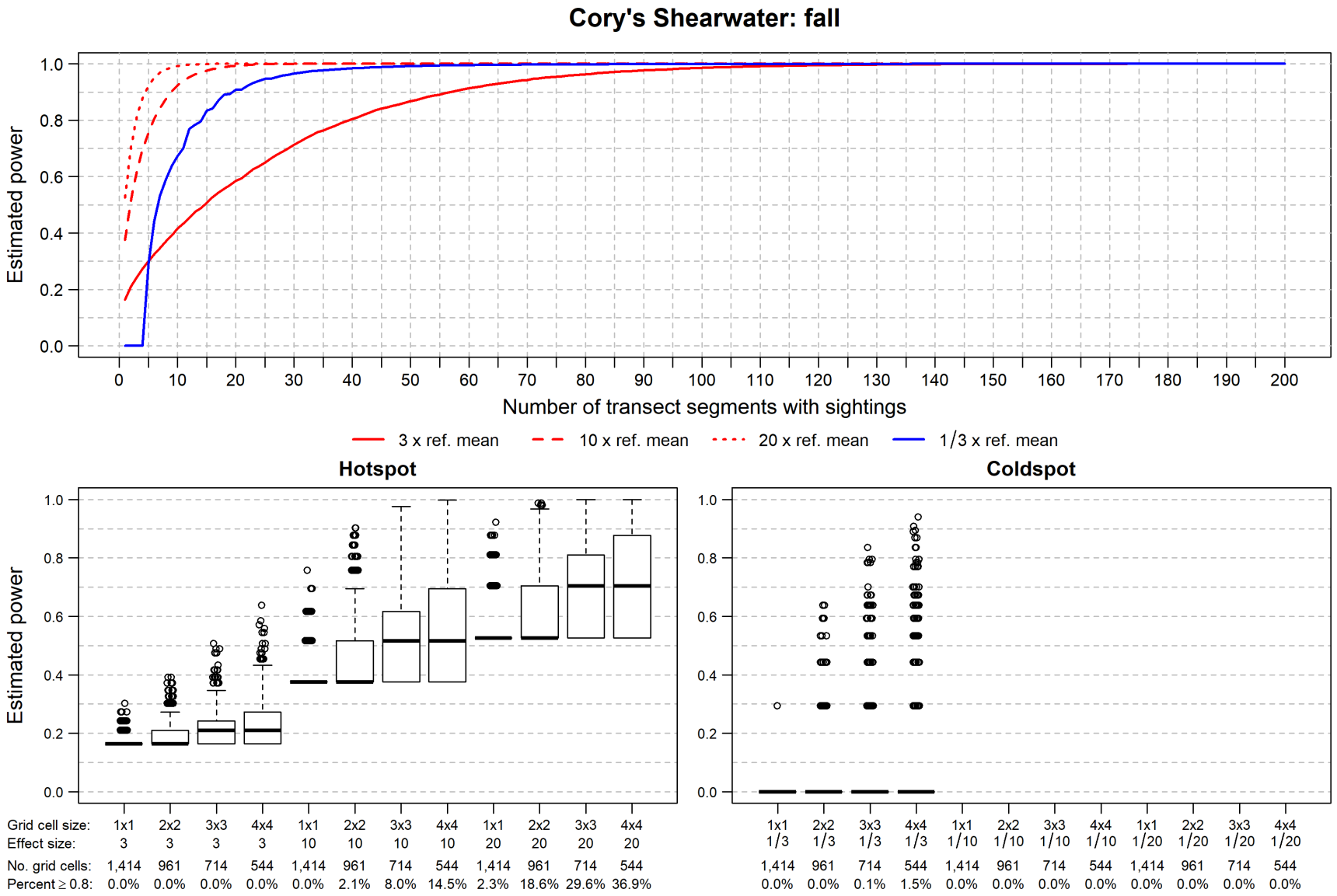

Figure D54. Power analysis results for Cory's Shearwater during fall based on the non-zero count model (type I error rate = 0.05)

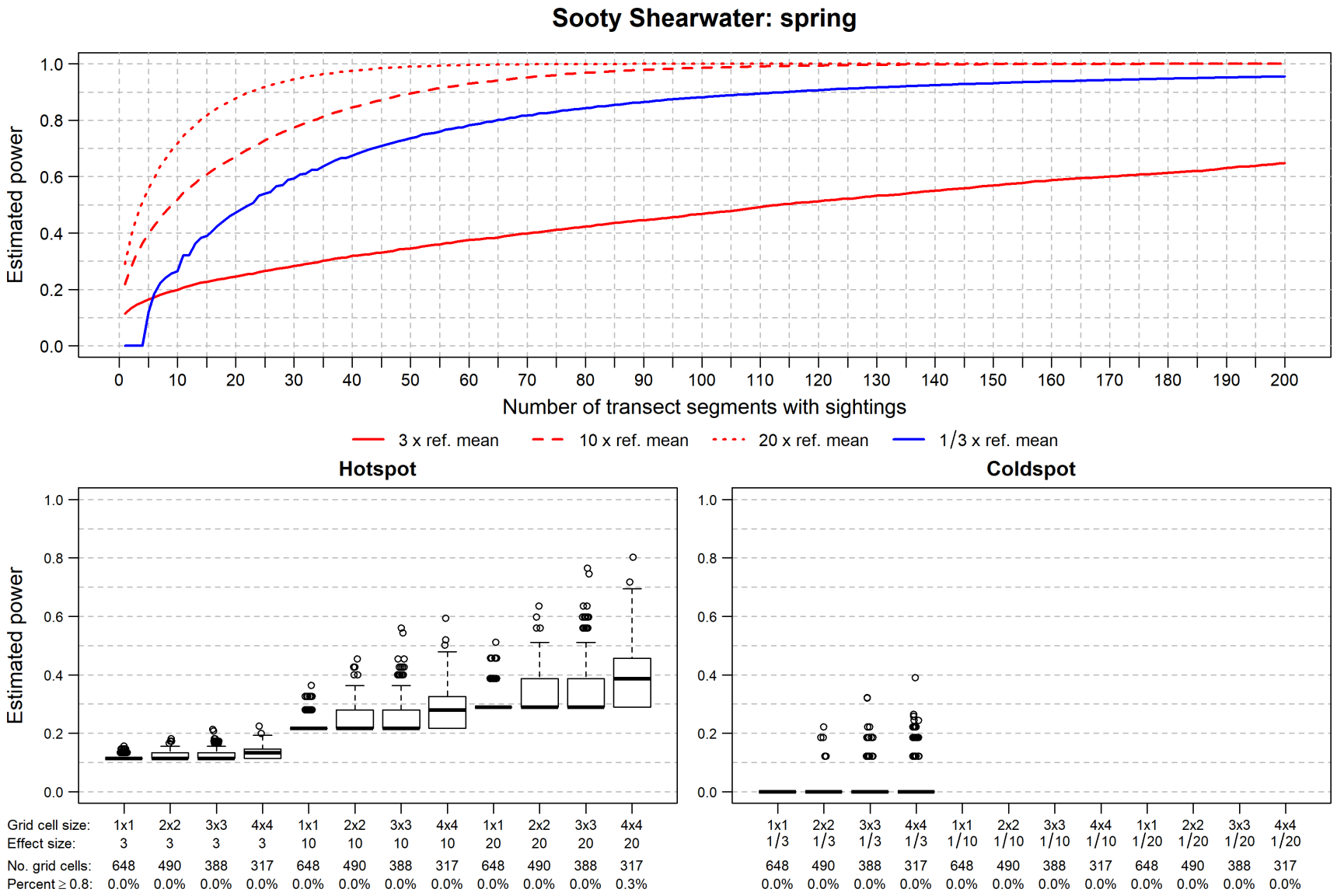

Figure D55. Power analysis results for Sooty Shearwater during spring based on the non-zero count model (type I error rate = 0.05)

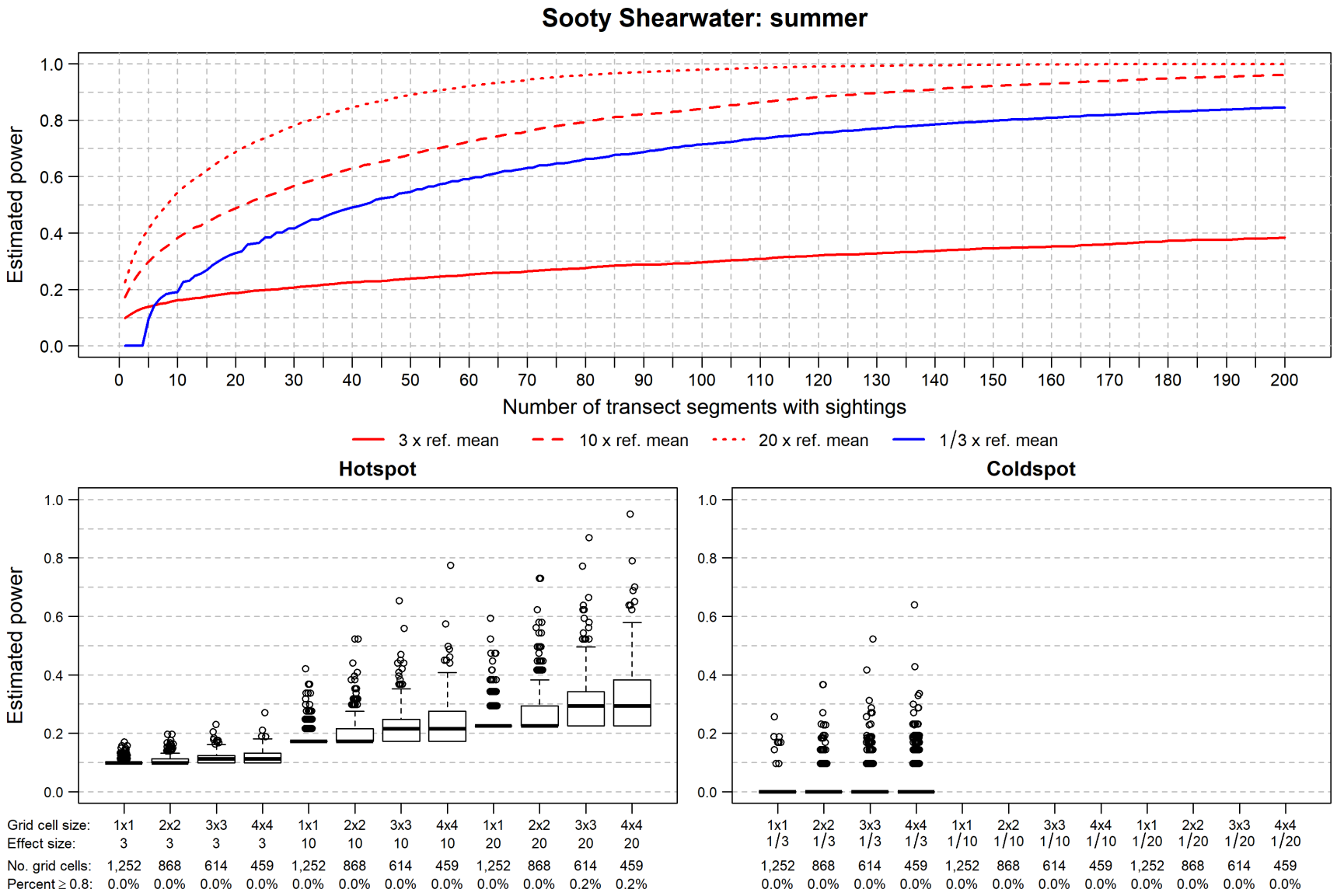

Figure D56. Power analysis results for Sooty Shearwater during summer based on the non-zero count model (type I error rate = 0.05)

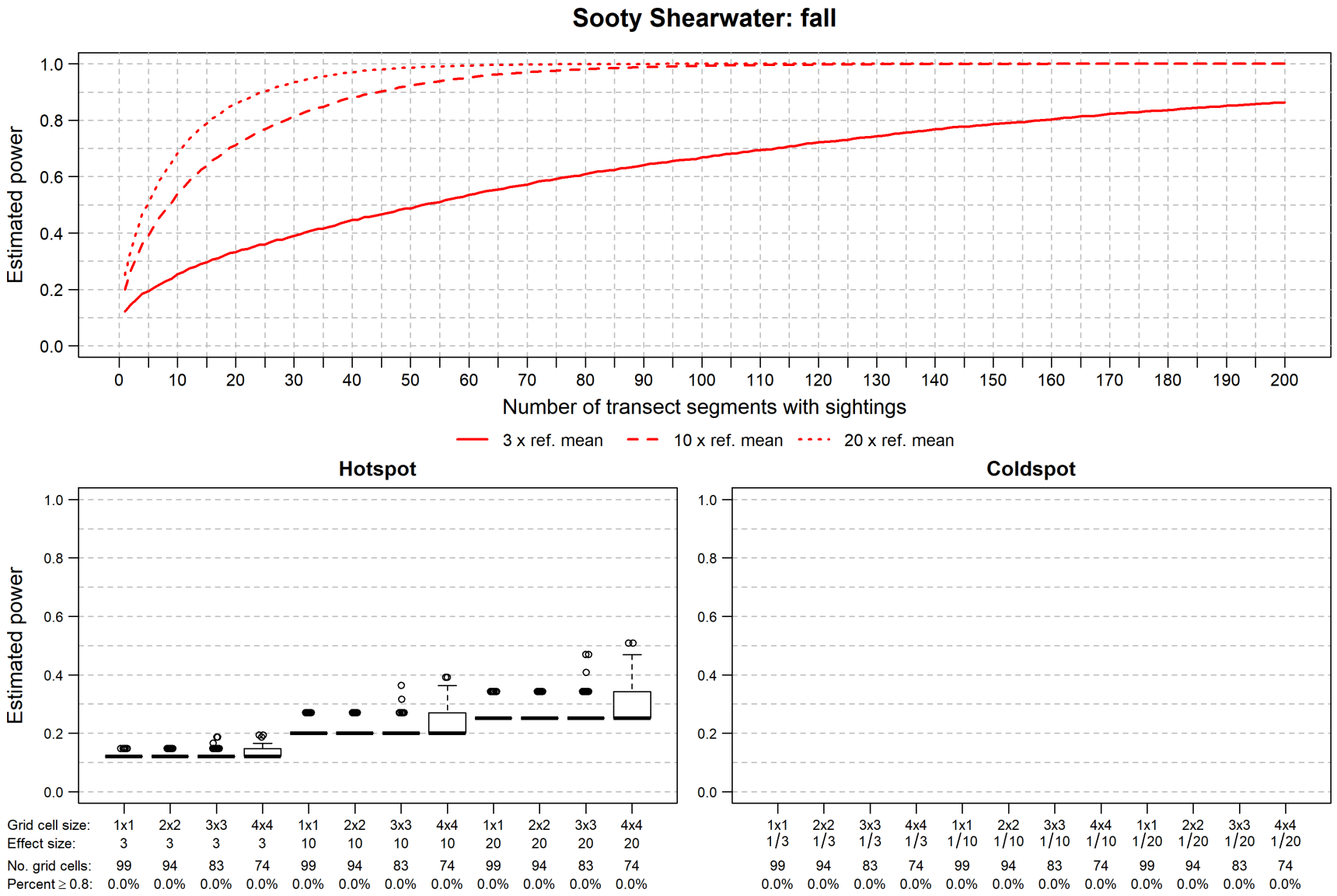

Figure D57. Power analysis results for Sooty Shearwater during fall based on the non-zero count model (type I error rate = 0.05)

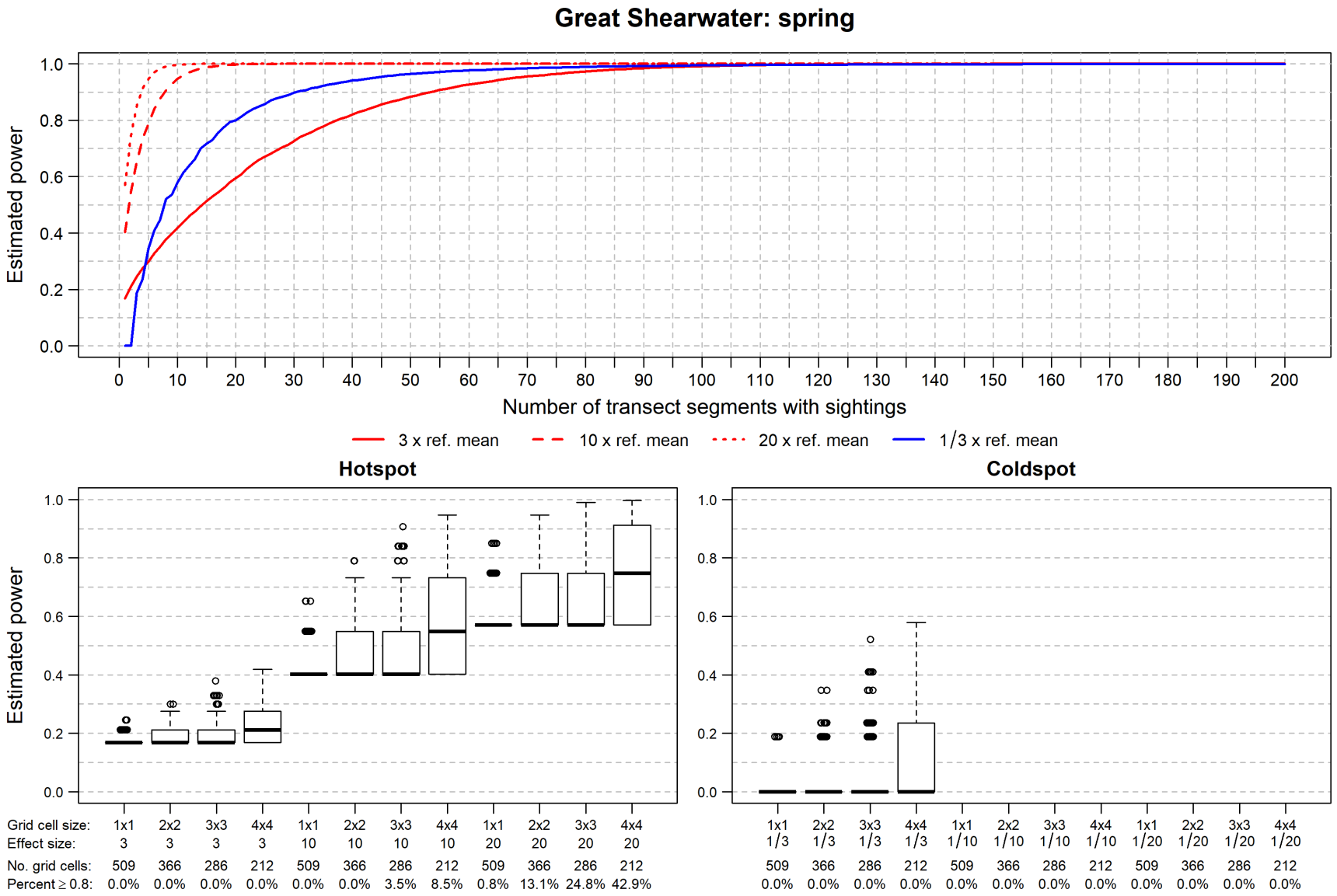

Figure D58. Power analysis results for Great Shearwater during spring based on the non-zero count model (type I error rate = 0.05)

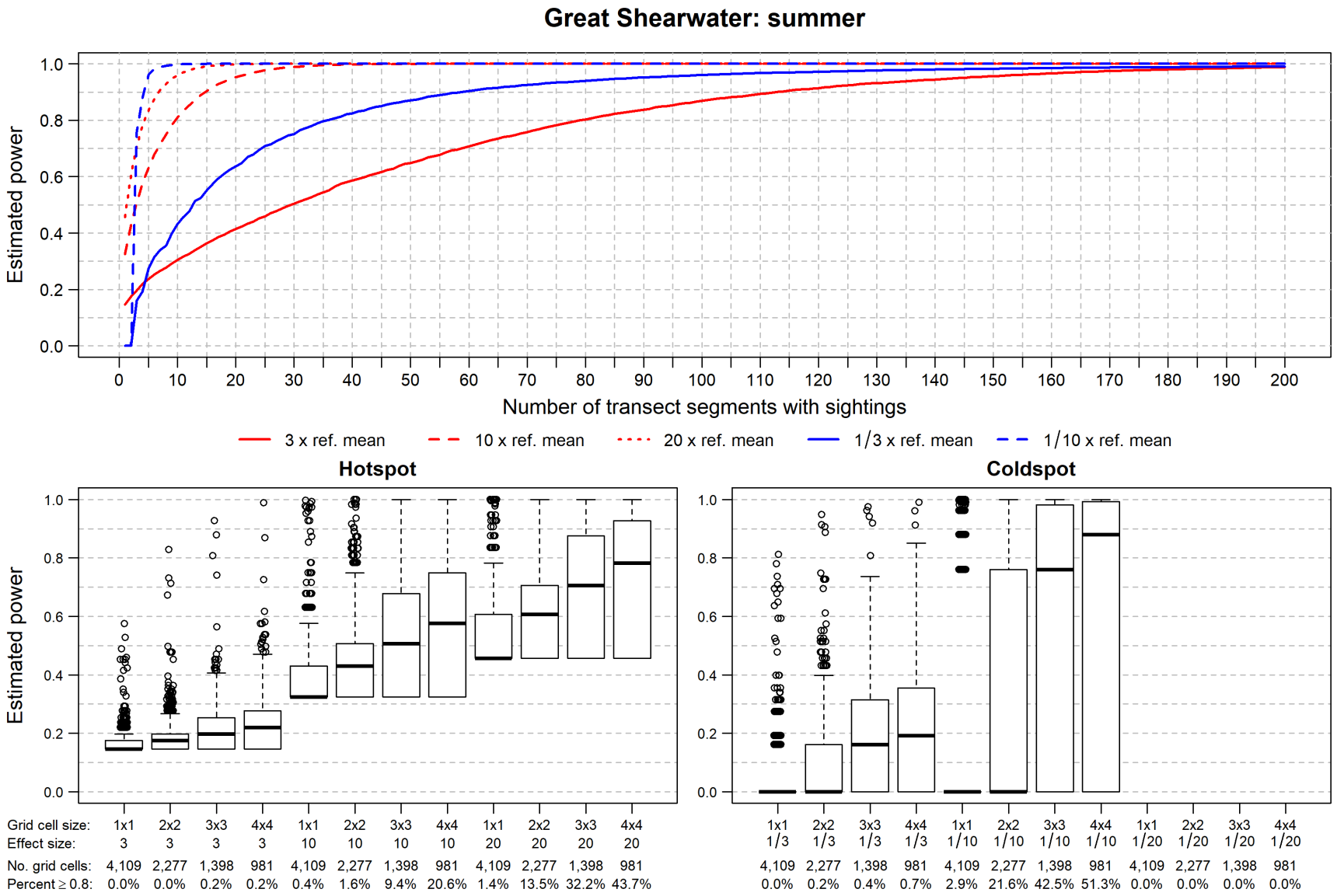

Figure D59. Power analysis results for Great Shearwater during summer based on the non-zero count model (type I error rate = 0.05)

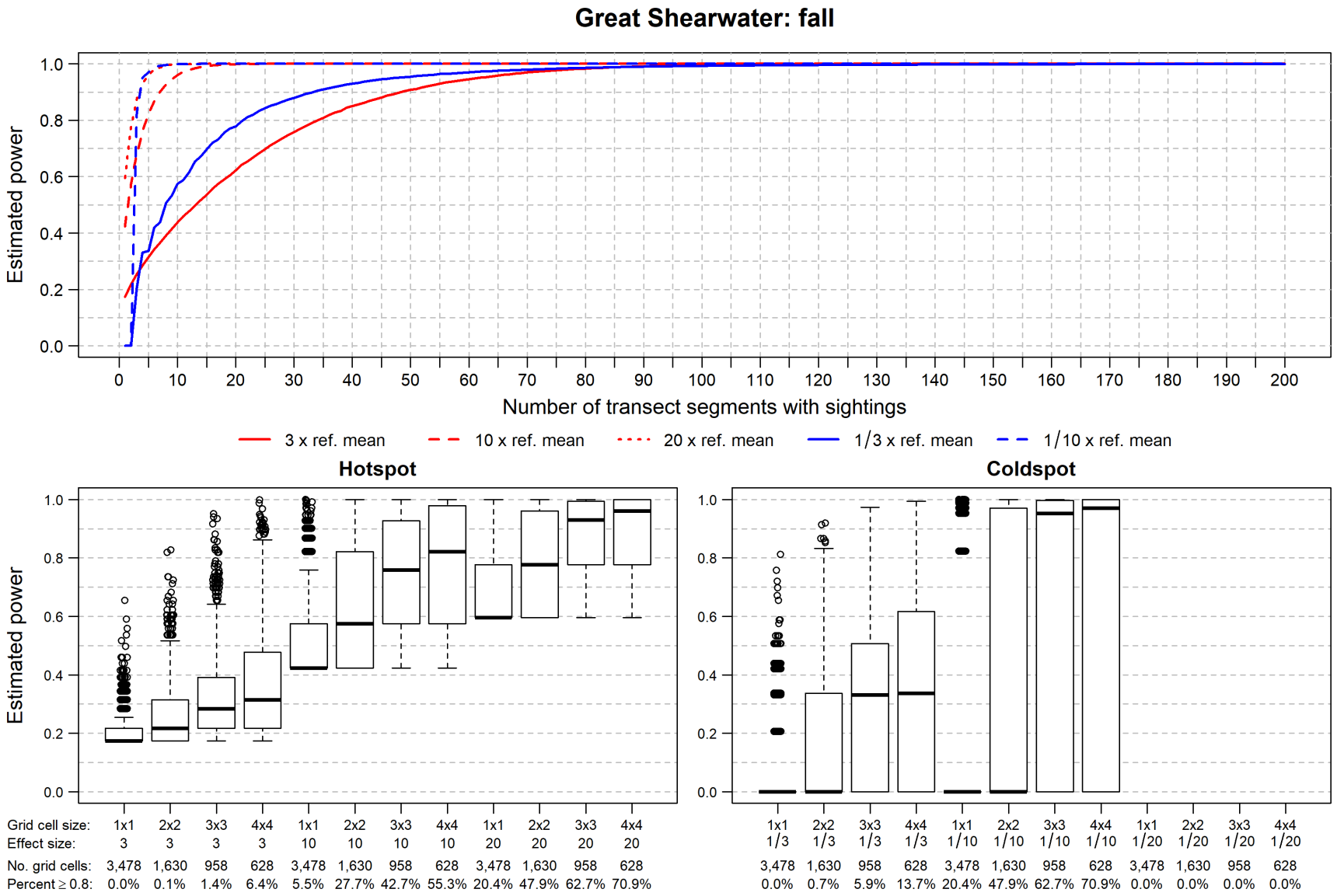

Figure D60. Power analysis results for Great Shearwater during fall based on the non-zero count model (type I error rate = 0.05)

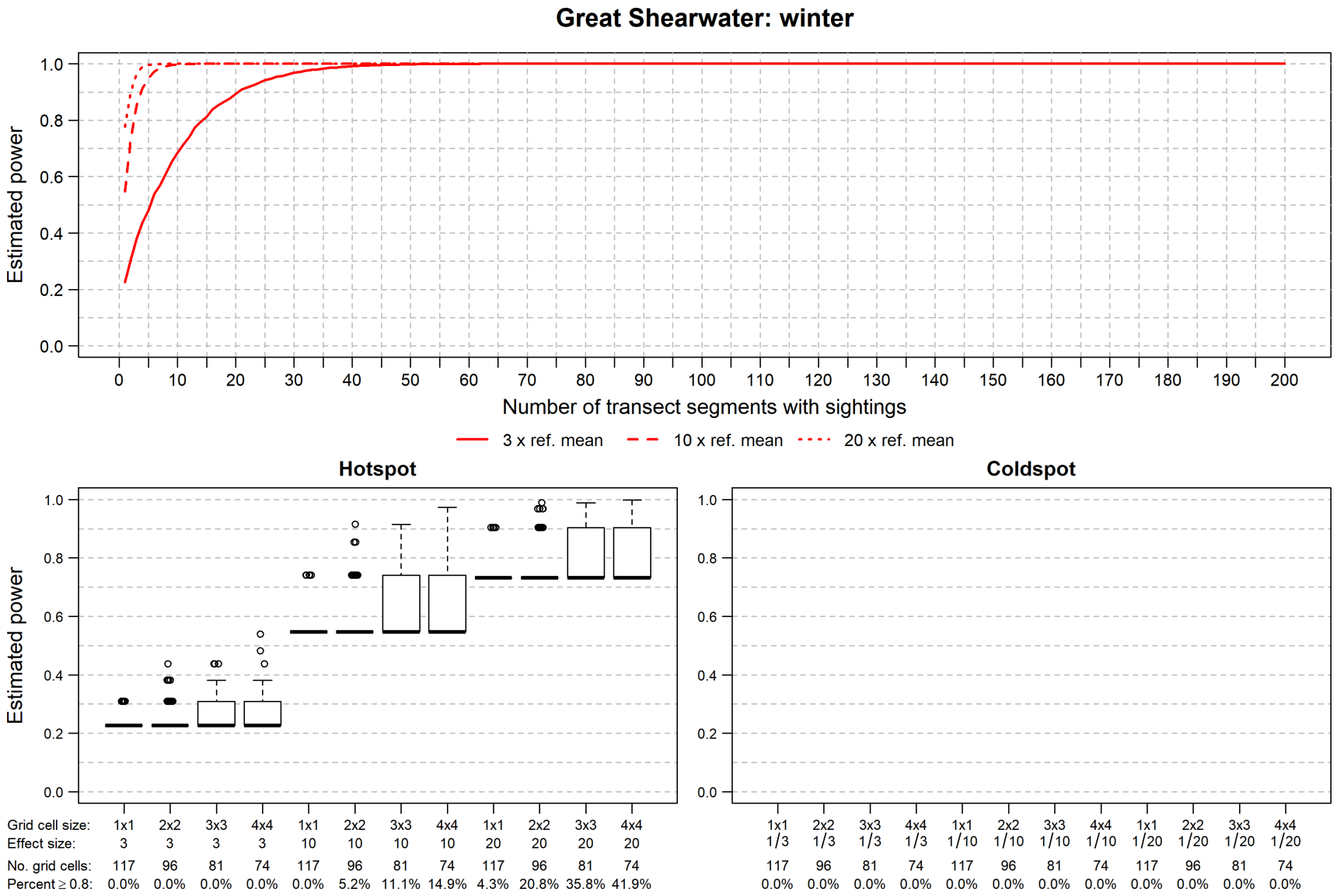

Figure D61. Power analysis results for Great Shearwater during winter based on the non-zero count model (type I error rate = 0.05)

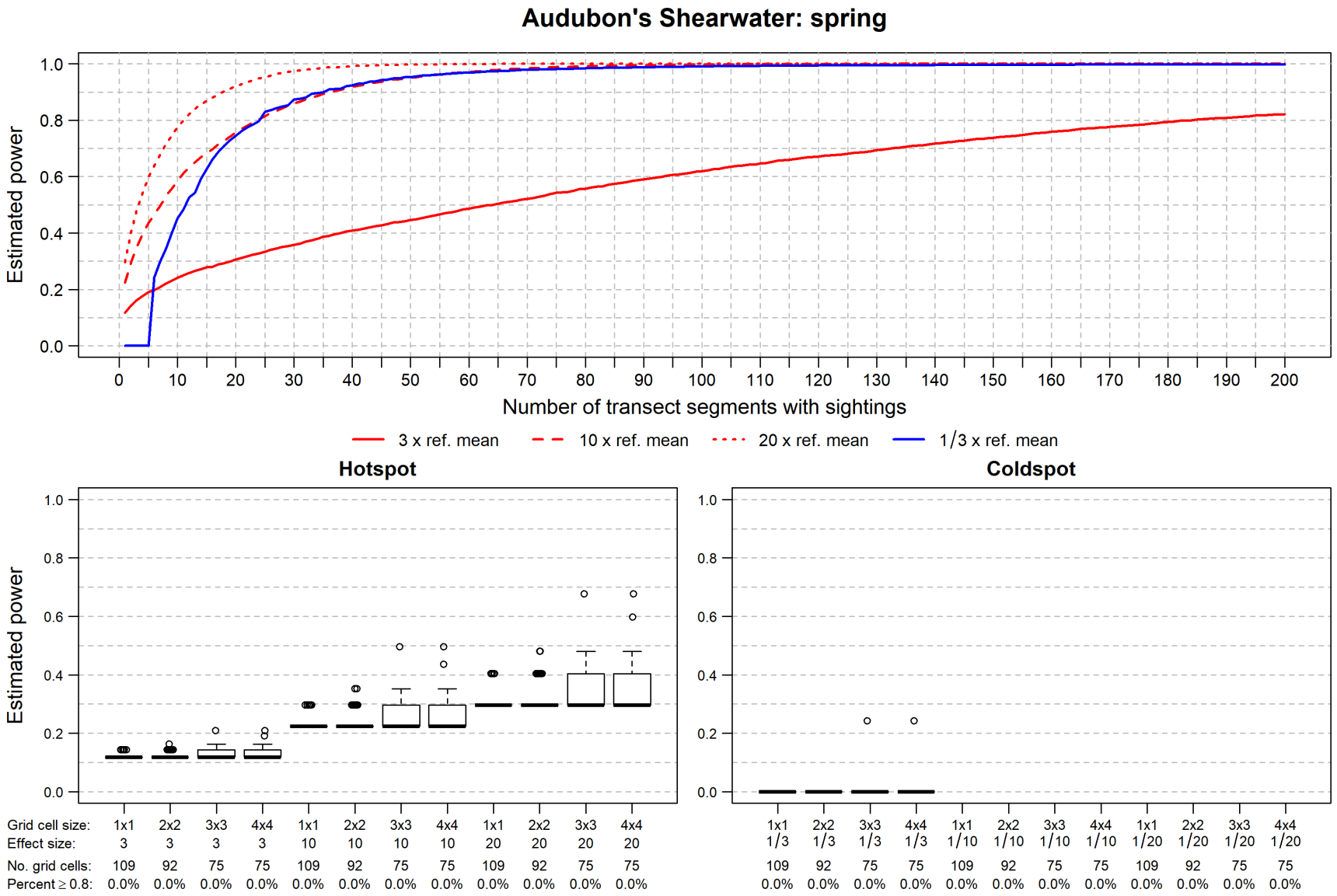

Figure D62. Power analysis results for Audubon's Shearwater during spring based on the non-zero count model (type I error rate = 0.05)

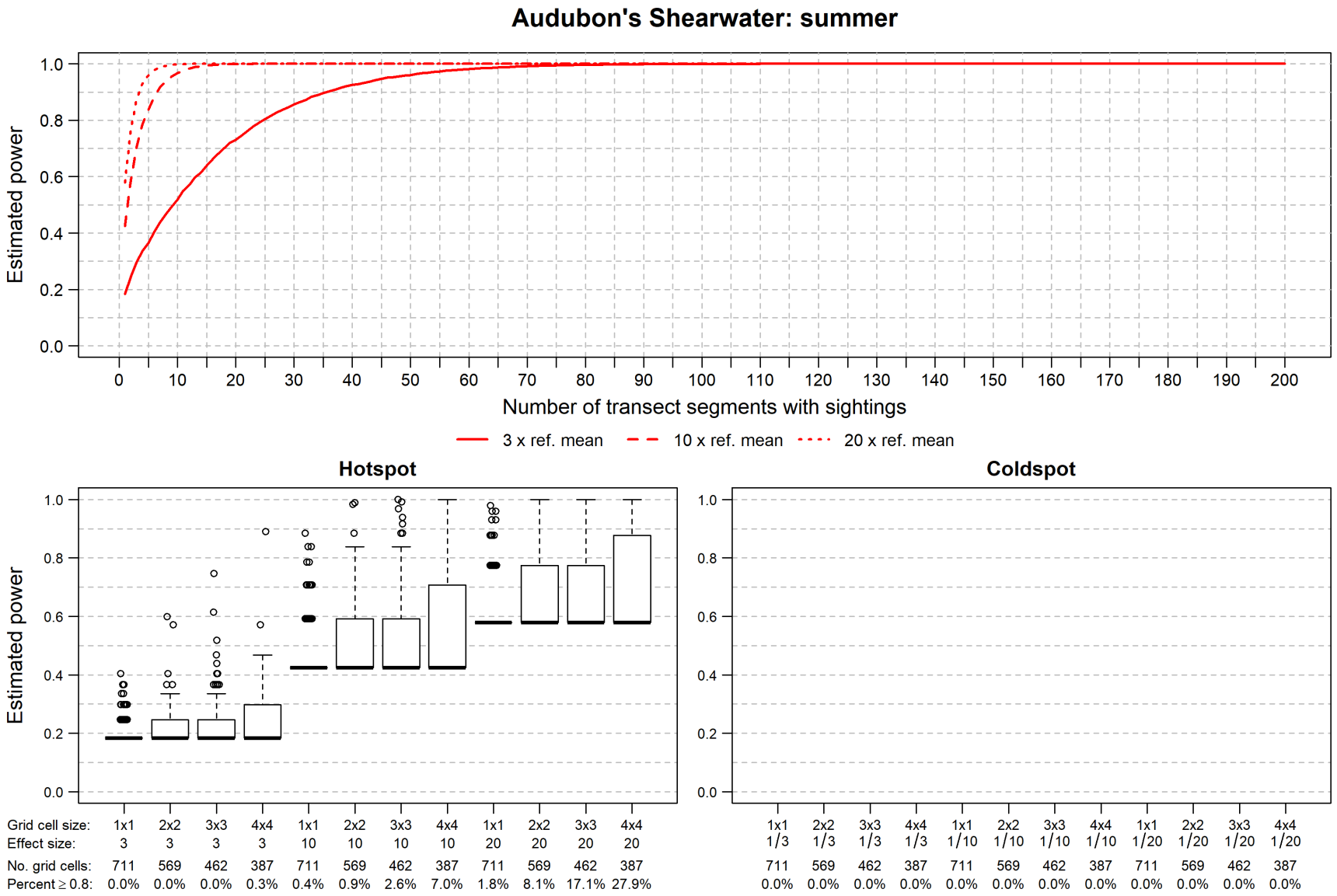

Figure D63. Power analysis results for Audubon's Shearwater during summer based on the non-zero count model (type I error rate = 0.05)

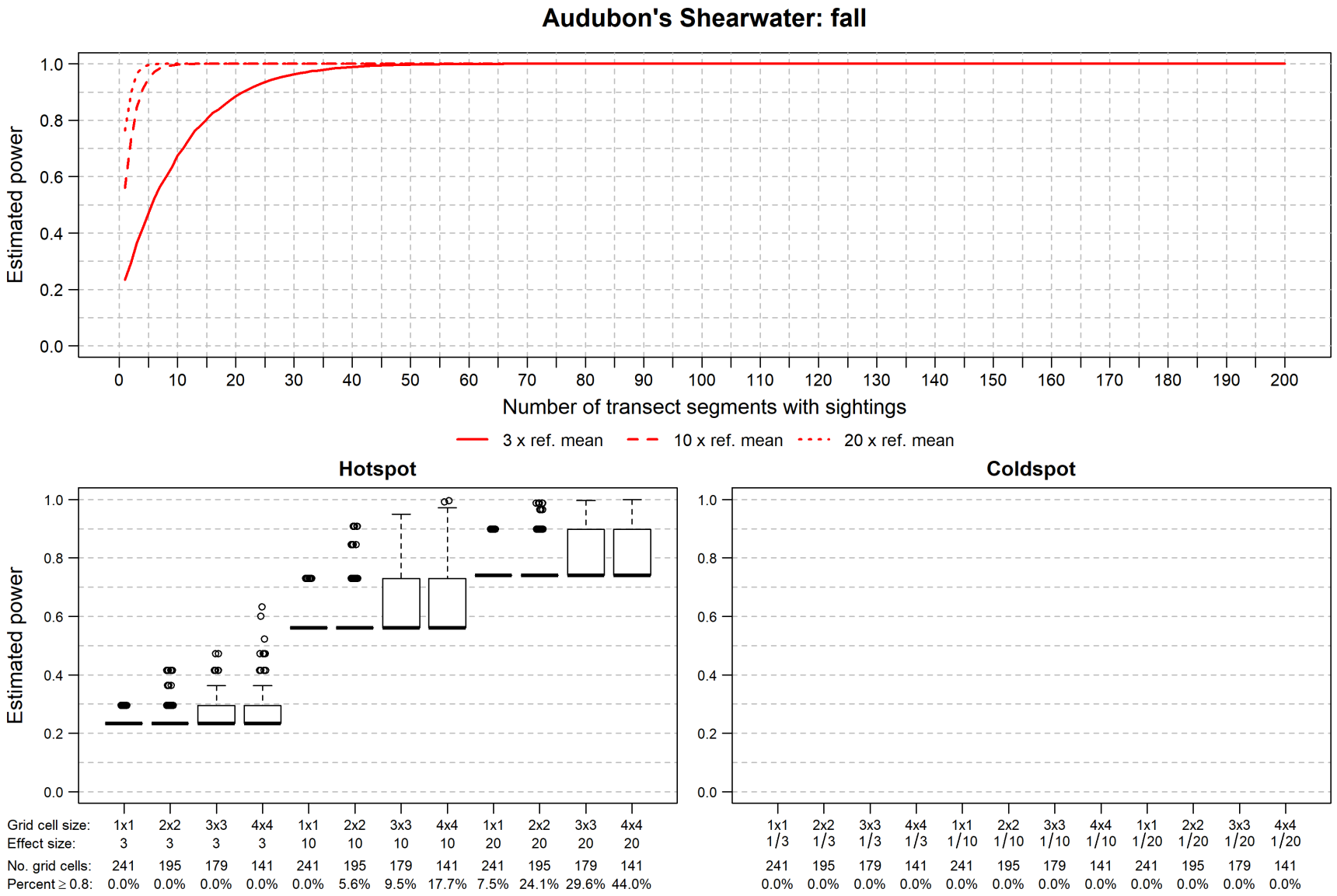

Figure D64. Power analysis results for Audubon's Shearwater during fall based on the non-zero count model (type I error rate = 0.05)

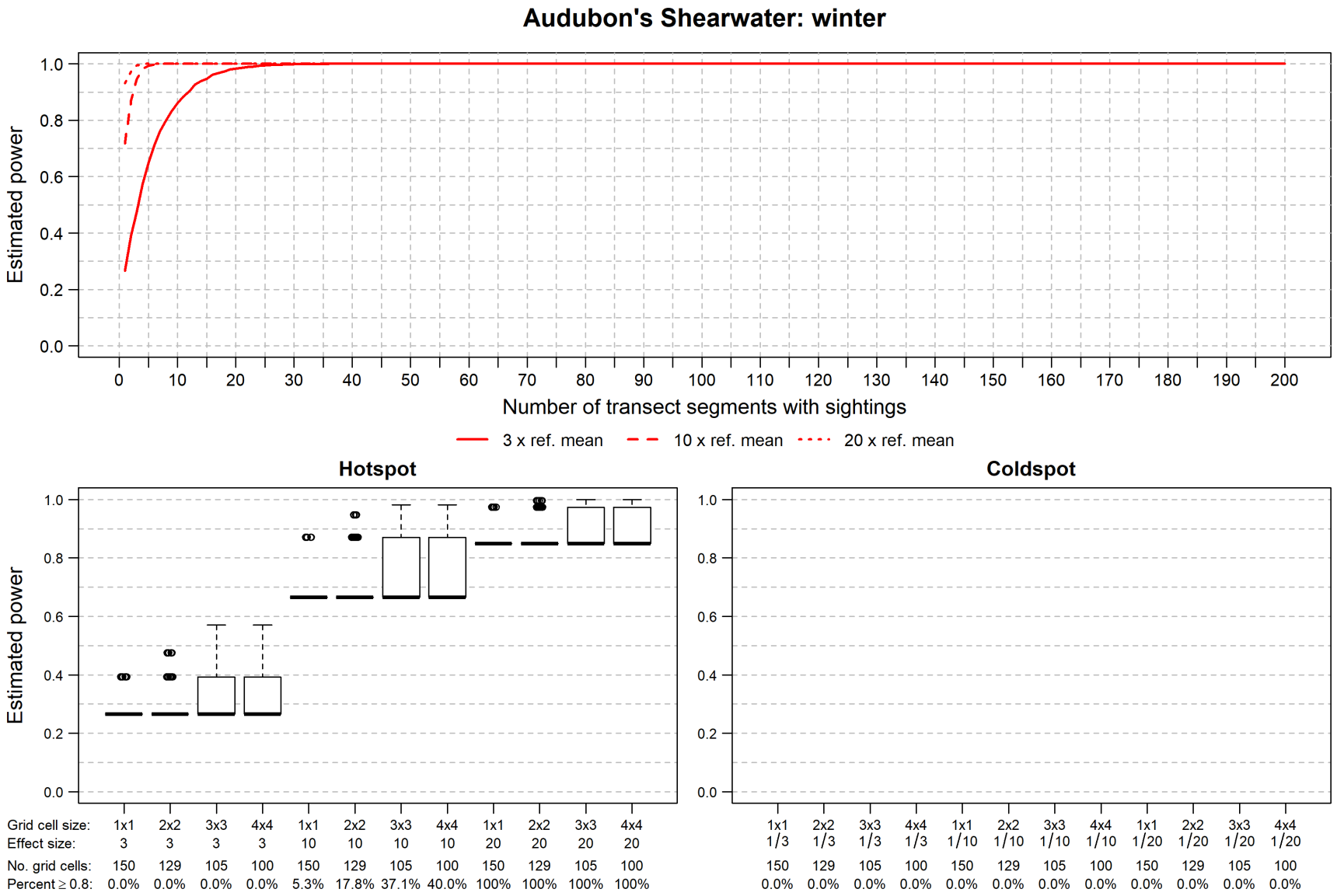

Figure D65. Power analysis results for Audubon's Shearwater during winter based on the non-zero count model (type I error rate = 0.05)

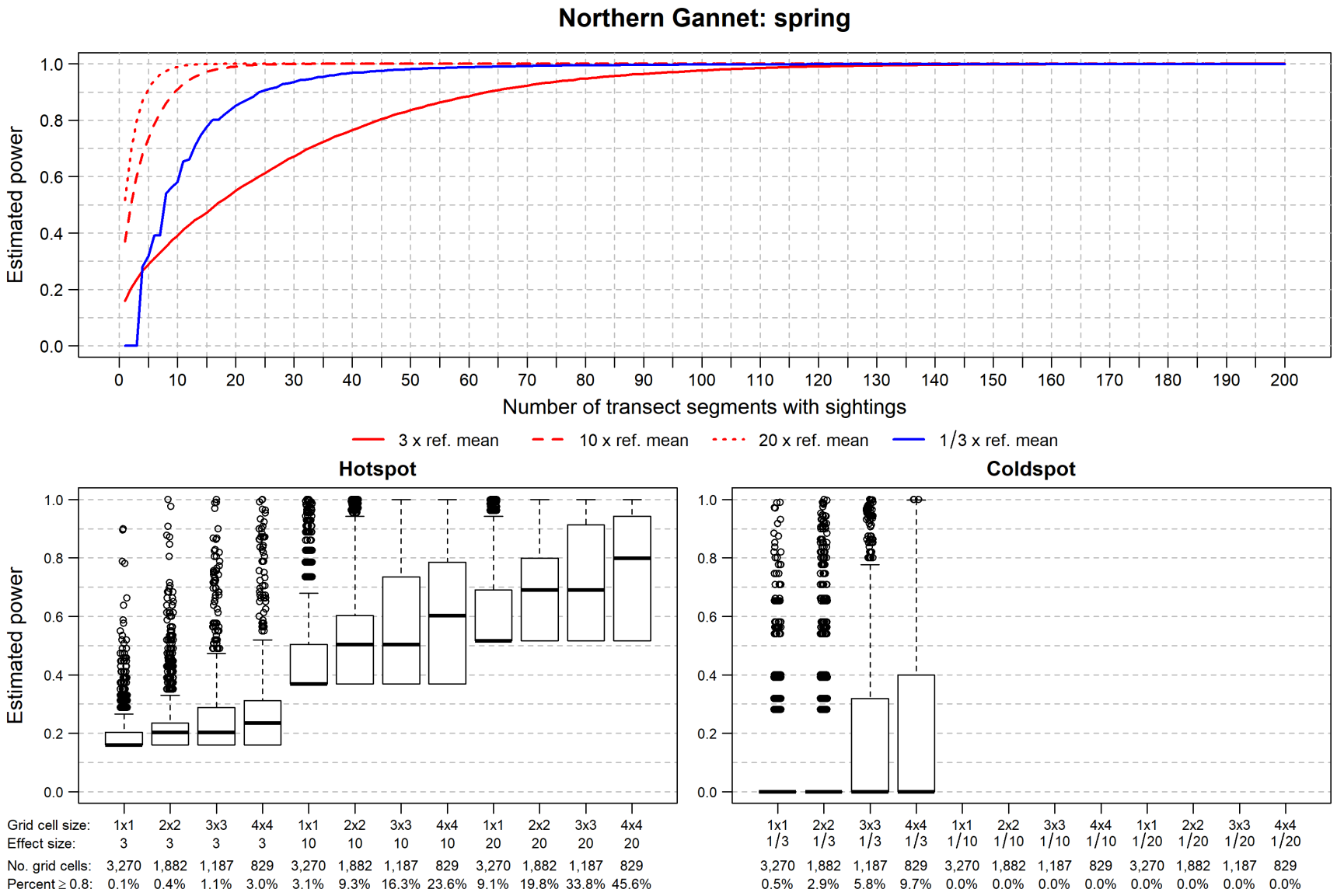

Figure D66. Power analysis results for Northern Gannet during spring based on the non-zero count model (type I error rate = 0.05)

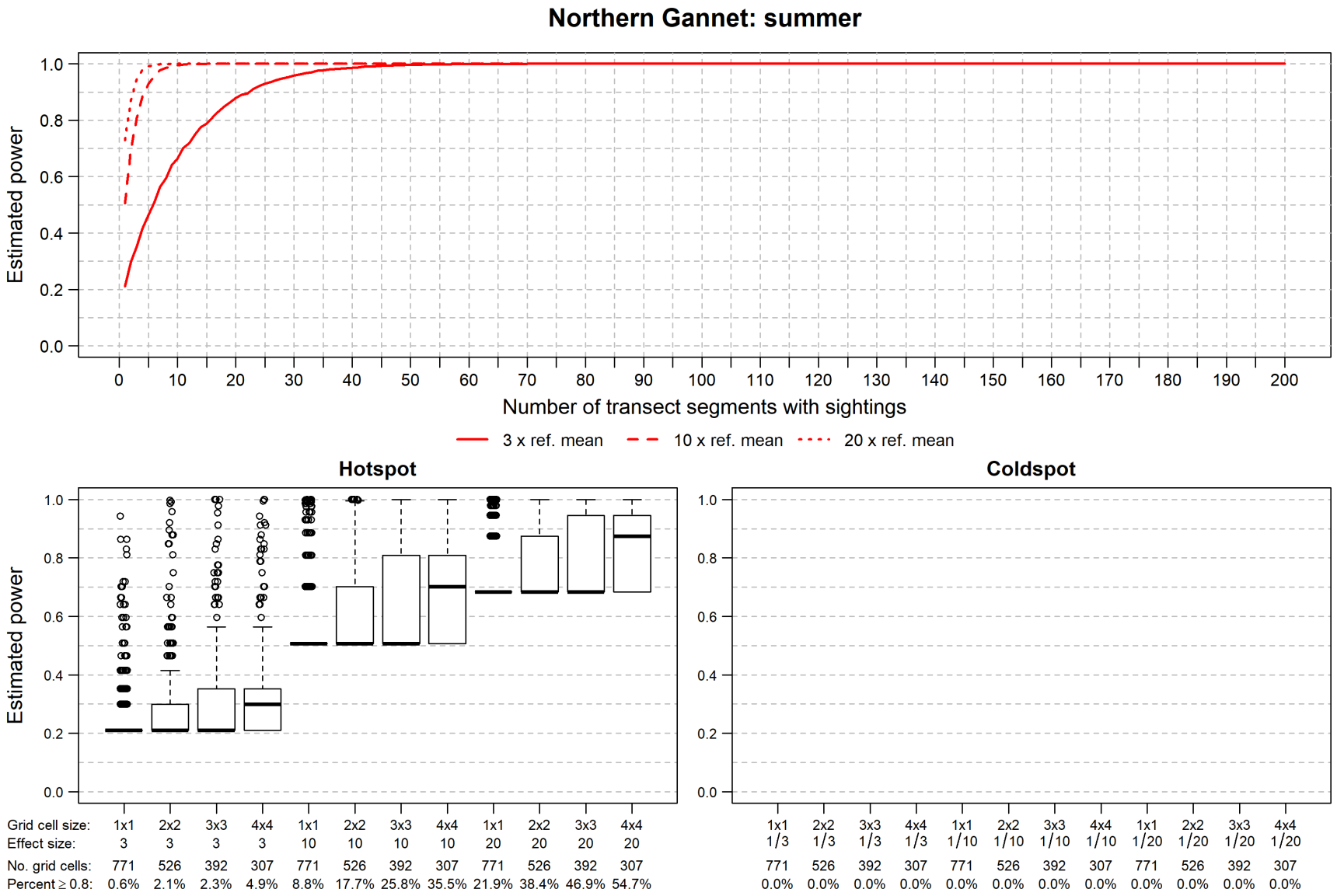

Figure D67. Power analysis results for Northern Gannet during summer based on the non-zero count model (type I error rate = 0.05)

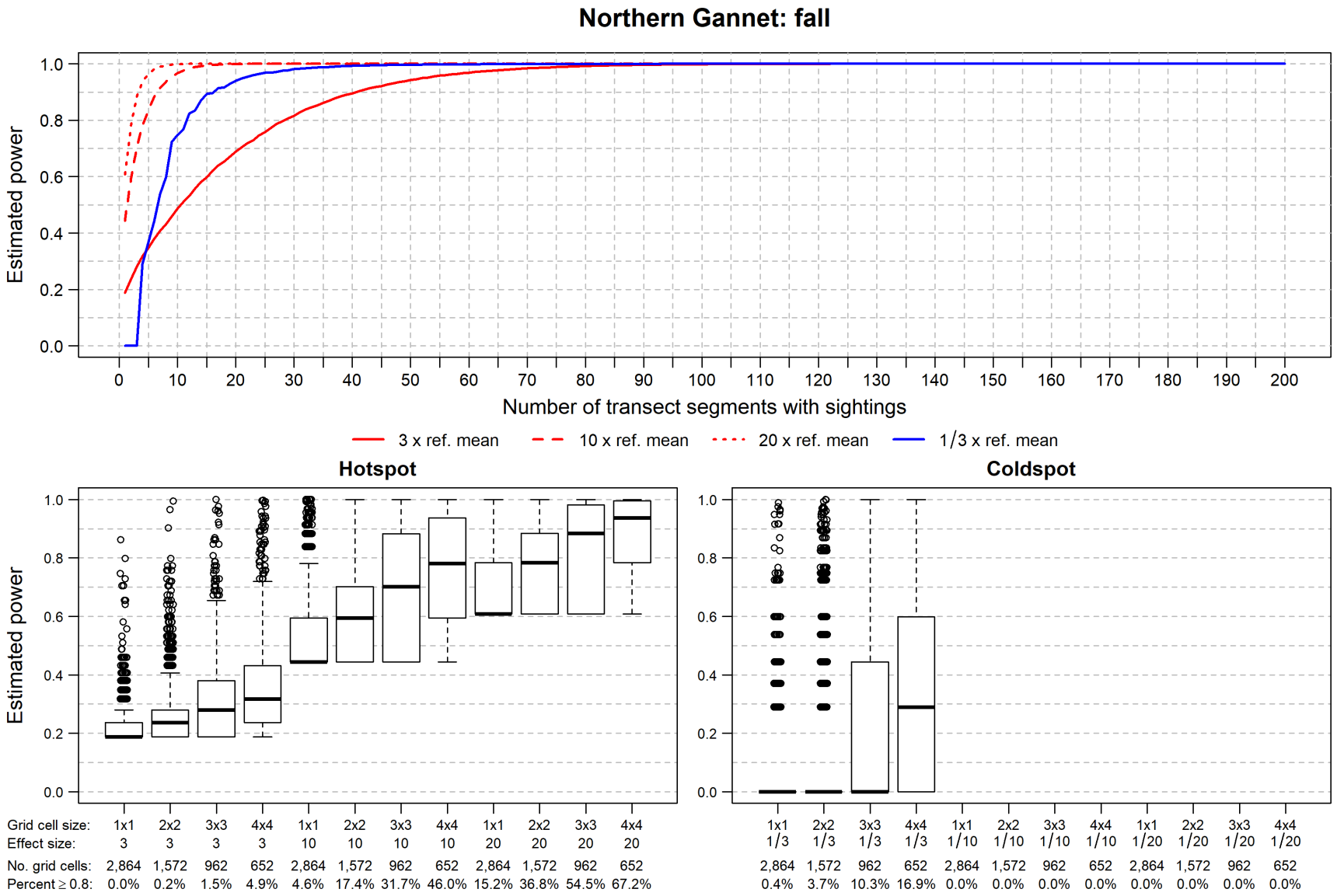

Figure D68. Power analysis results for Northern Gannet during fall based on the non-zero count model (type I error rate = 0.05)

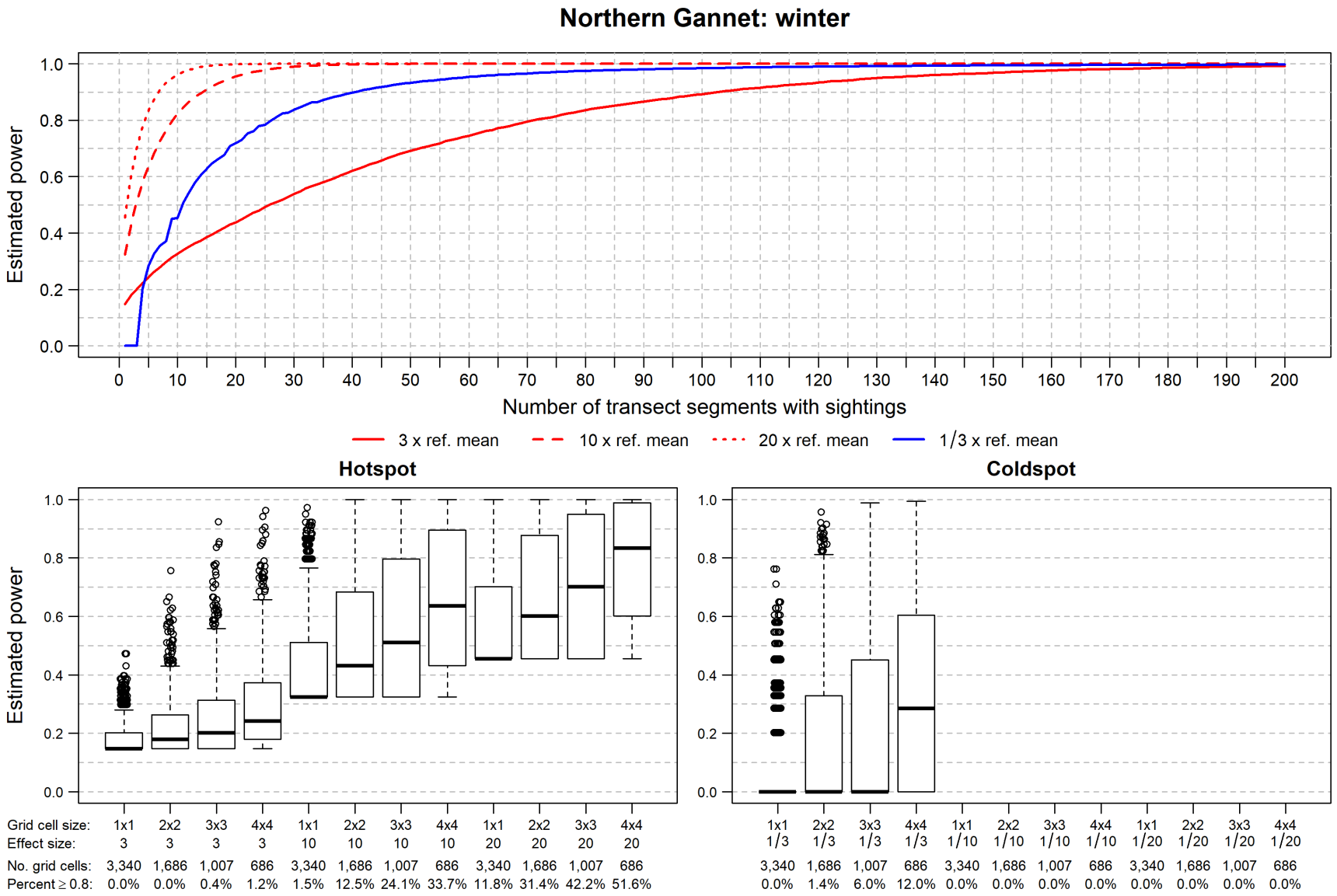

Figure D69. Power analysis results for Northern Gannet during winter based on the non-zero count model (type I error rate = 0.05)